THE
PHYSICAL REVIEW

A journal of experimental and theoretical physics established by E. L. Nichols in 1893

SECOND SERIES, VOL. 63, NOS. 11 AND 12 JUNE 1 AND 15, 1943

Measurements on X-Ray Production and Absorption in the Range 0.7 to 2.5 Mv

A. A. PETRAUSKAS,* L. C. VAN ATTA,** AND F. E. MYERS***
George Eastman Research Laboratory of Physics, Massachusetts Institute of Technology, Cambridge, Massachusetts
(Received April 9, 1942)

In the voltage range from 0.7 to 2.5 Mv, the intensity and the total mass absorption coefficient of the heterogeneous radiation produced in a thick gold target have been measured as a function of tube voltage, angle with respect to the electron beam, and thickness and material of the filter. Curves giving the dependence of absorption coefficient on voltage are presented for lead, tin, copper, aluminum, carbon, and water as absorbers. A method is described for calculating the absorption coefficient of the heterogeneous radiation produced at a given tube voltage and subjected to a given amount of filtration, utilizing accepted values for the absorption coefficient of homogeneous radiation. Measured and calculated values of the absorption coefficients for heterogeneous radiation are in good agreement. Curves giving the dependence of intensity on angle are in qualitative agreement with approximate theory. Curves giving the dependence of absorption coefficient on angle and the dependence of intensity in the forward direction on voltage are presented. A method for calculating the efficiency of x-ray production from these data is described and used to obtain results in satisfactory agreement with theory in the voltage range from 0.90 to 2.35 Mv.

I. INTRODUCTION

THIS research is concerned with the intensity and quality of the continuous radiation produced at a thick target of high atomic number by bombardment with high energy electrons, and with the absorption of this radiation by various materials.[1] Such information has application in high voltage x-ray research and therapy, and makes possible a limited comparison with existing theory.

Most previous precision measurements of absorption coefficients have been made with *homogeneous* radiation either at low voltage where homogeneous x-rays are obtainable by crystal reflection, or at high voltage as the homogeneous gamma-rays from radioactive materials. Such measurements have been made in various materials[2] up to 0.5 Mv with a probable error of one percent, up to 2.5 Mv with a probable error[3] of four percent, and in a few elements at isolated higher voltages[4] with less accuracy. Experiment and theory concerning the absorption of homogeneous radiation are in satisfactory agreement throughout the voltage range involved.

Measurements of the intensity and quality of the *heterogeneous* radiation produced at a thick target have been made up to 0.5 Mv, and to a limited extent up to 1.0 Mv. In the low voltage

* Now in the Physics Department, University of Notre Dame, Notre Dame, Indiana.

** Now in the Radiation Laboratory, Massachusetts Institute of Technology, Cambridge, Massachusetts.

*** On leave from the Physics Department, New York University, and now at the Frankford Arsenal, Frankford, Pennsylvania.

[1] Rough preliminary results were presented earlier: L. C. Van Atta and D. L. Northrup, Am. J. Roent. and Rad. Therapy **51**, 633 (1939); present authors, Phys. Rev. **59**, 688A (1941).

[2] J. Read and C. C. Lauritsen, Phys. Rev. **45**, 433 (1934).

[3] C. Y. Chao, Phys. Rev. **36**, 1519 (1930); G. T. P. Tarrant, Proc. Roy. Soc. **128A**, 345 (1930).

[4] L. A. Delsasso, W. A. Fowler, and C. C. Lauritsen, Phys. Rev. **51**, 391 (1937).

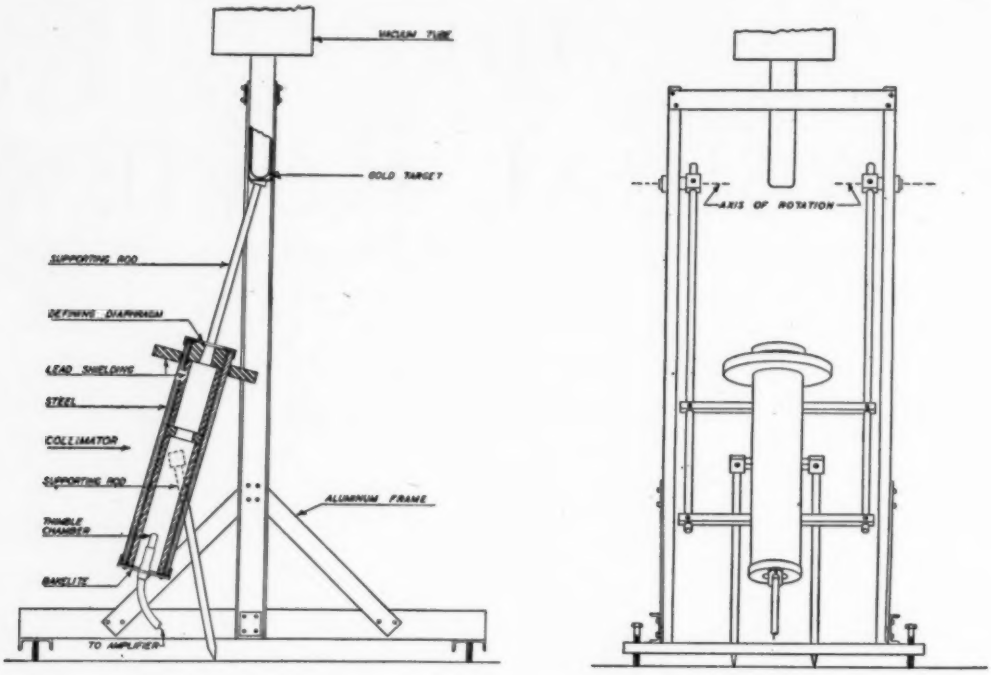

FIG. 1. General view of the x-ray target, collimator, and thimble chamber, and the structural frame supporting the collimator.

range the efficiency of production of x-rays, the angular distribution of the radiation from thin targets, and the absorption coefficients in various materials have been measured with considerable precision. In the region between 0.5 and 1.0 Mv, where characteristic radiation no longer plays an important part, much remains to be done. The variation of the intensity of heavily-filtered radiation with angle has been determined at 0.5 Mv.[5] The dependence of intensity on thickness in various absorbers has been measured for the heterogeneous radiation produced at voltages up to 1.0 Mv.[6]

II. APPARATUS

The general scheme is to make intensity measurements in a severely collimated x-ray beam with an air-equivalent thimble chamber. The collimation serves to define the angle with respect to the direction of the original electron beam, to exclude x-rays scattered in the absorber, and to exclude the background of x-rays scattered from various parts of the room. By varying the direction of the axis of the collimator with the x-ray target as a center, the intensity or the absorption coefficient of the radiation can be measured as a function of angle. Figure 1 shows the x-ray target, the collimator, the thimble chamber, and the aluminum structural frame which supports the collimator.

The collimator was subjected to two performance tests. Absorption measurements in lead for thicknesses up to 10 cm were made with 2.5- and 1.3-cm diameter defining diaphragms. The resulting curves (I/I_0 *versus* absorber thickness) were identical, showing that the 2.5-cm diameter diaphragm provided sufficient collimation. As the thickness of lead absorber was further increased to 15 cm the x-ray intensity at the thimble chamber continued to decrease exponentially, which indicated that the background radiation inside the collimator was negligible.

The thimble chamber was adopted for the measurement of x-ray intensity on the basis of considerable previous experimental[7] and theo-

[5] K. E. Corrigan and B. Cassen, Am. J. Roent. and Rad. Therapy **37**, 811 (1937).

[6] R. Phillips and G. S. Innes, Brit. J. Radiol. **11**, 498 (1938); J. C. Hudson, Radiol. **32**, 530 (1939). Also Folsom, Stone, Rose, Bouwers, and Hermann and Jaeger.

[7] O. Glasser and L. Rovner, Am. J. Roent. and Rad. Therapy **36**, 94 (1936); L. S. Taylor, G. Singer, and A. L. Charlton, Am. J. Roent. and Rad. Therapy **41**, 256 (1939); and others.

retical[8,9] work. This work has shown that the thimble chamber is the only practicable method for measuring radiation above 0.4 Mv, that measurements made by different observers with chambers of different geometries and different "air-equivalent" wall materials are accurately comparable, and that the corrections for wall effect necessary to reduce reading to roentgens, according to the accepted definition, are small and calculable.[8] An "air-equivalent" wall material is one in which the x-ray beam has the same equilibrium complement of electrons as it has in air. Theoretically the wall thickness should be at least as great as the range of secondary electrons in the material[9] if the chamber is to be used in a collimated beam, but experimentally the wall thickness can be somewhat less than this. In the case of carbon which is the element most nearly air-equivalent, the correction factor to obtain equivalent roentgens from the actual readings is 1.023 in the case of gamma-rays from radium in equilibrium with its decay products, and is 1.027 in the case of the total radiation at 0.6 Mv. Thus the x-ray intensity measured by a carbon-wall thimble chamber in the energy region from 0.6 to 2.5 Mv may be written $r=1.025(I/V)$ roentgens per min. where I=ionization current (stat-coulombs per min.) and V=volume of chamber (cc).

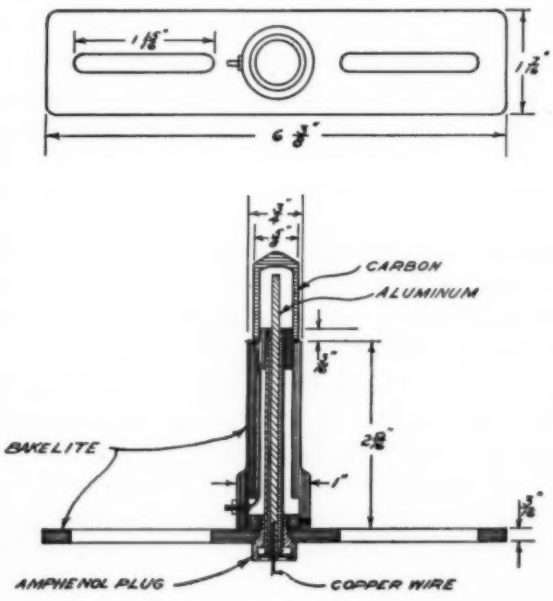

FIG. 2. Detailed view of the carbon-walled thimble chamber with its mounting strap.

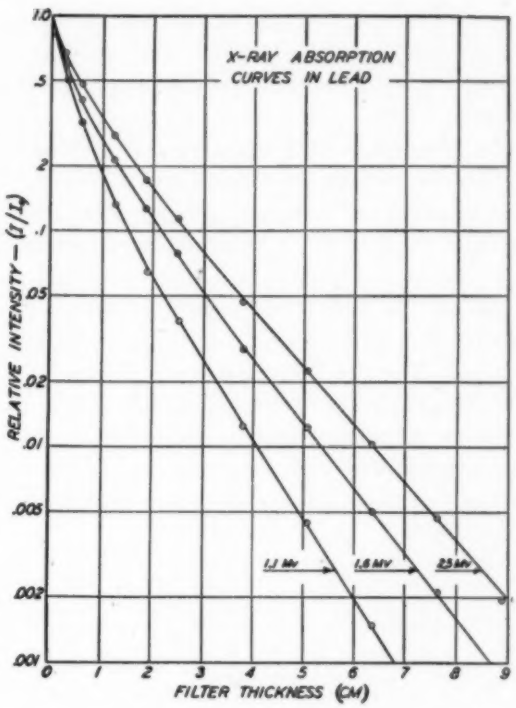

FIG. 3. Absorption curves in lead for the radiation produced at various voltages.

The thimble chamber used in these experiments is shown in cross section in Fig. 2, with a mounting strap for fastening the chamber to the lower end of the collimator. The volume of the chamber is 1.94 cc and the wall thickness is 2.4 mm on the sides. High voltage is applied to the carbon thimble by means of a wire leading to the side binding post. Ionization current is collected on the central aluminum wire and conducted to an amplifier. An aluminum tube connecting to the cable shield acts as a guard ring to reduce the effective leakage current. Saturation voltage for high x-ray intensities proved to be 270 v. This thimble chamber was subjected to several performance tests which proved it to be entirely satisfactory for the measurements involved.

The ionization produced in the carbon thimble chamber was measured with a current amplifier rather than by a condenser discharge method, in order to have a continuous reading of x-ray intensity and to avoid the necessity of maintaining constant conditions. The sensitivity ratios for the various ranges were measured with a constant

[8] G. C. Laurence, Can. J. Research **15A**, 67 (1937).
[9] L. H. Gray, Proc. Roy. Soc. **156A**, 578 (1936).

x-ray beam under actual conditions of use and were found to agree within the accuracy of reading with the ratios calculated from the input resistor values.

The construction of the target is indicated in Fig. 1. It is evident that much greater absorption must be expected in the neighborhood of 90° and that this effect must be considered in connection with angular distribution curves. Gold was chosen as the target material because it is the element of largest atomic number practicable for such use. The thickness used was required both for strength and for stopping the high speed electrons. An earlier target[1] of lead electroplated onto copper was not satisfactory because of a tendency of the lead to evaporate away from the target spot.

For the absorption coefficient measurements the absorber consisted of disks of the pure material 10 cm in diameter and each of such thickness as to reduce the intensity by 30 to 50 percent. In the case of water, distilled water of known temperature was used in a 15-cm diameter glass cylinder. The total thickness of absorber, in addition to a lead pre-filter, varied from 10 cm in the case of lead to 30 cm in the case of water.

III. MEASUREMENT OF ABSORPTION COEFFICIENTS

For the measurement of absorption coefficients, thimble chamber intensity readings in the collimated beam were taken as a function of thickness of absorber placed above the defining diaphragm. Comparable relative intensity readings were obtained by dividing each intensity reading by the corresponding electron current, averaging the results obtained with increasing and decreasing filter thickness, and dividing successive intensity values by the initial value. When such relative intensity (I/I_0) values are plotted against filter thickness on semi-logarithmic paper, the slope of the resulting curve provides a measure of the total mass absorption coefficient, $\mu_m = \ln (I_0/I)/\rho x$. Curvature in the initial part of these curves is an indication of a decreasing absorption coefficient because of the selective absorption of the softer components in the heterogeneous radiation. After sufficient filter has been used the wave-length distribution of the radiation in the beam becomes so narrow that the corresponding absorption coefficient is approximately constant. The resulting straight line portion of the logarithmic curve permits an accurate determination of the final constant value of absorption coefficient.

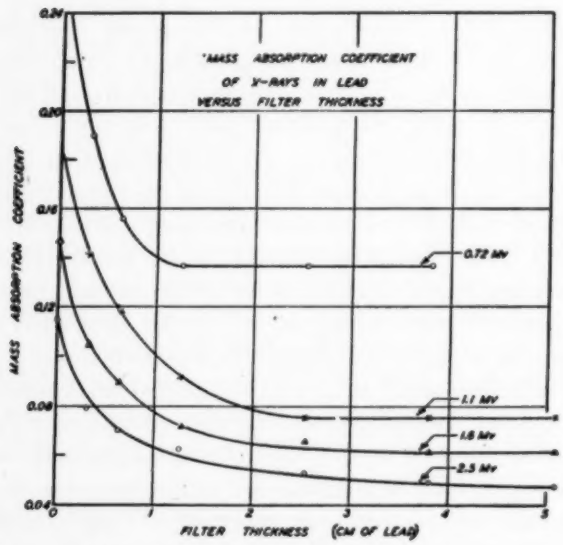

FIG. 4. Mass absorption coefficient in lead *versus* filter thickness for the radiation produced at various voltages.

Typical absorption curves are shown in Fig. 3, which gives the absorption in lead of the radiation produced at various voltages. It appears that the absorber thickness necessary for establishing the equilibrium condition increases with voltage, but that the final slope is constant over a wide range of absorption. This is more evident in Fig. 4, in which the mass absorption coefficient obtained from the slope of the logarithmic curves is plotted against filter thickness for the radiation produced at several voltages. From Fig. 4 we see that the initial absorption coefficient at each voltage is somewhat more than twice the final absorption coefficient and that the filter thickness necessary for obtaining the equilibrium condition is roughly proportional to the voltage.

In Fig. 5 is given the variation with voltage of the final value of absorption coefficient for several absorbing materials. The curves are drawn through the experimental points without regard to theory. In the case of absorbers other than lead a sufficient thickness of lead pre-filter was used to establish approximately the equilibrium condition.

The data presented in Fig. 5 represent the summary of approximately 1600 intensity readings on 83 absorption curves. For each absorption

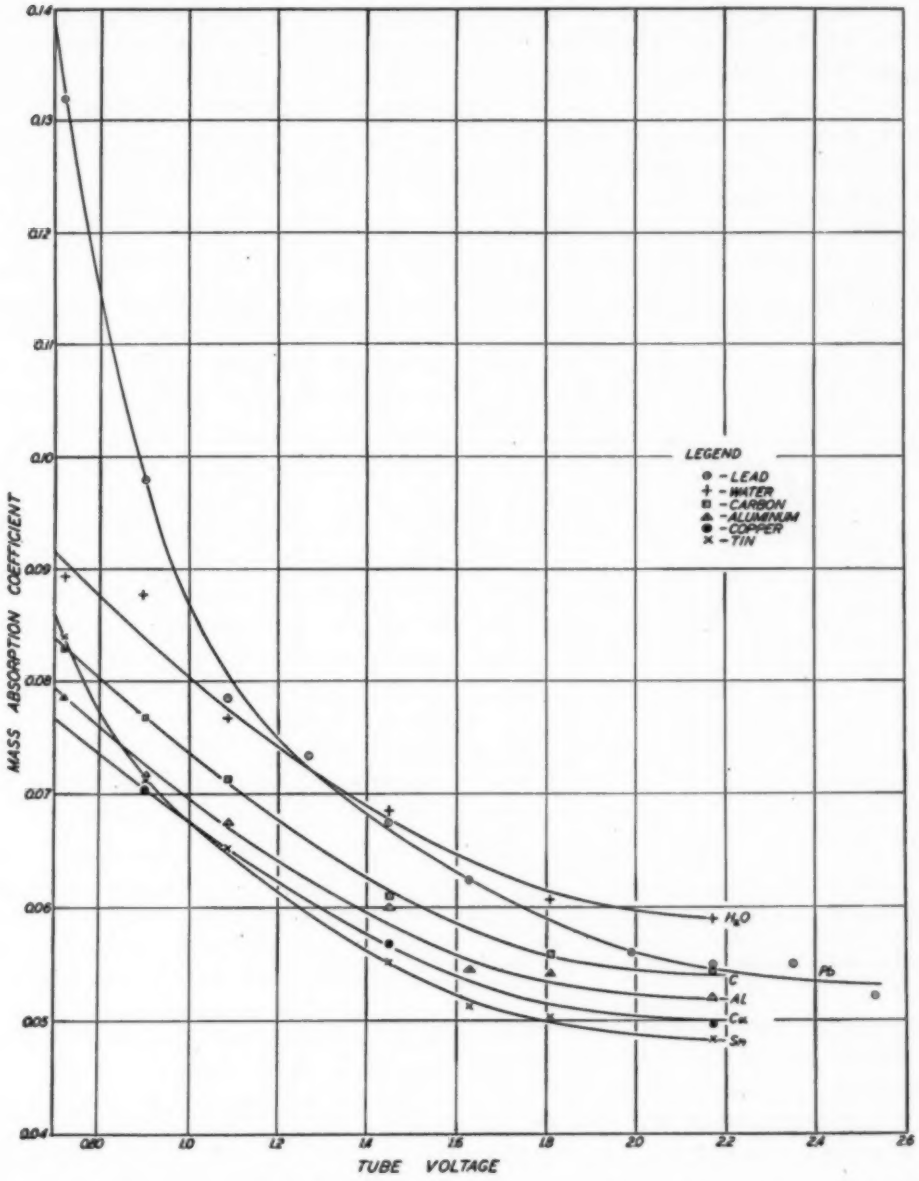

FIG. 5. Experimental values for the mass absorption coefficient in several materials of heavily filtered heterogeneous radiation plotted as a function of the tube voltage.

curve an estimated probable error in the slope can be obtained by considering the spread in the curves which might reasonably be used to represent the points. Such estimated probable errors for individual curves (i.e., for individual determinations of absorption coefficient) ranged from 0.3 percent to 4 percent with an average value of 1.2 percent.

It is evident from Fig. 5 that in four of the curves (H_2O, C, Al, and Cu) the same type of absorption is present, whereas in two of the curves (Pb and Sn) there is an additional absorption which becomes important at low voltage. In the higher part of the voltage range the order of increasing mass absorption coefficients (excepting Pb) is Sn, Cu, Al, C, and H_2O. These results are in agreement with theory in which the total absorption of energy from the x-ray beam is considered to be due to true absorption and scattering by free electrons (Compton absorption and

scattering),[10] absorption by bound electrons (photoelectric absorption),[11] and absorption due to the production of positron-electron pairs (pair production).[12]

Photoelectric absorption and pair production are appreciable in this voltage range only for lead and tin. Photoelectric absorption explains the steeper rise in the lead and tin curves of Fig. 5 at the low voltage end, and is appreciable throughout the entire voltage range in the case of lead.

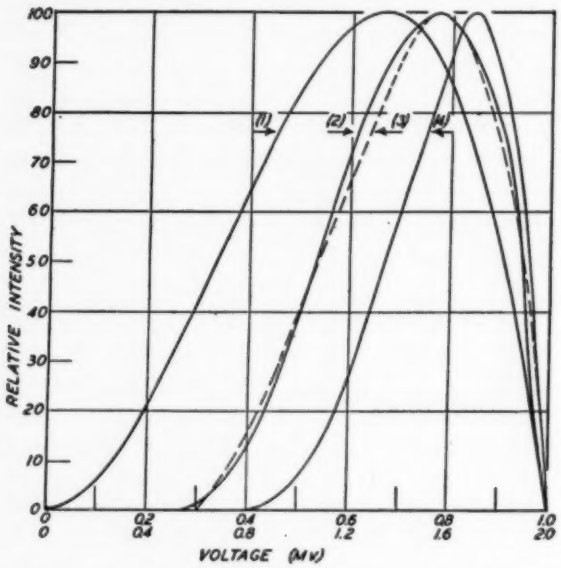

FIG. 6. Distribution in voltage of unfiltered (1) and filtered (2, 3, 4) radiation assuming Kramers' law and accepted values for lead absorption coefficients.

With the exception of lead, the absorption coefficient in the middle part of the voltage range is almost entirely due to Compton effect and therefore should be proportional to the number of electrons per gram of absorber, as is found experimentally to be the case. At the high voltage end, pair production[13] is responsible for about 12 percent of the absorption in lead and 7 percent in tin.

It appears therefore that the measured absorption coefficients for heterogeneous radiation are in general qualitative agreement with accepted theory for homogeneous radiation. In order to make a quantitative comparison, it is necessary to know the distribution in wavelength of the heterogeneous radiation. Kramers' theory[14] yields the relation

$$I_V = \text{constant} \cdot V^2(V_0 - V)$$

where V_0 = tube voltage. This relation was used to obtain curve (1) in Fig. 6 for the distribution in voltage of the unfiltered radiation produced either at 1.0 or 2.0 Mv. The change in the shape of this curve as the result of lead filtration can be calculated by using accepted values for the absorption coefficient of homogeneous radiation in lead at the different voltages. Curves (2) and (3) were obtained by assuming the thicknesses of lead pre-filter actually used at 1.0 and 2.0 Mv, respectively, in measuring the absorption coefficients of other materials. From these curves it appears that the distribution of the radiation after pre-filtering was very similar in the two cases. Curve (4) gives the distribution of the radiation produced at 2.0 Mv and filtered through 11.5 cm of lead. From curves (1), (3), and (4), together with accepted values for the absorption coefficient of homogeneous radiation in a given material, it is possible to calculate the absorption coefficient in that material of the heterogeneous radiation produced at 2.0 Mv and filtered through 0, 3.8, and 11.5 cm of lead. The results of these calculations for lead and aluminum absorbers are compared with the experimental values in Table I.

These calculations show the same effect of lead filter on heterogeneous radiation as was observed experimentally, i.e., that the initial high absorption coefficient *in lead* is reduced to roughly half-value and then becomes approximately constant

TABLE I. Calculated and measured values for the mass absorption coefficient in lead and aluminum of the heterogeneous radiation produced at 2.0 Mv after various amounts of lead filter.

Thickness of lead filter (cm)	Mass absorption coefficient (cm^2/g) Lead		Aluminum	
	Calculated	Measured	Calculated	Measured
0	0.090		0.059	
3.8	0.054	0.056	0.052	0.052
11.5	0.050		0.048	

[10] O. Klein and Y. Nishina, Zeits. f. Physik **52**, 853 (1929).
[11] H. R. Hulme, J. McDougall, R. A. Buckingham, and R. H. Fowler, Proc. Roy. Soc. **146A**, 83 (1934). M. T. Jones, Phys. Rev. **50**, 110 (1936).
[12] H. Bethe and W. Heitler, Proc. Roy. Soc. **146A**, 83 (1934).
[13] For the calculation of absorption by pair production, we are indebted to Dr. R. D. Evans, "Introduction to the Atomic Nucleus," M.I.T. course notes.
[14] H. A. Kramers, Phil. Mag. **46**, 863 (1923).

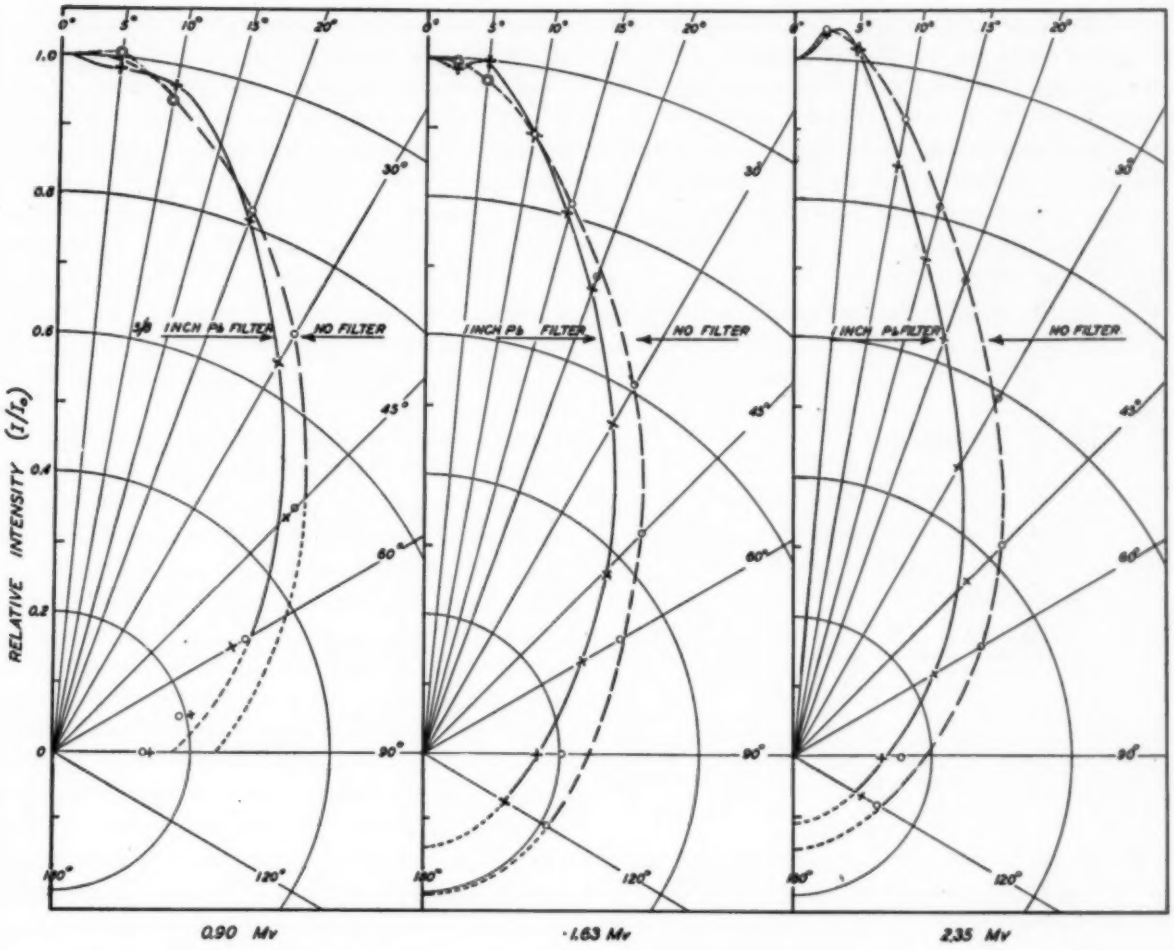

FIG. 7. Variation of intensity with angle for the unfiltered and filtered radiation at three values of tube voltage.

as the filter thickness is further increased. The absorption coefficient at small filter thicknesses could not be determined accurately because it changed so rapidly with added absorber. There was not sufficient intensity left after 11.5 cm of lead filter to permit an accurate measurement of the absorption coefficient of the resulting radiation. However, for lead thicknesses between 3.8 cm and 11.5 cm no appreciable change in absorption coefficient was observed. The calculated and measured values for both lead and aluminum absorbers after 3.8 cm of lead filter are in very satisfactory agreement. This agreement tends to confirm the values for the absorption coefficient of homogeneous radiation and to indicate that the distribution function given by Kramers' theory represents a reasonable approximation in spite of its theoretical limitations. Furthermore it tends to justify the method outlined above for calculating the absorption coefficient of the heterogeneous radiation in a severely collimated beam of x-rays produced at a given tube voltage and subjected to a given amount of filtration.

IV. MEASUREMENT OF ANGULAR DISTRIBUTION

To measure the x-ray intensity as a function of angle with respect to the forward direction of the electron beam, the collimator was pivoted in its support to swing about the x-ray target as a center. The thimble chamber in the collimated beam then provides an approximately true measure of the intensity as a function of angle. Having the collimated beam also permits insertion of absorbing material into the beam to obtain a measure of the quality of the radiation as a function of angle.

With the tube voltage held constant the collimator was set at various angles, and the intensity and electron current were recorded. The intensity readings were divided by the corresponding electron currents and by the specific intensity in the forward direction to obtain comparable relative intensity readings. This procedure was followed with no filter and with a heavy lead filter for three values of tube voltage.

The results of the angular intensity measurements are presented in Fig. 7. These curves show the strong predominance of the radiation in the forward direction. The intensity ratio between 0° and 90° varies from 4.2 for the unfiltered radiation at 0.90 Mv to 7.3 for the filtered radiation at 2.35 Mv. No attempt was made to pass these curves through the 90° experimental points because of the excessive absorption introduced by the target in that direction.

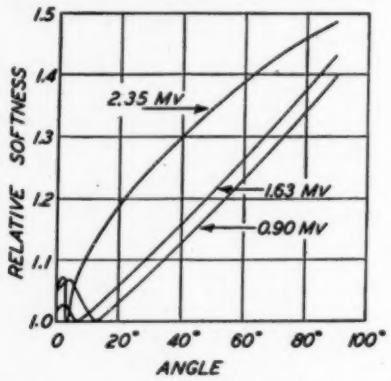

FIG. 8. Relative softness of the radiation produced at several voltages as a function of angle, where relative softness is defined as the ratio of unfiltered to filtered intensity.

In Fig. 7, the unfiltered and filtered relative intensity values are compared for three values of tube voltage. This comparison shows that the radiation is considerably softer at larger angles. The softening of the unfiltered radiation with increasing angle is an effect which increases with voltage, as is shown by Fig. 8 in which the ratio of unfiltered to filtered relative intensities is plotted against angle for three values of tube voltage. The ratios have been adjusted to unity at the angle of hardest radiation, rather than at 0°. These curves of an arbitrarily defined quantity are presented primarily because of the way in which they emphasize the angle of maximum hardness of the radiation.

A detailed examination of the curves of Fig. 7 at small angles reveals an interesting fine structure. There is a maximum in the curves which becomes more pronounced and which moves in to smaller angles as the voltage is increased. This effect is so small at 0.90 and 1.63 Mv that the small angle points on these curves were taken with great care. The additional maximum at 0° on the 0.90- and 1.63-Mv curves can be obtained by combining two slightly overlapping angular distribution patterns of conventional shape, and is therefore assumed to be of no especial theoretical interest.

The angular positions of the intensity maximum at the several voltages are given in Table II with an estimated probable error of 0.5°. Examination of the curves shows that the maximum moves in to smaller angles as the voltage is increased, but for a given voltage the harder components of the radiation have their maxima at larger angles. If these curves are thought of as the combination of two slightly overlapping angular distribution patterns on opposite sides of the axis, resolving the lobes would increase appreciably the angle of the maximum.

The dependence of x-ray quality on angle for the heavily filtered radiation from a thick target was obtained by measuring the final value of the mass absorption coefficient in lead at a number of angles with a fixed tube voltage. The dependence on angle of this absorption coefficient is given in Fig. 9 for the radiation produced at 1.09 and at 1.63 Mv. A pronounced dip in the curves at about 7° is followed by a regular rise as the angle is further increased. These curves illustrate the advantage of working in the forward direction rather than at 90° when penetrating radiation is required, and the additional advantage of working at a small angle from the forward direction if a small portal is used.

TABLE II. Angular position of the intensity maximum at several tube voltages.

Voltage	Positions of the intensity maximum: Unfiltered radiation	Filtered radiation	Sommerfeld theory	Positions of hardness maximum (Fig. 8)
0.90		9.0°	13°	13°
1.63	3.8°	4.5°	8°	7°
2.35	2.8°	3.3°	6°	3.7°

There is no available theory strictly applicable to the problem of calculating the angular distribution of the radiation produced in a thick target of high atomic number at high voltage. This is not surprising in view of the extreme difficulties imposed by these conditions. Sommerfeld's classical theory[15] is relativistic but assumes a thin target and complete stopping of the electron without change in direction. His wave mechanical theory[16] is non-relativistic and therefore not applicable. Later theories[12,17] are too complicated to justify calculation in that they are approximations for elements as heavy as gold. In spite of its limitations, therefore, Sommerfeld's classical theory has been used to calculate the positions of the intensity maximum in the angular distribution curves (last column, Table II). Actually the angular position of the hardest radiation (minimum in Fig. 8) is in better agreement with Sommerfeld's predicted angle than is the position of the intensity maximum. In general, theory predicts that the maximum will move toward smaller angles and will become more pronounced as the voltage is increased, but that for a given voltage the harder components of the radiation will have their maxima at larger angles. In these respects theory and experiment are in qualitative agreement.

V. EFFICIENCY OF X-RAY PRODUCTION

In all the measurements described previously the results have not depended on the absolute calibration of the thimble chamber, and not sensitively upon the variation of this calibration with x-ray quality. The results presented in Fig. 10, however, depend on the carbon thimble chamber for the absolute measurement of intensity in r-units. The x-ray intensity in the forward direction is plotted on double logarithmic paper as a function of voltage for the unfiltered radiation (except for the 2.3-mm lead equivalent thickness introduced by the target) and for radiation filtered through 2.5 cm of lead. The unfiltered radiation increases approximately as the third power of the tube voltage. The filtered radiation shows a more uniform increase as the 4.7 power of the voltage. This emphasizes the importance of having high voltage for producing radiation which is to be used through considerable absorbing material.

From a consideration of the x-ray intensity available at high voltage and the low value of the absorption coefficient after moderate filtration, it is evident that radiographical examination of very thick specimens, such as heavy steel castings, becomes feasible. If the target-to-specimen distance is made large, sufficient pre-filter is used, and stray radiation is carefully eliminated, good resolution should be obtained for thickness as great as 12 in. of steel.

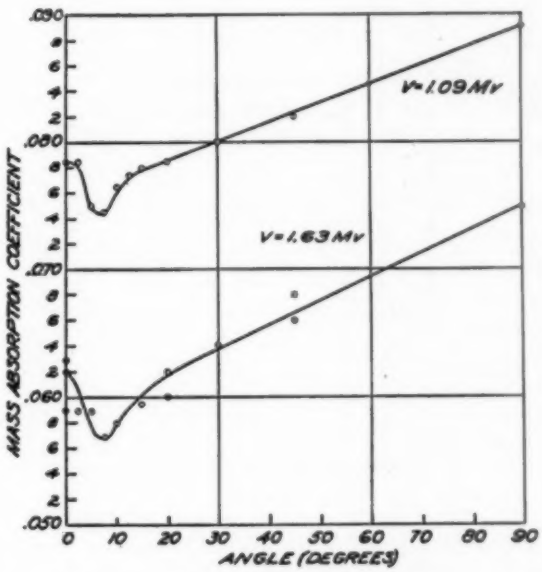

FIG. 9. Dependence on angle of the final value of the mass absorption coefficient in lead for the radiation produced at 1.09 and 1.63 Mv.

The efficiency of x-ray production may be defined as the ratio of the power radiated from the target as x-rays to the power received at the target as the result of electron bombardment. The power radiated as x-rays at a given tube voltage and beam current can be determined from a knowledge of the x-ray intensity (in roentgens) in all directions from the target, provided that the proper correction be made for true absorption in the target.

The rate at which energy passes through unit area at a distance r from the target and at an angle θ with respect to the forward direction of the beam is given in terms of the reading of an

[15] A. Sommerfeld, Physik. Zeits. **10**, 969 (1919).
[16] A. Sommerfeld, Ann. d. Physik **11**, 257 (1931).
[17] W. Heitler and F. Sauter, Nature **132**, 892 (1933); F. Sauter, Ann. d. Physik **20**, 404 (1934).

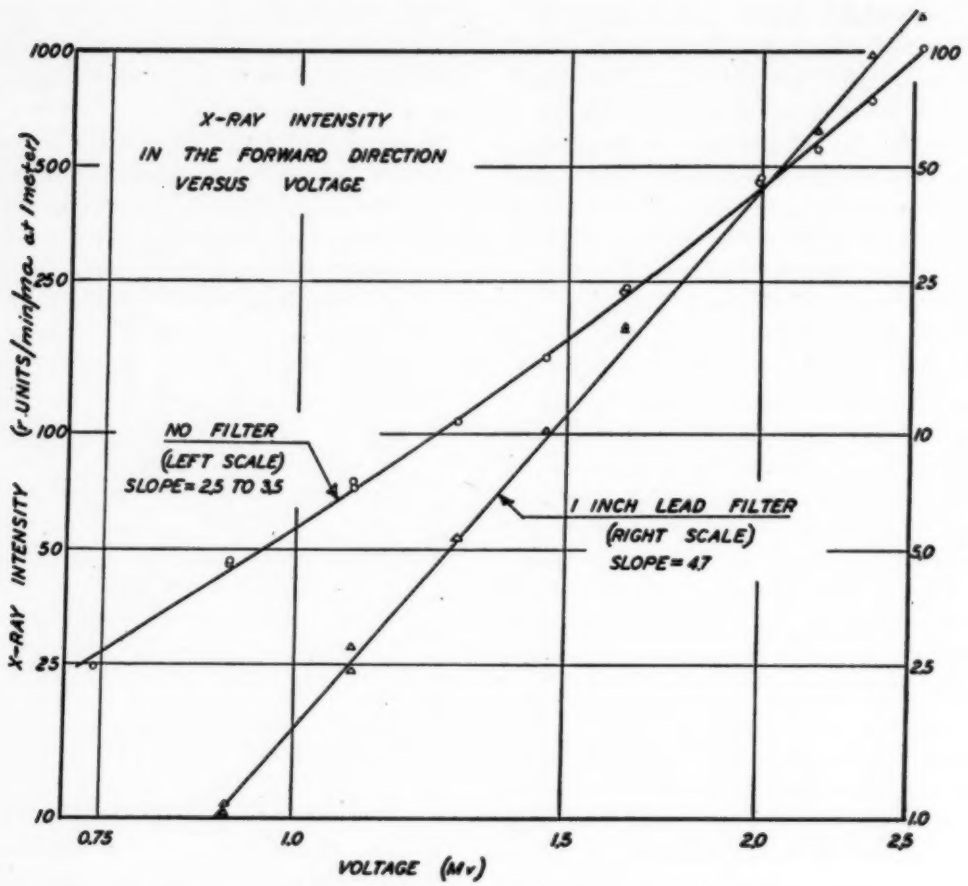

FIG. 10. Dependence of absolute intensity in the forward direction on voltage for unfiltered and filtered radiation.

air-wall thimble chamber at that point by

$$P_{r,\theta}=\int_r^\infty I dr = I_{r,\theta}/\mu \text{ roentgen cm/min.}$$

where μ is the linear coefficient for true absorption in air of the heterogeneous radiation incident upon the thimble chamber. If we accept a value of 45.5 ev per ion pair as the energy required for x-ray ionization in air,[19] we may write this expression in terms of a more conventional unit for radiation density

$$P_{r,\theta}=2.53\times10^{-10} I_{r,\theta}/\mu \text{ watt/cm}^2.$$

The total rate at which energy passes through a sphere of radius r is

$$P_r=1.59\times10^{-9} r^2 \int_0^\pi (I_{r,\theta}/\mu)\sin\theta d\theta \text{ watt.}$$

If we introduce I_f, the x-ray intensity in the

TABLE III. Efficiency of x-ray production: a comparison of experiment with theory.

Voltage (Mv)	Experiment I_f	$\int I_\theta \sin\theta d\theta$	μ	Target Correction Factor	η	Theory η
2.35	750	0.52	3.08×10^{-5}	1.22	10.4%	8.3%
1.63	240	0.61	3.30×10^{-5}	1.35	5.8	5.6
0.90	44	0.68	3.48×10^{-5}	2.00	3.0	3.4

[19] The generally accepted value of 32 ev per ion pair is apparently based on H. Geiger's early value of 33 ev obtained from alpha-particle ionization experiments (Proc. Roy. Soc. **82A**, 486 (1909)). The value of 45.5±1.0 ev obtained from the excellent work of J. F. Lehmann and T. H. Osgood on ionization in air by electrons in the energy range 200 to 1000 ev (Proc. Roy. Soc. **115A**, 609 (1927)) more properly applies to the case of x-ray ionization. We are indebted to Dr. M. S. Livingston, who brought these references to our attention as well as his own confirming calculation based on ionization by radium gamma-rays.

forward direction expressed in roentgens per min. and milliampere at one meter from the target and I_θ, the intensity at angle θ relative to that in the forward direction, and if we recognize the fact that the coefficient for true absorption in air does not depend appreciably on angle, we may write

$$P_1 = 1.59 \times 10^{-5}(I_f/\mu)\int_0^\pi I_\theta \sin\theta d\theta \text{ watt/ma.}$$

Then the efficiency of x-ray production is

$$\eta = 1.59(I_f/\mu V)\int_0^\pi I_\theta \sin\theta d\theta \text{ percent}$$

where V is the tube drop in volts.

Experimental data already presented make it possible to calculate the efficiency at three voltages: 2.35, 1.63, and 0.90 Mv. Values of I_f are obtained from Fig. 10 and values of the integral are calculated from the dashed curves of Fig. 7. The values of μ, the linear coefficient for true absorption in air of the heterogeneous radiation incident upon the thimble chamber, were calculated as weighted averages from the corresponding coefficients for homogeneous radiation. From curves similar to those shown in Fig. 6 it is possible to obtain directly factors to correct for true absorption of x-ray power in the target. The ratio of the area under the Kramers' distribution to that under the reduced distribution gives the factor by which the power has been reduced in passage through the target. The correction is not serious except at the lowest voltage. Values of I_f, the integral, μ, the correction factor, and η are presented in Table III.

The theoretical values for the efficiency given in the last column were computed from curves calculated from Bethe and Heitler's theory by Arcimovic and Chramov.[20] In view of limitations in the theory when applied to targets of high atomic number, the agreement between theory and experiment throughout this voltage range may be considered quite satisfactory.

The writers are indebted to Dr. G. G. Harvey for helpful discussions and to Mr. Zigmond Wilchinsky, Mr. W. B. Nowak, and Mr. Howard Rowland for much capable assistance in making measurements and calculations. The research was supported in part by grants from Research Corporation and the Carnegie Corporation of New York.

[20] L. A. Arcimovic and V. A. Chramov, Comptes Rendus Acad. Sci. U.S.S.R., **18**, 415 (1938).

Errata: Quantization of Molecules, Inter- and Intramolecular Forces

[Phys. Rev. **63**, 309 (1943)]

KASIMIR FAJANS AND THEODORE BERLIN
Department of Chemistry, University of Michigan, Ann Arbor, Michigan

THE sentence on page 310, left column, lines 8–6 from the bottom should read: "In Fig. 1A, two Li^+ cores are placed at the internuclear distance 0.74A of H_2 ($n=I$)."

On page 311, left column, line 7 from the bottom should have $n=3$ instead of $n=III$.

Erratum: The Carbon Arc in Oxygen for the Spectrochemical Determination of Potassium

[Phys. Rev. **63**, 322 (1943)]

L. T. STEADMAN
Department of Radiology, The University of Rochester, School of Medicine and Dentistry, Rochester, New York

THE last paragraph, beginning line 8 from the bottom, should read: "To the cathode is added 0.01 ml of serum, which amount in the human normally contains 33.0 gamma (micrograms) Na, 2.0 gamma K, 1.0 gamma Ca, 0.27 gamma Mg, and 1.3 gamma P. Also, 2.5 gamma Rb is added as the internal standard for K and 100 gamma Cd as the internal standard for all the other elements. The spectrum lines measured are Na 2680.3A, K 4044.1A, Ca 3006.9A, Mg 2783.0A, P 2535.6A, Rb 4201.8A, and Cd 2677.6A."

PHYSICAL REVIEW VOLUME 63, NUMBERS 11 AND 12 JUNE 1 AND 15, 1943

On the Theory of a Mixed Pseudoscalar and a Vector Meson Field

W. PAULI AND S. KUSAKA
The Institute for Advanced Study, Princeton, New Jersey
(Received March 24, 1943)

Schwinger's modification of the Møller-Rosenfeld theory of nuclear forces based on a mixture of pseudoscalar and vector meson field is investigated in the strong coupling theory. The isobar separation turns out to be $\frac{1}{4}$ of its value in the pseudoscalar theory. The interaction energy between two nucleons is calculated, and in the most interesting case of the symmetrical theory, it is the same as the corresponding expression in the weak coupling theory with the spin and isotopic spin vectors replaced by the $\mathbf{e}^{\alpha}$ vectors of Pauli and Dancoff. A classification of the states of the two-nucleon system is made, and the lowest state for the deuteron is found to be the triplet state. An estimate is made for the values of the constants involved, and we find that a suitable choice of the coupling constant and the masses of the mesons can be made in such a way that the binding energy and the quadrupole moment of the deuteron agree with the observed values, and such that the conditions for small source (compared to the Compton wavelengths of the mesons) and for small effect of the higher spin states on the ground state are fulfilled. However the theory gives for the magnetic moment of the deuteron a value only a few percent of the observed value, and according to this theory highly charged nuclei would be unstable. We therefore conclude that the strong coupling theory, based on the assumption of an extended source, should be abandoned in favor of a weak coupling theory, based on a point source with the singularities of its field eliminated by means of a subtraction formalism.

I. INTRODUCTION

THE usual theories of nuclear forces derived from one type of meson field give rise, both in the weak and strong coupling approximations, to tensor forces with inadmissible r^{-3} singularity for small r, which consequently has to be cut off at a certain arbitrary radius. Møller and Rosenfeld[1] showed that the singularity can be removed by taking a mixture of pseudoscalar and vector meson fields with the same coupling constant. They, however, also took the masses of the two types of meson equal, and found that the tensor force vanished in the first approximation. Schwinger[2] then pointed out that the tensor force can be retained with only an admissible r^{-1} dependence at small distances if the masses are taken unequal, and that the right sign for the quadrupole moment is obtained if the vector meson has the larger mass. This is in agreement with the hypothesis that the vector meson is highly unstable and that it is responsible for the β-decay in the nucleus.

It may be argued that the introduction of the vector meson field is just another way of removing the inadmissible singularities by an arbitrary constant, and in a much more complicated way at that. The introduction of a new particle is admittedly undesirable, but we feel that further investigation in this direction is justified for the reason that this may be a first step in the direction of a more far-reaching theory in which the vector meson enters, not as a new independent particle, but as an excited state of the pseudoscalar meson.

We have investigated in this paper the mixed meson theory in the strong coupling approximation. The calculations of Section II for the isobar separation follows closely the development for the pseudoscalar meson given by Pauli and Dancoff.[3] The theory of nuclear forces in the strong coupling approximation has been developed by Serber and Dancoff[4] who treated the charged scalar and the neutral pseudoscalar meson fields, and the calculation in Section III follows their procedure. Hence the computations in these sections are not given in detail. However we wish to point out that in contrast to Serber and Dancoff, we do not consider the nucleons to be at rest, and consequently we do not discuss here the small oscillations around the minimum of the potential energy which occurs for sufficiently small separation of the nucleons. The

[1] C. Møller and L. Rosenfeld, K. Danske vidensk. Selsk. **17** (1940).
[2] J. Schwinger, Phys. Rev. **61**, 387A (1942).
[3] W. Pauli and S. M. Dancoff, Phys. Rev. **62**, 85 (1942). This paper will henceforth be quoted as P-D.
[4] R. Serber and S. M. Dancoff, Phys. Rev. **63**, 143 (1943). This paper will henceforth be quoted as S-D. We wish to thank these authors for letting us see their calculations before publication.

results of these sections are applied in Sections IV and V to the deuteron and the heavy nuclei, respectively.

II. ISOBAR SEPARATION

We describe the pseudoscalar part by the real quantities $\varphi^\alpha(x)$ and the vector part by $\psi_i^\alpha(x)$, where the subscript i denotes the components in the ordinary space and takes the values 1, 2, 3. The superscript α in both cases denotes the components in the isotopic spin space. In the symmetrical theory it takes the three values 1, 2, 3; in the charged theory the values 1, 2; and in the neutral theory only the value 3. In the following we do not restrict the values which α may assume so that the results for these three types of theories may be obtained by making suitable restrictions on the values for α. However, unless otherwise stated, we restrict our attention to the most interesting case of the symmetrical theory. The Hamiltonian of the field and its interaction with a nucleon is given by

$$\begin{aligned} H=&\tfrac{1}{2}\sum_\alpha\int\{(\pi^\alpha)^2+(\nabla\varphi^\alpha)^2+\kappa^2(\varphi^\alpha)^2\}dV \\ &+\tfrac{1}{2}\sum_{\alpha,i}\int\{(\omega_i^\alpha)^2+(\nabla\psi_i^\alpha)^2+\mu^2(\psi_i^\alpha)^2\}dV \\ &-(4\pi)^{\frac{1}{2}}\sum_{\alpha,i,j}\int\left\{f\frac{\partial\varphi^\alpha}{\partial x_i}\sigma_i\right. \\ &\left.+\frac{g}{2}\left(\frac{\partial\psi_j^\alpha}{\partial x_i}-\frac{\partial\psi_i^\alpha}{\partial x_j}\right)\sigma_{ij}\right\}\tau^\alpha U(x)dV, \end{aligned} \tag{1}$$

where π^α and ω_i^α are the momenta conjugate to φ^α and ψ_i^α, respectively; κ and μ are the rest masses of the pseudoscalar and the vector meson, respectively (we are using natural units where $\hbar=c=1$); σ_i and τ^α are the spin and isotopic spin matrices, respectively, with $\sigma_{ij}=-\sigma_{ji}=\sigma_k$ if i, j, k are cyclic permutations of 1, 2, 3; and f and g are coupling constants for the pseudoscalar and vector field, respectively.[5] For the time being we do not make the assumption $f=g$. $U(x)$ is the source function of the nucleon which we assume to be spherically symmetrical and normalized according to

$$\int U(x)dV=1. \tag{2}$$

It determines a radius a of the nucleon

$$\frac{1}{a}=\int\int\frac{U(x)U(x')}{R}dVdV' \tag{3}$$

where $R=|\mathbf{x}-\mathbf{x}'|$.

As in P-D, we split the fields into two parts and write

$$\begin{aligned} \varphi_i^{0\alpha}&=-(4\pi)^{\frac{1}{2}}\int\frac{\partial\varphi^\alpha}{\partial x_i}U(x)dV=(4\pi)^{\frac{1}{2}}\int\varphi^\alpha\frac{\partial U}{\partial x_i}dV, \\ \psi_{ij}^{0\alpha}&=(2\pi)^{\frac{1}{2}}\int\left\{\frac{\partial\psi_j^\alpha}{\partial x_i}-\frac{\partial\psi_i^\alpha}{\partial x_j}\right\}U(x)dV \\ &=(2\pi)^{\frac{1}{2}}\int\left\{\psi_i^\alpha\frac{\partial U}{\partial x_j}-\psi_j^\alpha\frac{\partial U}{\partial x_i}\right\}dV, \end{aligned} \tag{4}$$

$$\begin{aligned} \int\varphi'^\alpha\frac{\partial U}{\partial x_i}dV&=0, \\ \int\left\{\psi_i'^\alpha\frac{\partial U}{\partial x_j}-\psi_j'^\alpha\frac{\partial U}{\partial x_i}\right\}dV&=0. \end{aligned} \tag{5}$$

$\psi_{ij}^{0\alpha}$ is antisymmetric in i and j, and we shall sometimes write $\psi_{ij}^{0\alpha}\equiv\psi_k^{0\alpha}$ for i, j, k cyclic. The source function generates the potentials $X(x)$ and $Y(x)$ according to

$$(-\Delta+\kappa^2)X=4\pi U,\quad(-\Delta+\mu^2)Y=4\pi U; \tag{6}$$

so that

$$\begin{aligned} X(x)&=\int U(x')(e^{-\kappa R}/R)dV', \\ Y(x)&=\int U(x')(e^{-\mu R}/R)dV', \end{aligned} \tag{7}$$

with $R=|\mathbf{x}-\mathbf{x}'|$. We define

$$I\delta_{ij}=\int\frac{\partial X}{\partial x_i}\frac{\partial U}{\partial x_j}dV, \tag{8}$$

and if we assume both κa and $\mu a\ll1$, we have

$$\int\frac{\partial X}{\partial x_i}\frac{\partial U}{\partial x_i}dV\backsimeq\int\frac{dY}{\partial x_i}\frac{\partial U}{\partial x_i}dV. \tag{9}$$

[5] In this paper we find it more convenient to use these constants which have the dimension of κ^{-1}. Thus our f is equal to $g/\sqrt{2}\kappa$ where g is the coupling constant for the pseudoscalar field used in P-D.

This approximation gives some formal, although unessential, simplification and we shall make use of it. We therefore write

$$\xi(x)=X(x)/I, \quad \eta(x)=Y(x)/I; \tag{10}$$

then

$$\int \frac{\partial \xi}{\partial x_i}\frac{\partial U}{\partial x_j}dV=\int \frac{\partial \eta}{\partial x_i}\frac{\partial U}{\partial x_j}=\delta_{ij}. \tag{11}$$

We thus obtain from (4) and (5)

$$\begin{aligned}\varphi^\alpha(x)&=(4\pi)^{-\frac{1}{2}}\sum_i \varphi_i^{0\alpha}\frac{\partial \xi(x)}{\partial x_i}+\varphi'^\alpha(x),\\ \psi_i{}^\alpha(x)&=(8\pi)^{-\frac{1}{2}}\sum_j \psi_{ij}^{0\alpha}\frac{\partial \eta(x)}{\partial x_j}+\psi_i'^\alpha(x).\end{aligned} \tag{12}$$

The corresponding decompositions of the momenta are given by

$$\begin{aligned}\pi_i^{0\alpha}&=(4\pi)^{-\frac{1}{2}}\int \pi^\alpha\frac{\partial \xi}{\partial x_i}dV,\\ \omega_{ij}^{0\alpha}&=(8\pi)^{-\frac{1}{2}}\int\left\{\omega_i{}^\alpha\frac{\partial \eta}{\partial x_j}-\omega_j{}^\alpha\frac{\partial \eta}{\partial x_i}\right\}dV,\end{aligned} \tag{13}$$

with $\omega_{ij}^{0\alpha}\equiv-\omega_{ji}^{0\alpha}\equiv\omega_k^{0\alpha}$ (i, j, k cyclic);

$$\begin{aligned}\int \pi'^\alpha\frac{\partial \xi}{\partial x_i}dV&=0,\\ \int\left\{\omega_i'^\alpha\frac{\partial \eta}{\partial x_j}-\omega_j'^\alpha\frac{\partial \eta}{\partial x_i}\right\}dV&=0;\end{aligned} \tag{14}$$

$$N\delta_{ij}=4\pi\int \frac{\partial U}{\partial x_i}\frac{\partial U}{\partial x_j}dV; \tag{15}$$

$$\begin{aligned}\pi^\alpha(x)&=(4\pi)^{\frac{1}{2}}\sum_i \pi_i^{0\alpha}\frac{\partial U(x)}{\partial x_i}+\pi'^\alpha(x),\\ \omega_i{}^\alpha(x)&=(2\pi)^{\frac{1}{2}}\sum_j \omega_{ij}^{0\alpha}\frac{\partial U(x)}{\partial x_j}+\omega_i'^\alpha(x).\end{aligned} \tag{16}$$

The commutation relations are

$$\begin{aligned}i[\pi_i^{0\alpha}, \varphi_j^{0\beta}]&=\delta_{\alpha\beta}\delta_{ij},\\ i[\omega_{ij}^{0\alpha}, \psi_{kl}^{0\beta}]&=\delta_{\alpha\beta}(\delta_{ik}\delta_{jl}-\delta_{il}\delta_{jk}).\end{aligned} \tag{17}$$

The Hamiltonian (1) becomes

$$\begin{aligned}H=&\frac{N}{2}\sum_{\alpha,i}\{(\pi_i^{0\alpha})^2+(\omega_i^{0\alpha})^2\}\\ &+\frac{1}{2I}\sum_{\alpha,i}\{(\varphi_i^{0\alpha})^2+(\psi_i^{0\alpha})^2\}\\ &+\sum_{\alpha,i}\{f\varphi_i^{0\alpha}+\sqrt{2}g\psi_i^{0\alpha}\}\sigma_i\tau^\alpha\\ &+(4\pi)^{\frac{1}{2}}\sum_{\alpha,i,j}\left\{\pi_i^{0\alpha}\int \pi'^\alpha\frac{\partial U}{\partial x_i}dV\right.\\ &\left.+\frac{\omega_{ij}^{0\alpha}}{\sqrt{2}}\int \omega_i'^\alpha\frac{\partial U}{\partial x_j}dV\right\}\\ &+\tfrac{1}{2}\sum_{\alpha,i}\int\{(\pi'^\alpha)^2+(\omega_i'^\alpha)^2\}dV\\ &+\tfrac{1}{2}\sum_{\alpha,i}\int\{\varphi'^\alpha(-\Delta+\kappa^2)\varphi'^\alpha\\ &+\psi_i'^\alpha(-\Delta+\mu^2)\psi_i'^\alpha\}dV,\end{aligned} \tag{18}$$

and the potential energy in the zero state E^0 is given by

$$\begin{aligned}E^0=\sum_{\alpha,i}\Big[&\frac{1}{2I}\{(\varphi_i^{0\alpha})^2+(\psi_i^{0\alpha})^2\}\\ &+\{f\varphi_i^{0\alpha}+\sqrt{2}g\psi_i^{0\alpha}\}\sigma_i\tau^\alpha\Big].\end{aligned} \tag{19}$$

The total angular momentum of the field and the nucleon is

$$\begin{aligned}L_{ij}=&-\sum_\alpha\int\left\{\pi^\alpha\left(x_i\frac{\partial \varphi^\alpha}{\partial x_j}-x_j\frac{\partial \varphi^\alpha}{\partial x_i}\right)\right\}dV\\ &-\sum_{\alpha,k}\int\left\{\omega_k{}^\alpha\left(x_i\frac{\partial \psi_k{}^\alpha}{\partial x_j}-x_j\frac{\partial \psi_k{}^\alpha}{\partial x_i}\right)\right\}dV\\ &+\sum_\alpha\int\{\psi_i{}^\alpha\omega_j{}^\alpha-\psi_j{}^\alpha\omega_i{}^\alpha\}dV+\tfrac{1}{2}\sigma_{ij};\end{aligned} \tag{20}$$

and the part $L_{ij}{}^0$ due to the zero state of the field is

$$L_{ij}{}^0=\sum_\alpha(\varphi_i^{0\alpha}\pi_j^{0\alpha}-\varphi_j^{0\alpha}\pi_i^{0\alpha})+\sum_{\alpha,k}(\psi_{ik}^{0\alpha}\omega_{jk}^{0\alpha}-\psi_{jk}^{0\alpha}\omega_{ik}^{0\alpha}),$$

or

$$\begin{aligned}L_{ij}{}^0=\sum_\alpha\{&\varphi_i^{0\alpha}\pi_j^{0\alpha}-\varphi_j^{0\alpha}\pi_i^{0\alpha}\\ &+\psi_i^{0\alpha}\omega_j^{0\alpha}-\psi_j^{0\alpha}\omega_i^{0\alpha}\}.\end{aligned} \tag{21}$$

Now E^0 takes its minimum value when

$$\varphi_i^{0\alpha}=fIe_i{}^\alpha, \quad \psi_i^{0\alpha}=\sqrt{2}gIe_i{}^\alpha; \tag{22}$$

so that it is convenient to introduce new variables defined by the orthogonal transformation

$$\begin{aligned}\Phi_i^{0\alpha}&=(f^2+2g^2)^{-\frac{1}{2}}\{f\varphi_i^{0\alpha}+\sqrt{2}g\psi_i^{0\alpha}\},\\ \Psi_i^{0\alpha}&=(f^2+2g^2)^{-\frac{1}{2}}\{\sqrt{2}g\varphi_i^{0\alpha}-f\psi_i^{0\alpha}\};\end{aligned}\tag{23}$$

with the inverse transformation

$$\begin{aligned}\varphi_i^{0\alpha}&=(f^2+2g^2)^{-\frac{1}{2}}\{f\Phi_i^{0\alpha}+\sqrt{2}g\Psi_i^{0\alpha}\},\\ \psi_i^{0\alpha}&=(f^2+2g^2)^{-\frac{1}{2}}\{\sqrt{2}g\Phi_i^{0\alpha}-f\Psi_i^{0\alpha}\}.\end{aligned}\tag{24}$$

The corresponding transformation equations for the momenta are

$$\begin{aligned}\Pi_i^{0\alpha}&=(f^2+2g^2)^{-\frac{1}{2}}\{f\pi_i^{0\alpha}+\sqrt{2}g\omega_i^{0\alpha}\},\\ \Omega_i^{0\alpha}&=(f^2+2g^2)^{-\frac{1}{2}}\{\sqrt{2}g\pi_i^{0\alpha}-f\omega_i^{0\alpha}\};\end{aligned}\tag{25}$$

with the inverse

$$\begin{aligned}\pi_i^{0\alpha}&=(f^2+2g^2)^{-\frac{1}{2}}\{f\Pi_i^{0\alpha}+\sqrt{2}g\Omega_i^{0\alpha}\},\\ \omega_i^{0\alpha}&=(f^2+2g^2)^{-\frac{1}{2}}\{\sqrt{2}g\Pi_i^{0\alpha}-f\Omega_i^{0\alpha}\}.\end{aligned}\tag{26}$$

Then we have

$$L_{ij}^{0}=L_{ij}^{00}+L_{ij}^{01},\tag{27}$$

where

$$L_{ij}^{00}=\sum_\alpha\{\Phi_i^{0\alpha}\Pi_j^{0\alpha}-\Phi_j^{0\alpha}\Pi_i^{0\alpha}\},\tag{28}$$

$$L_{ij}^{01}=\sum_\alpha\{\Psi_i^{0\alpha}\Omega_j^{0\alpha}-\Psi_j^{0\alpha}\Omega_i^{0\alpha}\}.\tag{29}$$

As in P-D, we write

$$\Phi_i^{0\alpha}=De_i^\alpha+\sum_\beta q^{\alpha\beta}e_i^\beta,\tag{30}$$

where $q^{\alpha\beta}\equiv q^{\beta\alpha}$, e_i^α are the components of an orthogonal matrix introduced in Eqs. (51), (51a) of P-D and can be considered as components of an orthogonal system of three unit vectors, and according to (22)

$$D=(f^2+2g^2)^{\frac{1}{2}}I;\tag{31}$$

and

$$\Pi_i^{0\alpha}=\sum_\beta\{p^{\alpha\beta}+(1/2D)L^{00\alpha\beta}\}e_i^\beta,\tag{32}$$

where $p^{\alpha\beta}\equiv p^{\beta\alpha}$ and

$$L^{00\alpha\beta}=\sum_{i,j}e_i^\alpha e_j^\beta L_{ij}^{00}=-D\sum_i\{e_i^\alpha\Pi_i^{0\beta}-e_i^\beta\Pi_i^{0\alpha}\}.\tag{33}$$

In (32) and (33) terms of higher order in $q^{\alpha\beta}/D$ have been neglected [cf. P-D, Eq. (72)]. $p^{\alpha\beta}$ and $q^{\alpha\beta}$ satisfy the commutation relation

$$i[p^{\alpha\beta},q^{\gamma\delta}]=\tfrac{1}{2}(\delta_{\alpha\gamma}\delta_{\beta\delta}+\delta_{\alpha\delta}\delta_{\beta\gamma}),\tag{34}$$

[cf. P-D, Eq. (57)]. If we insert these new variables in (18) and perform the S-transformation, we obtain for the Hamiltonian

$$\begin{aligned}H=&\frac{N}{4D^2}\mathbf{s}^2-\tfrac{3}{2}(f^2+2g^2)I\\&+\frac{\pi^{\frac{1}{2}}f}{D(f^2+2g^2)^{\frac{1}{2}}}\sum_{\alpha,\beta,i}L^{00\alpha\beta}e_i^\beta\int\frac{\partial U}{\partial x_i}\pi'^\alpha dV\\&+\frac{\pi^{\frac{1}{2}}g}{D(f^2+2g^2)^{\frac{1}{2}}}\sum_{\alpha,\beta,i}L^{00\alpha\beta}\int[\boldsymbol{\nabla}U\times\mathbf{e}^\beta]_i\omega_i'^\alpha dV\\&+\tfrac{1}{2}\sum_{\alpha,i}\int\{(\pi_i'^\alpha)^2+(\omega_i'^\alpha)^2\}dV\\&+\frac{1}{2I^2}\sum_{\alpha,\beta}(q^{\alpha\beta})^2,\end{aligned}\tag{35}$$

where

$$\mathbf{s}^2=\tfrac{1}{2}\sum_{\alpha,\beta}(L^{00\alpha\beta})^2.$$[6]

The terms which do not influence the isobar separation have been omitted; in particular the terms due to $\Psi_i^{0\alpha}$ and $\Omega_i^{0\alpha}$ which describe free mesons. By shifting the origin of π'^α and $\omega_i'^\alpha$ according to

$$\begin{aligned}\pi'^\alpha=\pi''^\alpha&-\frac{\pi^{\frac{1}{2}}f}{D(f^2+2g^2)^{\frac{1}{2}}}\sum_{\beta,i}L^{00\alpha\beta}e_i^\beta\\&\times\left\{\frac{\partial U}{\partial x_i}-\frac{3\partial\xi/\partial x_i}{\int(\boldsymbol{\nabla}\xi)^2dV}\right\},\end{aligned}\tag{36}$$

$$\begin{aligned}\omega_i'^\alpha=\omega_i''^\alpha&+\frac{\pi^{\frac{1}{2}}g}{D(f^2+2g^2)^{\frac{1}{2}}}\sum_\beta L^{00\alpha\beta}\\&\times\left[\mathbf{e}^\beta\times\left(\boldsymbol{\nabla}U-\frac{3\boldsymbol{\nabla}\xi}{\int(\boldsymbol{\nabla}\xi)^2dV}\right)\right]_i,\end{aligned}\tag{36}$$

we can get rid of the terms linear in π'^α and $\omega_i'^\alpha$ and of the order $1/D$, and still retain the orthogonality relations (14) [cf. P-D, Eq. (75)].

The final result for the isobar energy is

$$\frac{3}{4}\frac{\mathbf{s}^2}{(f^2+2g^2)}\frac{4\pi}{\int(\boldsymbol{\nabla}X)^2dV},$$

and the isobar separation ΔE is given by

$$\Delta E=\frac{3}{4}\frac{\{s(s+1)-\frac{3}{4}\}}{(f^2+2g^2)}\frac{4\pi}{\int(\boldsymbol{\nabla}X)^2dV}.\tag{37}$$

Now for a small source (κa and μa both$\ll1$)

$$\frac{4\pi}{\int(\boldsymbol{\nabla}X)^2dV}\cong\frac{1}{a}$$

[6] We have $\mathbf{s}$ instead of $\mathbf{L}$ as in P-D since we want to use the usual spectroscopic notation in the discussion of the two-nucleon system in Section IV.

[cf. P-D, Eq. (80a)], hence

$$\Delta E=\frac{3a}{4(f^2+2g^2)}\{s(s+1)-\tfrac{3}{4}\}. \quad (38)$$

We obtain the result (80a) in P-D for pseudoscalar meson alone if we put $g=0$ and $f=g/\sqrt{2}\kappa$. For the vector theory alone, we put $f=0$ and find that in this case ΔE is 1/2 of the value in the pseudoscalar theory (for the same coupling constant). For the Møller-Rosenfeld mixture, we put $f=g$ and find ΔE in this case is 1/3 of the value in the pseudoscalar theory.

III. NUCLEAR FORCES

A. Pseudoscalar Theory

We make the simplifying assumptions that the source size a is small compared to both κ^{-1} and the distance $r=|\mathbf{x}_{\rm I}-\mathbf{x}_{\rm II}|$ between the two nucleons. Let $U_{\rm I}(x)$ and $U_{\rm II}(x)$ be the source functions for particles I and II, respectively, and normalize them according to

$$\int U_A(x)dV=1 \text{ for } A=\text{I, II}. \quad (39)$$

The potentials $X_{\rm I}(x)$ and $X_{\rm II}(x)$ which they generate according to

$$(-\Delta+\kappa^2)X_A=4\pi U_A \text{ for } A=\text{I, II}, \quad (40)$$

are given by

$$X_A(x)=\int U_A(x')\frac{e^{-\kappa R}}{R}dV', \quad (41)$$

where $R=|\mathbf{x}-\mathbf{x}'|$. Also let

$$I\delta_{ij}=\int \frac{\partial X_A}{\partial x_i}\frac{\partial U_A}{\partial x_j}dV \text{ for } A=\text{I, II}; \quad (42)$$

$$J_{ij}=\int \frac{\partial X_A}{\partial x_i}\frac{\partial U_B}{\partial x_j}dV \text{ for } A, B=\text{I, II and } A\neq B$$
$$=-\int\int U_{\rm I}(x)U_{\rm II}(x')\frac{\partial^2}{\partial x_i\partial x_j}\left(\frac{e^{-\kappa R}}{R}\right)dVdV'. \quad (43)$$

It is evident that $J_{ij}=J_{ji}$. Now I is of the order a^{-3}, and J_{ij} is for small r of the order r^{-3} so that in the following we can neglect all quantities of the second and higher orders in J_{ij}/I.[7] Moreover we can substitute for J_{ij} its value for point sources;[8] i.e.,

$$J_{ij}=-\frac{\partial^2}{\partial x_{{\rm I}i}\partial x_{{\rm I}j}}\left(\frac{e^{-\kappa r}}{r}\right) \quad (44)$$

where $r=|\mathbf{x}_{\rm I}-\mathbf{x}_{\rm II}|$.

To obtain the interaction energy between two nucleons, it is sufficient to consider just the potential energy of the system E which is

$$E=\sum_\alpha\int\varphi^\alpha(-\Delta+\kappa^2)\varphi^\alpha dV$$
$$-(4\pi)^{\frac{1}{2}}f\sum_{A,\alpha,i}\int\frac{\partial\varphi^\alpha}{\partial x_i}\sigma_{Ai}\tau_A{}^\alpha U_A(x)dV, \quad (45)$$

where the subscript A is summed over I and II. As in S-D, Eq. (71), we split the field as follows:

$$\varphi^\alpha(x)=(4\pi)^{-\frac{1}{2}}\sum_{A,i}{}^{0\alpha}\varphi_{Ai}\xi_{Ai}(x)+\varphi'^\alpha(x), \quad (46)$$

where φ'^α satisfies the condition

$$\int\varphi'^\alpha\frac{\partial U_A}{\partial x_i}dV=0 \text{ for } A=\text{I, II}, \quad (47)$$

and where the functions ξ_{Ai} span the linear subspace of the functions $\partial X_A/\partial x_i$ in such a way that

$$\int\xi_{Ai}\frac{\partial U_B}{\partial x_j}dV=\delta_{AB}\delta_{ij}. \quad (48)$$

From these relations we obtain

$${}^{0\alpha}\varphi_{Ai}=(4\pi)^{\frac{1}{2}}\int\varphi^\alpha\frac{\partial U_A}{\partial x_i}dV. \quad (49)$$

The above conditions are fulfilled up to terms of the order J_{ij}/I if we put

$$\xi_{Ai}=\frac{1}{I}\frac{\partial X_A}{\partial x_i}-\frac{1}{I^2}\sum_j J_{ij}\frac{\partial X_B}{\partial x_j}$$
$$\text{for } A, B=\text{I, II and } A\neq B. \quad (50)$$

In terms of these variables, the potential energy (45) becomes

$$E=\sum_{A,\alpha,i,j}\left\{\frac{1}{2I}({}^{0\alpha}\varphi_{Ai})^2-\frac{J_{ij}}{I^2}{}^{0\alpha}\varphi_{{\rm I}i}{}^{0\alpha}\varphi_{{\rm II}j}\right\}+f\sum_{A,\alpha,i}{}^{0\alpha}\varphi_{Ai}\sigma_{Ai}\tau_A{}^\alpha$$
$$+\sum_\alpha\int\varphi'^\alpha(-\Delta+\kappa^2)\varphi'^\alpha dV. \quad (51)$$

[7] A similar situation holds for the integral $\int(\partial X_{\rm I}/\partial x_i)\times(\partial X_{\rm II}/\partial x_j)dV$ in comparison to $\int(\partial X_{\rm I}/\partial x_i)(\partial X_{\rm I}/\partial x_i)dV$ which are of the order of magnitude r^{-1} and a^{-1}, respectively. It is shown in S-D that, due to this circumstance, the neglect of the dependence of the isobar levels on r is justified as long as the latter integral is large compared to the former.

[8] The substitution of the point source is in reality not so simple and holds only for distances r considerably larger than a. This was pointed out by Oppenheimer and Serber.

The justification for the assumed decomposition of φ^α lies in the circumstance that no cross terms between $\overset{0\alpha}{\varphi}_{Ai}$ and φ'^α occur in (51). φ'^α describes free mesons and can be omitted for our purpose.

For the case of infinite separation of the two nucleons ($J_{ij}=0$), the lowest eigenvalue of the interaction energy is obtained analogously to the treatment of the one-source problem in P-D [cf. Eqs. (82), (64), (65), (67) there]. We put

$$\overset{0\alpha}{\varphi}_{Ai}=fI\overset{\alpha}{e}_{Ai} \tag{52}$$

where the $\overset{\alpha}{e}_{Ai}$ satisfy the conditions

$$\sum_\alpha \overset{\alpha}{e}_{Ai}\overset{\alpha}{e}_{Aj}=\delta_{ij},\quad \sum_i \overset{\alpha}{e}_{Ai}\overset{\beta}{e}_{Ai}=\delta_{\alpha\beta},\quad \text{for } A=\text{I, II}; \tag{53}$$

and by selecting the state where

$$\sum_{\alpha,i} \sigma_{Ai}\tau_A{}^\alpha \overset{\alpha}{e}_{Ai}=-3 \text{ for } A=\text{I, II}; \tag{54}$$

we obtain for $A=$ I, II

$$\sigma_A{}'^\alpha\tau_A{}^\alpha=-1 \text{ for each value of } \alpha \tag{55}$$

with

$$\sigma_A{}'^\alpha=\sum_i \overset{\alpha}{e}_{Ai}\sigma_{Ai} \tag{56}$$

and

$$\sigma_A{}'^\alpha\tau_A{}^\beta+\sigma_A{}'^\beta\tau_A{}^\alpha=0 \text{ for } \alpha\neq\beta. \tag{57}$$

To obtain the minimum value E^0 of E to the first order in J_{ij}/I in the absence of free mesons, we simply insert (52), (53), (54) in (51). The result is[9]

$$E^0=-3f^2I-f^2\sum_{\alpha,i,j} J_{ij}\overset{\alpha}{e}_{\text{I}i}\overset{\alpha}{e}_{\text{II}j}, \tag{58}$$

or omitting the first term which gives the self-energy, we have for the interaction energy

$$E^0_{\text{I II}}=-f^2\sum_{\alpha,i,j} J_{ij}\overset{\alpha}{e}_{\text{I}i}\overset{\alpha}{e}_{\text{II}j}. \tag{59}$$

Inserting for J_{ij} the expression (44), we obtain

$$E^0_{\text{I II}}=f^2\sum_\alpha (\mathbf{e}_\text{I}{}^\alpha\cdot\nabla)(\mathbf{e}_\text{II}{}^\alpha\cdot\nabla)(e^{-\kappa r}/r), \tag{60}$$

and if the differentiation is carried out,

$$E^0_{\text{I II}}=\frac{f^2}{3}\left\{\Gamma\frac{\kappa^2}{r}e^{-\kappa r}+\Lambda\frac{1}{r^3}(3+3\kappa r+\kappa^2r^2)e^{-\kappa r}\right\} \tag{61}$$

where

$$\Gamma=\sum_\alpha (\mathbf{e}_\text{I}{}^\alpha\cdot\mathbf{e}_\text{II}{}^\alpha),$$

$$\Lambda=\sum_\alpha\left\{\frac{3}{r^2}(\mathbf{e}_\text{I}{}^\alpha\cdot\mathbf{x})(\mathbf{e}_\text{II}{}^\alpha\cdot\mathbf{x})-(\mathbf{e}_\text{I}{}^\alpha\cdot\mathbf{e}_\text{II}{}^\alpha)\right\} \tag{62}$$

with $\mathbf{x}=\mathbf{x}_\text{I}-\mathbf{x}_\text{II}$.

It follows from the method of derivation that our theory differs from the usual perturbation treatment in the weak coupling theory only in the fact that $\sigma_A\tau_A{}^\alpha$ is replaced by $\mathbf{e}_A{}^\alpha$ ($A=$ I, II).

As stated at the beginning of Section II, the symmetrical theory is obtained by letting α take the values 1, 2, 3; the charged theory for α taking the values 1, 2; and the neutral theory for α restricted to the single value 3.

B. Mixed Theory

As in Part A we consider two source functions normalized according to (39). They generate the potentials according to

$$\begin{aligned}(-\Delta+\kappa^2)X_A&=4\pi U_A\\(-\Delta+\mu^2)Y_A&=4\pi U_A\end{aligned}\quad\text{for } A=\text{I, II}; \tag{63}$$

and hence

$$\begin{aligned}X_A(x)&=\int U_A(x')\frac{e^{-\kappa R}}{R}dV'\\Y_A(x)&=\int U_A(x')\frac{e^{-\mu R}}{R}dV'\end{aligned}\quad\text{for } A=\text{I, II}. \tag{64}$$

We have

$$I\delta_{ij}=\int\frac{\partial X_A}{\partial x_i}\frac{\partial U_A}{\partial x_j}dV\backsimeq\int\frac{\partial Y_A}{\partial x_i}\frac{\partial U_A}{\partial x_j}dV \quad\text{for } A=\text{I, II}; \tag{65}$$

$$J_{ij}=J_{ji}=\int\frac{\partial X_A}{\partial x_i}\frac{\partial U_B}{\partial x_j}dV\backsimeq-\frac{\partial^2}{\partial x_{\text{I}i}\partial x_{\text{I}j}}\left(\frac{e^{-\kappa r}}{r}\right) \quad\text{for } A, B=\text{I, II and } A\neq B. \tag{66}$$

$$K_{ij}=K_{ji}=\int\frac{\partial Y_A}{\partial x_i}\frac{\partial U_B}{\partial x_j}dV\backsimeq-\frac{\partial^2}{\partial x_{\text{I}i}\partial x_{\text{I}j}}\left(\frac{e^{-\mu r}}{r}\right)$$

The potential energy of the system is given by

$$\begin{aligned}E=\sum_{\alpha,i}\int\{&\varphi^\alpha(-\Delta+\kappa^2)\varphi^\alpha+\psi_i{}^\alpha(-\Delta+\mu^2)\psi_i{}^\alpha\}dV\\&-(4\pi)^{\frac{1}{2}}f\sum_{A,\alpha,i,j}\int\left\{\frac{\partial\varphi^\alpha}{\partial x_i}\sigma_{Ai}\right.\\&\left.+\frac{1}{2}\left(\frac{\partial\psi_j{}^\alpha}{\partial x_i}-\frac{\partial\psi_i{}^\alpha}{\partial x_j}\right)\sigma_{Aij}\right\}\tau_A{}^\alpha U_A dV,\end{aligned} \tag{67}$$

[9] If we had taken a more general expression

$$\overset{0\alpha}{\varphi}_{Ai}=\Sigma_\beta(fI\delta_{\alpha\beta}+q_A{}^{\alpha\beta})\overset{\alpha}{e}_{Ai}$$

instead of (52), we would have obtained in the expression for E^0 terms in $q_A{}^{\alpha\beta}$ which are of the relative order J_{ij}/I, and hence give corrections of the order $(J_{ij}/I)^2$ to E^0.

where we have assumed the equality of the coupling constants.

As before, we split the field as follows:

$$\varphi^\alpha(x)=(4\pi)^{-\frac{1}{2}}\sum_{A,i}\overset{0\alpha}{\varphi}_{Ai}\xi_{Ai}(x)+\varphi'^\alpha(x),$$
$$\psi_i^\alpha(x)=(8\pi)^{-\frac{1}{2}}\sum_{A,j}\overset{0\alpha}{\psi}_{Aij}\eta_{Aj}(x)+\psi_i'^\alpha(x); \tag{68}$$

with the orthogonality conditions

$$\int\varphi'^\alpha\frac{\partial U_A}{\partial x_i}dV=0 \quad \text{for } A=\text{I, II;} \tag{69}$$
$$\int\psi_i'^\alpha\frac{\partial U_A}{\partial x_j}dV=0$$

and

$$\int\xi_{Ai}\frac{\partial U_B}{\partial x_j}dV=\delta_{AB}\delta_{ij},$$
$$\int\eta_{Ai}\frac{\partial U_B}{\partial x_j}dV=\delta_{AB}\delta_{ij}. \tag{70}$$

Then

$$\overset{0\alpha}{\varphi}_{Ai}=(4\pi)^{\frac{1}{2}}\int\varphi^\alpha\frac{\partial U_A}{\partial x_i}dV \quad \text{for } A=\text{I, II,} \tag{71}$$
$$\overset{0\alpha}{\psi}_{Aij}=(8\pi)^{\frac{1}{2}}\int\psi_i^\alpha\frac{\partial U_A}{\partial x_j}dV$$

where we do not assume yet the antisymmetry of $\overset{0\alpha}{\psi}_{Aij}$ in i and j. The above conditions are satisfied up to term linear in J_{ij}/I and K_{ij}/I by

$$\xi_{Ai}=\frac{1}{I}\frac{\partial X_A}{\partial x_i}-\frac{1}{I^2}\sum_j J_{ij}\frac{\partial X_B}{\partial x_j} \quad \text{for } A, B=\text{I, II and } A\neq B. \tag{72}$$
$$\eta_{Ai}=\frac{1}{I}\frac{\partial Y_A}{\partial x_i}-\frac{1}{I^2}\sum_j K_{ij}\frac{\partial Y_A}{\partial x_j}$$

The potential energy now becomes

$$E=\frac{1}{2I}\sum_{A,\alpha,i,j}\{(\overset{0\alpha}{\varphi}_{Ai})^2+\tfrac{1}{2}(\overset{0\alpha}{\psi}_{Aij})^2\}$$
$$-\frac{1}{I^2}\sum_{\alpha,i,j,k}\{J_{ij}\overset{0\alpha}{\varphi}_{\text{I}i}\overset{0\alpha}{\varphi}_{\text{II}j}+\tfrac{1}{2}K_{ij}\overset{0\alpha}{\psi}_{\text{I}ik}\overset{0\alpha}{\psi}_{\text{II}jk}\}$$
$$-f\sum_{A,\alpha,i,j}\left\{\sigma_{Ai}\tau_A{}^\alpha\overset{0\alpha}{\varphi}_{Ai}+\frac{1}{\sqrt{2}}\sigma_{Aij}\tau_A{}^\alpha\overset{0\alpha}{\psi}_{Aij}\right\}$$
$$+\sum_{\alpha,i}\int\{\varphi'^\alpha(-\Delta+\kappa^2)\varphi'^\alpha$$
$$+\psi_i'^\alpha(-\Delta+\mu^2)\psi_i'^\alpha\}. \tag{73}$$

To obtain the minimum value of E to the first order in J_{ij}/I and K_{ij}/I, it is sufficient to put

$$\overset{0\alpha}{\varphi}_{Ai}=fI\overset{\alpha}{e}_{Ai}$$
for $A=$ I, II and i, j, k cyclic, (74)

$$\overset{0\alpha}{\psi}_{Aij}=-\overset{0\alpha}{\psi}_{Aji}\equiv\overset{0\alpha}{\psi}_{Ak}=\sqrt{2}fI\overset{\alpha}{e}_{Ak}$$
$$\tfrac{1}{2}\sum_i\{\sigma_{Ai}\tau_A\overset{\alpha}{e}_{Ai}\overset{\beta}{e}_{Ai}+\sigma_{Ai}\tau_A\overset{\beta}{e}_{Ai}\overset{\alpha}{e}_{Ai}\}=\delta_{\alpha\beta}$$
for $A=$ I, II. (75)

We find the interaction energy to be

$$E^0_{\text{I II}}=-f^2\sum_{\alpha,i,j}\{(J_{ij}-K_{ij})\overset{\alpha}{e}_{\text{I}i}\overset{\alpha}{e}_{\text{II}j}-K_{ii}\overset{\alpha}{e}_{\text{I}j}\overset{\alpha}{e}_{\text{II}j}\}, \tag{76}$$

and inserting the expressions (66) for J_{ij}, K_{ij} for point source, we obtain

$$E^0_{\text{I II}}=f^2\sum_\alpha\left\{(\mathbf{e}_{\text{I}}{}^\alpha\cdot\nabla)(\mathbf{e}_{\text{II}}{}^\alpha\cdot\nabla)\left(\frac{e^{-\kappa r}-e^{-\mu r}}{r}\right)\right.$$
$$\left.+(\mathbf{e}_{\text{I}}{}^\alpha\cdot\mathbf{e}_{\text{II}}{}^\alpha)\Delta\left(\frac{e^{-\mu r}}{r}\right)\right\}. \tag{77}$$

The evaluation of the differential operators yields

$$E^0_{\text{I II}}=\tfrac{1}{3}\{\Gamma J(r)+\Lambda K(r)\} \tag{78}$$

with Γ and Λ as defined in (62) and with the radial functions

$$J(r)=\frac{f^2}{r}(\kappa^2e^{-\kappa r}+2\mu^2e^{-\mu r}),$$
$$K(r)=\frac{f^2}{r^3}\{(3+3\kappa r+\kappa^2r^2)e^{-\kappa r}$$
$$-(3+3\mu r+\mu^2r^2)e^{-\mu r}\}. \tag{79}$$

It is to be noted that for small r, both J and K behave as r^{-1}, and $K(r)\equiv0$ for $\kappa=\mu$ in agreement with the results of Møller and Rosenfeld for the weak coupling theory.

The remarks made at the end of Part A also hold in this case; i.e., by letting α take the values 1, 2, 3; 1, 2; or 3, we obtain the symmetrical, the charged, and the neutral theory, respectively.

IV. THE DEUTERON

A. Classification of the States

The stationary states of the one-nuclear system in the symmetrical theory can be described completely by the numbers s, m, and n which

are the eigenvalues of the following operators:[10]

$$\mathbf{s}^2=\mathbf{t}^2=s(s+1), \quad s_3=m, \quad t^3=n. \tag{80}$$

s is a positive half-odd integer, and m and n are half-odd integers such that $-s\leqq m,n\leqq s$. It is to be noted that there is complete symmetry between spin and isotopic spin.

For a system containing two nucleons, the Hamiltonian is

$$H=\frac{1}{M}\left\{p_r^2+\frac{\mathbf{L}^2}{r^2}\right\}+\frac{a}{4f^2}\{\mathbf{s}_{\mathrm{I}}^2+\mathbf{s}_{\mathrm{II}}^2-\tfrac{3}{2}\}+\tfrac{1}{3}\{\Gamma J(r)+\Lambda K(r)\}. \tag{81}$$

The first part gives the kinetic energy of relative motion,[11] the second the isobar energy, and the third the interaction energy. The motion of the center of gravity of the system is not considered, and of course this is in the non-relativistic approximation.

Let us first consider states with no orbital angular momentum ($\mathbf{L}=0$); then there is still complete symmetry between spin and isotopic spin as in the one-nucleon system. Their operators $\mathbf{S}=\mathbf{s}_{\mathrm{I}}+\mathbf{s}_{\mathrm{II}}$ and $\mathbf{T}=\mathbf{t}_{\mathrm{I}}+\mathbf{t}_{\mathrm{II}}$ are still constant, but now their magnitude need not be the same. Hence the stationary states can be described by the eigenvalues S, T, M, and N of the following operators:

$$\begin{aligned}&\mathbf{S}^2=S(S+1),\\ &\mathbf{T}^2=T(T+1),\\ &S_3=M,\\ &T^3=N,\end{aligned} \tag{82}$$

where S and T are positive integers or zero such that $|s_{\mathrm{I}}-s_{\mathrm{II}}|\leqq S$, $T\leqq(s_{\mathrm{I}}+s_{\mathrm{II}})$, and M and N are integers or zero such that $-S\leqq M\leqq S$ and $-T\leqq N\leqq T$. If there is an orbital angular momentum $\mathbf{L}$, then the spin angular momentum $\mathbf{S}$ is no longer constant, and it has to be replaced by the total angular momentum $\mathbf{J}$ given by

$$\mathbf{J}=\mathbf{L}+\mathbf{S}, \tag{83}$$

and the eigenvalues S and M by J and J_M, respectively, where

$$\mathbf{J}^2=J(J+1), \quad J_M=L_M+M. \tag{84}$$

In addition there is the quantum number provided by the parity, the eigenvalue of the spatial reflection operator. The Hamiltonian (81) is also invariant under any rotation in the isotopic spin space. Such a rotation leaves the s_{Ai} unchanged and transforms the t_A^{α} and e_{Ai}^{α} (for each i) in the same way. In particular, a rotation which changes the sign of the 3-component, as for instance the rotation about the 1-axis through 180° which results in the transformation

$$\begin{aligned}&t_A^1\rightarrow t_A^1, \quad t_A^2\rightarrow -t_A^2, \quad t_A^3\rightarrow -t_A^3,\\ &\mathbf{e}_A^1\rightarrow\mathbf{e}_A^1, \quad \mathbf{e}_A^2\rightarrow -\mathbf{e}_A^2, \quad \mathbf{e}_A^3\rightarrow -\mathbf{e}_A^3,\end{aligned} \tag{85}$$

will turn out to be very useful. [Note that this transformation conserves the commutation relations satisfied by the e_i^{α} given in (135) of the Appendix.] The transformation (85) multiplies the spin function by a phase factor $e^{iN\times\text{const}}$, and changes the sign of n_{I}, n_{II}, and N. Thus the operator shows the degeneracy in the energy levels of the excited spin states which differ only by the sign of N. In particular for the case $N=0$, that is for the deuteron, the phase factor is unity, and the transformation does not change the state to which the spin function belongs. Consequently this operator provides another quantum number which is the signature of the spin function under the substitution $n_{\mathrm{I}}\rightarrow -n_{\mathrm{I}}$, $n_{\mathrm{II}}\rightarrow -n_{\mathrm{II}}$.

With the aid of these quantum numbers the complete wave function of a stationary state can be written in the form

$$\Psi(r,\vartheta,\varphi;J,T,J_M,N)=\sum_{\substack{L,S\\ L_M+M=J_M}} c^J_{L_M M}\frac{u_{L,S}(r)}{r}\times Y_L^{L_M}(\vartheta,\varphi)\Xi(S,T,M,N), \tag{86}$$

where $c^J_{L_M M}$ is the normalized coefficient of the Clebsch-Gordon series; $u_{L,S}(r)$ is the radial function which we normalize, for bound states where this is possible, according to

$$\sum_{L,S}\int_0^{\infty}\bar{u}_{L,S}(r)u_{L,S}(r)dr=1; \tag{87}$$

$Y_L{}^{L_M}(\vartheta,\varphi)$ is the normalized spherical harmonic;

[10] Cf. P-D. We use s instead of j there to denote the eigenvalue of the spin. Also we denote the spin operator by $\mathbf{s}$ instead of $\mathbf{L}$ as mentioned already in footnote 6, and the isotopic spin operator by $\mathbf{t}$ instead of $\mathbf{T}$.

[11] We identify M with the empirical mass of the nucleon from which the part of the mass due to the meson field has been subtracted. It was pointed out to one of us by Dr. Schwinger that in the neutral theories the latter is a tensor with respect to the direction of $\mathbf{e}^3$. In the symmetrical theories, however, the field mass is also a scalar.

and $\Xi(S, T, M, N)$ is the spin-isotopic spin function (we shall refer to this hereafter simply as the spin function when no possibility of ambiguity exists). Of course the numbers L and S do not determine the radial functions uniquely since there is still the radial quantum number, but in the present work we consider only the radial functions belonging to the lowest energy level. In accordance with the exclusion principle, we assume Ψ to be antisymmetric in the interchange of particle I and II. Then since the interchange of the space coordinates gives rise to a factor $(-1)^L$, the spin function Ξ must be symmetric or antisymmetric in the interchange of particles I and II depending on whether L is odd or even, respectively. Further since the parity quantum number is $(-1)^L$, any state is restricted to spherical harmonics of even or of odd orders.

In order to evaluate the eigenvalues of the operators Γ and Λ, it is necessary to evaluate the matrix elements of e_i^a in the (s, m, n) representation and express the spin function $\Xi(S, T, M, N)$ in terms of the one-nucleon spin functions $\xi_{\rm I}(s_{\rm I}, m_{\rm I}, n_{\rm I})$ and $\xi_{\rm II}(s_{\rm II}, m_{\rm II}, n_{\rm II})$. The calculation of the matrix elements of e_i^a is given in the Appendix. The expression for $\Xi(S, T, M, N)$ in terms of $\xi_{\rm I}(s_{\rm I}, m_{\rm I}, n_{\rm I})$ and $\xi_{\rm II}(s_{\rm II}, m_{\rm II}, n_{\rm II})$ is obtained by means of the Clebsch-Gordon series. In fact they can be expressed as products of the spin and isotopic spin functions

$$\Xi(S, T, M, N) = \mathrm{X}(S, M)\mathrm{Z}(T, N), \tag{88}$$

$$\xi_A(s_A, m_A, n_A) = \chi_A(s_A, m_A)\zeta_A(s_A, n_A) \quad \text{for } A = \mathrm{I}, \mathrm{II}; \tag{89}$$

and

$$\mathrm{X}(S, M) = \sum_{\substack{s_{\rm I}, s_{\rm II} \\ m_{\rm I}+m_{\rm II}=M}} C^{S}_{m_{\rm I}m_{\rm II}}\{\chi_{\rm I}(s_{\rm I}, m_{\rm I})\chi_{\rm II}(s_{\rm II}, m_{\rm II}) \pm \chi_{\rm II}(s_{\rm I}, m_{\rm I})\chi_{\rm I}(s_{\rm II}, m_{\rm II})\}, \tag{90}$$

$$\mathrm{Z}(T, N) = \sum_{\substack{s_{\rm I}, s_{\rm II} \\ n_{\rm I}+n_{\rm II}=N}} C^{T}_{n_{\rm I}n_{\rm II}}\{\zeta_{\rm I}(s_{\rm I}, n_{\rm I})\zeta_{\rm II}(s_{\rm II}, n_{\rm II}) \pm \zeta_{\rm II}(s_{\rm I}, n_{\rm I})\zeta_{\rm I}(s_{\rm II}, n_{\rm II})\}.$$

The symmetrization of these expressions in particles I and II is necessary for the reason given above. However since Γ and Λ have matrix elements between states with values of $s_{\rm I}$ and $s_{\rm II}$ which differ by 1, $s_{\rm I}$ and $s_{\rm II}$ are not constants of the motion, and hence the series (90) are actually infinite series, and the calculation of the eigenvalues of Γ and Λ are very complicated.

We therefore make the following approximation: we replace Γ and Λ by Γ_0 and Λ_0 which are the parts of Γ and Λ diagonal in $s_{\rm I}$ and $s_{\rm II}$. This treatment is of course rigorous in the limit of infinitely large isobar energy. We shall show for the ground state of the deuteron, by treating the off-diagonal parts Γ_1 and Λ_1 of Γ and Λ as perturbations, that even when the isobar energy is not too large, the effect of the perturbing terms is small. This justifies our method of approximation at least of the ground state of the deuteron in which we are interested.

In the unperturbed system, $s_{\rm I}$ and $s_{\rm II}$ are also quantum numbers of the system, and hence, combining (88), (89), and (90), we obtain for the spin functions of the unperturbed system

$$\Xi(s_{\rm I}, s_{\rm II}; S, T, M, N) = \sum_{\substack{m_{\rm I}+m_{\rm II}=M \\ n_{\rm I}+n_{\rm II}=N}} C^{S}_{m_{\rm I}m_{\rm II}}C^{T}_{n_{\rm I}n_{\rm II}} \times\{\xi_{\rm I}(s_{\rm I}, m_{\rm I}, n_{\rm I})\xi_{\rm II}(s_{\rm II}, m_{\rm II}, n_{\rm II}) \pm \xi_{\rm II}(s_{\rm I}, m_{\rm I}, n_{\rm I})\xi_{\rm I}(s_{\rm II}, m_{\rm II}, n_{\rm II})\}. \tag{91}$$

It is readily seen that these spin functions are eigenfunctions of the operator given in (85) with the eigenvalues $(-1)^{s_{\rm I}+s_{\rm II}-T}$. It is only necessary to use the following property of the Clebsch-Gordon coefficients:

$$C^{T}_{n_{\rm I}n_{\rm II}} = (-1)^{s_{\rm I}+s_{\rm II}-T}C^{T}_{-n_{\rm I}-n_{\rm II}}, \tag{92}$$

and to remember that the operation (85) on the spin functions (91) for the deuteron simply replaces $n_{\rm I}$ and $n_{\rm II}$ by $-n_{\rm I}$ and $-n_{\rm II}$, respectively.

The spin functions (91) are also eigenfunctions of the operator Γ_0, and its eigenvalues are found by simple calculation with the matrix elements of the e_i^a. They are given by the general formula

$$\Gamma_0 = \frac{\{S(S+1)-s_{\rm I}(s_{\rm I}+1)-s_{\rm II}(s_{\rm II}+1)\} \times\{T(T+1)-s_{\rm I}(s_{\rm I}+1)-s_{\rm II}(s_{\rm II}+1)\}}{4s_{\rm I}(s_{\rm I}+1)s_{\rm II}(s_{\rm II}+1)}. \tag{93}$$

Thus if s is the smaller and t the larger of the two numbers $s_{\rm I}$ and $s_{\rm II}$, we have

$$-\frac{s}{s+1} \leqq \Gamma_0 \leqq \frac{s(t+1)}{(s+1)t}; \tag{94}$$

TABLE I. Classification of the deuteron states.

s_I	s_{II}	S	T	(I, II)	$(n\to -n)$	Γ_0
1/2	1/2	0	0	+	−	+1
1/2	1/2	0	1	−	+	−1/3
1/2	1/2	1	0	−	−	−1/3
1/2	1/2	1	1	+	+	+1/9
3/2	1/2	1	1	+, −	−	+5/9
3/2	1/2	1	2	+, −	+	−1/3
3/2	1/2	2	1	+, −	−	−1/3
3/2	1/2	2	2	+, −	+	+1/5
3/2	3/2	0	0	+	−	+1
3/2	3/2	0	1	−	+	+11/15
3/2	3/2	0	2	+	−	+2/5
3/2	3/2	0	3	−	+	−3/5
3/2	3/2	1	0	−	−	+11/15
3/2	3/2	1	1	+	+	+121/225
3/2	3/2	1	2	−	−	+11/75
3/2	3/2	1	3	+	+	−11/25
3/2	3/2	2	0	+	−	+2/5
3/2	3/2	2	1	−	+	+11/75
3/2	3/2	2	2	+	−	+1/25
3/2	3/2	2	3	−	+	−3/25
3/2	3/2	3	0	−	−	−3/5
3/2	3/2	3	1	+	+	−11/25
3/2	3/2	3	2	−	−	−3/25
3/2	3/2	3	3	+	+	+9/25

so that for large s_I and s_{II}, Γ_0 lies between -1 and 1. Furthermore, Γ_0 is negative when either S or T is near the maximum value s_I+s_{II} and the other near the minimum value $|s_I-s_{II}|$, while Γ_0 is positive when both S and T are either near their maximum or near their minimum value. This result is very useful since $\frac{1}{3}\Gamma_0 J(r)$ is the dominant part of the interaction energy, and, in general, the sign of Γ_0 determines whether the interaction is attractive or repulsive. Since the operator Λ_0 contains angular coordinates besides the operators e^{α}_{Ai}, the calculation of its eigenvalues is too complicated in the general case, and they are computed only for the special states considered in Part B.

The first few states of the deuteron system are classified according to their quantum numbers in Table I. The fifth column under (I, II) indicates the symmetry of the spin function under the interchange of particles I and II. For $s_I\neq s_{II}$, both symmetric and antisymmetric functions are possible for each value of S and T; but for $s_I=s_{II}$, only a symmetric or an antisymmetric function is possible for a given value of S and T, depending on whether $(S+T)$ is even or odd, respectively. The sixth column under $(n\to -n)$ indicates the signature of the spin functions under the operation (85). As mentioned above, it is positive or negative depending on whether $(s_I+s_{II}-T)$ is even or odd. The last column under Γ_0 gives the eigenvalues of this operator.

B. The Ground State

The lowest state of the unperturbed system is for $s_I=s_{II}=\frac{1}{2}$, and for the spatial part of the wave function to consist mostly of the S-wave $(L=0)$, we must consider antisymmetric spin functions (in the interchange of particles). We see from Table I that both the singlet $(S=0)$ and the triplet $(S=1)$ states have $\Gamma_0=-\frac{1}{3}$. Thus these states will evidently be bound states. Now the tensor interaction given by Λ_0 vanishes for the singlet state, and we shall find below that it contributes additional attractive potential to the triplet state. Thus in agreement with experiment the ground state is the triplet state.

To obtain the matrix elements of Λ_0, we use the matrix elements of the e_i^{α} and the expansion (91) for Ξ in terms of ξ_I and ξ_{II}. The result is[12]

$$\Lambda_0\Xi_0(1,0,M)=-\frac{4(2\pi)^{\frac{1}{2}}}{3}\times\sum_{M'+M''=M}{}^{1}c_{M'M''}Y_2^{M'}\Xi_0(1,0,M''). \quad (95)$$

Now if we use the spectroscopic notation to designate the states; i.e. write $^3S_M{}^1$ for the triplet S state with $J=1$ and $J_M=M$, $^3D_M{}^1$ for the triplet D state etc., and if we let $\Sigma_0(^3S_M{}^1)$, $\Sigma_0(^3D_M{}^1)$, etc. denote the spin and angular parts of the wave function, we have

$$\begin{aligned}\Sigma_0(^3S_M{}^1)&=(4\pi)^{-\frac{1}{2}}\Xi_0(1,0,M),\\ \Sigma_0(^3D_M{}^1)&=\sum_{M'+M''=M}{}^{1}c_{M'M''}Y_2^{M'}\Xi_0(1,0,M'').\end{aligned} \quad (96)$$

Thus combining (95) and (96) we obtain

$$\begin{aligned}\Lambda_0\Sigma_0(^3S_M{}^1)&=-\frac{2\sqrt{2}}{3}\Sigma_0(^3D_M{}^1),\\ \Lambda_0\Sigma_0(^3D_M{}^1)&=\tfrac{2}{3}\Sigma\ (^3D_M{}^1)-\frac{2\sqrt{3}}{3}\Sigma_0(^3S_M{}^1).\end{aligned} \quad (97)$$

No higher values of the angular momentum

[12] Instead of writing the spin values s_I and s_{II} as in (91), we now use the subscripts 0, 1, and 2 to denote quantities belonging to the states $s_I=s_{II}=\frac{1}{2}$; $s_I=\frac{1}{2}$, $s_{II}=\frac{3}{2}$; and $s_I=s_{II}=\frac{3}{2}$, respectively. Also we drop the designation 0 for N since we do not consider states where N has values different from 0.

occur in this state, and we have

$$\Psi_0(r,\vartheta,\varphi;1,0,M)=\frac{u_0(r)}{r}\sum_0(^3S_M{}^1)+\frac{v_0(r)}{r}\sum_0(^3D_M{}^1). \quad (98)$$

Inserting this expression into the Schrödinger equation

$$H\Psi=E\Psi, \quad (99)$$

and using the expression (81) for H, we obtain with the aid of (97) the simultaneous set of differential equations for $u_0(r)$ and $v_0(r)$

$$\begin{aligned}&\frac{d^2u_0}{dr^2}+M\left\{E_0+\frac{1}{9}J(r)\right\}u_0=-\frac{2\sqrt{2}}{9}MK(r)v_0,\\&\frac{d^2v_0}{dr^2}-\frac{6v_0}{r^2}+M\left\{E_0+\frac{1}{9}J(r)-\frac{2}{9}K(r)\right\}v_0\\&\qquad=-\frac{2\sqrt{2}}{9}MK(r)u_0.\end{aligned} \quad (100)$$

Thus we see that the tensor force contributes additional attractive potential. The above equations are to be solved with the normalization condition

$$\int_0^\infty(u_0{}^2+v_0{}^2)dr=1, \quad (101)$$

and the boundary conditions u_0, $v_0=0$ at both $r=0$ and $r=\infty$. The solution of these equations will be studied in Part C.

First we want to see whether (98) is a good approximation to the actual ground state wave function; i.e., to see whether the approximation we have made in taking only the parts of Γ and Λ diagonal in s_{I} and s_{II} is justified. We do this by calculating the matrix elements of the perturbations Γ_1 and Λ_1 between the state described by (98) and the other states. The first excited spin state occurs when one of the particles has spin 3/2 while the other has the unexcited value 1/2. We see from Table I, however, that none of the states for this case has the same eigenvalues as any of the states with $s_{\mathrm{I}}=s_{\mathrm{II}}=\frac{1}{2}$, and since neither Γ_1 nor Λ_1 change these quantum numbers (except s_{I} and s_{II}), both Γ_1 and Λ_1 have no matrix element between these states.

For the second excited spin state, $s_{\mathrm{I}}=s_{\mathrm{II}}=\frac{3}{2}$, the states which combine with the ground state ($S=1$, $T=0$) are only the triplet and the septet terms with $T=0$ (cf. Table I). The spin-angular functions which occur in this state are

$$\begin{aligned}&\Sigma_2(^3S_M{}^1)=(4\pi)^{-\frac{1}{2}}\Xi_2(1,0,M),\\&\Sigma_2(^3D_M{}^1)=\sum_{M'+M''=M}{}^1c_{M'M''}Y_2^{M'}\Xi_2(1,0,M''),\\&\Sigma_2(^7D_M{}^1)=\sum_{M'+M''=M}{}^1c_{M'M''}Y_2^{M'}\Xi_2(3,0,M''),\\&\Sigma_2(^7G_M{}^1)=\sum_{M'+M''=M}{}^1c_{M'M''}Y_4^{M'}\Xi_2(3,0,M'').\end{aligned} \quad (102)$$

The operator Λ_0 applied to these functions gives the following results:

$$\begin{aligned}\Lambda_0\Sigma_2(^3S_M{}^1)&=\frac{4\sqrt{7}}{25}\Sigma_2(^7D_M{}^1)-\frac{34\sqrt{2}}{75}\Sigma_2(^3D_M{}^1),\\\Lambda_0\Sigma_2(^3D_M{}^1)&=\frac{12\sqrt{6}}{25\sqrt{7}}\Sigma_2(^7G_M{}^1)-\frac{4\sqrt{2}}{25\sqrt{7}}\Sigma_2(^7D_M{}^1)\\&\quad+\frac{34}{75}\Sigma_2(^3D_M{}^1)-\frac{34\sqrt{2}}{75}\Sigma_2(^3S_M{}^1),\\\Lambda_0\Sigma_2(^7D_M{}^1)&=-\frac{12\sqrt{3}}{175}\Sigma_2(^7G_M{}^1)+\frac{144}{175}\Sigma_2(^7D_M{}^1)\\&\quad-\frac{4\sqrt{2}}{25\sqrt{7}}\Sigma_2(^3D_M{}^1)+\frac{4\sqrt{7}}{25}\Sigma_2(^3S_M{}^1),\\\Lambda_0\Sigma_2(^7G_M{}^1)&=\frac{6}{7}\Sigma_2(^7G_M{}^1)-\frac{12\sqrt{3}}{175}\Sigma_2(^7D_M{}^1)\\&\quad+\frac{12\sqrt{6}}{25\sqrt{7}}\Sigma_2(^3D_M{}^1).\end{aligned} \quad (103)$$

Writing the wave function in the form

$$\Psi_2(r,\vartheta,\varphi;1,0,M)=\frac{u_2(r)}{r}\Sigma_2(^3S_M{}^1)+\frac{v_2(r)}{r}\Sigma_2(^3D_M{}^1)+\frac{w_2(r)}{r}\Sigma_2(^7D_M{}^1)+\frac{y_2(r)}{r}\Sigma_2(^7G_M{}^1), \quad (104)$$

we find the following set of equations for the

radial functions:

$$\frac{d^2u_2}{dr^2}+M\left\{E_2-\frac{3a}{2f^2}-\frac{11}{15}J(r)\right\}u_2$$
$$=-\frac{2}{225}MK(r)\{17\sqrt{2}\,v_2-6\sqrt{7}\,w_2\},$$
$$\frac{d^2v_2}{dr^2}-\frac{6v_2}{r^2}+M\left\{E_2-\frac{3a}{2f^2}-\frac{11}{15}J(r)-\frac{34}{225}K(r)\right\}v_2$$
$$=-\frac{2}{225}MK(r)\left\{17\sqrt{2}\,u_2+\frac{6\sqrt{2}}{7}w_2-\frac{18\sqrt{6}}{\sqrt{7}}y_2\right\},$$
$$\frac{d^2w_2}{dr^2}-\frac{6w_2}{r^2}+M\left\{E_2-\frac{3a}{2f^2}+\frac{1}{5}J(r)-\frac{48}{175}K(r)\right\}w_2 \tag{105}$$
$$=-\frac{4}{75}MK(r)\left\{-\sqrt{2}\,u_2+\frac{\sqrt{2}}{\sqrt{7}}v_2+\frac{3\sqrt{3}}{\sqrt{7}}y_2\right\},$$
$$\frac{d^2y_2}{dr^2}-\frac{20y_2}{r^2}+M\left\{E_2-\frac{3a}{2f^2}+\frac{1}{5}J(r)-\frac{2}{7}K(r)\right\}y_2$$
$$=-\frac{4}{25}MK(r)\left\{-\frac{\sqrt{6}}{\sqrt{7}}v_2+\frac{\sqrt{3}}{\sqrt{7}}w_2\right\}.$$

No higher spin states need be considered since neither Γ_1 nor Λ_1 has matrix elements between states whose spin value differ by more than 1. Hence the excited state considered above is the only state which combines with the ground state (98).

To calculate the matrix elements between them, we have

$$\Gamma_1\Sigma_0(^3S_M{}^1)=\frac{\sqrt{5}}{3}\Sigma_2(^3S_M{}^1),$$
$$\Gamma_1\Sigma_0(^3D_M{}^1)=\frac{\sqrt{5}}{3}\Sigma_2(^3D_M{}^1),$$
$$\Lambda_1\Sigma_0(^3S_M{}^1)=-\frac{\sqrt{7}}{\sqrt{5}}\Sigma_2(^7D_M{}^1)+\frac{\sqrt{2}}{3\sqrt{5}}\Sigma_2(^3D_M{}^1), \tag{106}$$
$$\Lambda_1\Sigma_0(^3D_M{}^1)=-\frac{3\sqrt{6}}{\sqrt{35}}\Sigma_2(^7G_M{}^1)+\frac{\sqrt{2}}{\sqrt{35}}\Sigma_2(^7D_M{}^1)$$
$$-\frac{1}{3\sqrt{5}}\Sigma_2(^3D_M{}^1)+\frac{\sqrt{2}}{3\sqrt{5}}\Sigma_2(^3S_M{}^1).$$

Hence if we write $(2|H|0)$ for the matrix element of the perturbation

$$H_1=\tfrac{1}{3}\{\Gamma_1J(r)+\Lambda_1K(r)\} \tag{107}$$

between these states, we have

$$(2|H|0)=\frac{1}{3}\int_0^\infty\left[\frac{\sqrt{5}}{3}\{\bar{u}_2u_0+\bar{v}_2v_0\}J(r)\right.$$
$$+\left\{\frac{\sqrt{2}}{3\sqrt{5}}\bar{u}_2v_0+\frac{1}{3\sqrt{5}}\bar{v}_2(\sqrt{2}\,u_0-v_0)\right.$$
$$-\frac{1}{\sqrt{35}}\bar{w}_2(7u_0-\sqrt{2}\,v_0)$$
$$\left.\left.-\frac{3\sqrt{6}}{\sqrt{35}}\bar{y}_2v_0\right\}K(r)\right]dr. \tag{108}$$

From (105) we see that for the dominant S part u_2 of the wave function the direct interaction gives rise to a repulsive potential $11/15J(r)$. The tensor force gives rise to an attractive potential when coupled with the triplet D part v_2, and a repulsive potential when coupled with the septet D part w_2, but these contributions will be small compared to the direct interaction. Hence it seems that the state (104) will not be a bound state. Assuming this to be the case, we can estimate the correction to the wave function (98) due to the perturbation (107) by approximating the wave function (104) with a plane wave. If we denote this correction term by Ψ_{01}, then we find

$$\int|\Psi_{01}|^2dV\sim0.2, \tag{109}$$

by using numerical values for the constants a, f, κ and μ which will be found in Part C and for isobar separation of 20 Mev. Thus the correction is quite small, and it will not alter appreciably the results obtained for the unperturbed ground state.

On the other hand, if the state (105) is a bound state, the effect of the perturbation is proportional to the ratio

$$(2|H|0)/(E_2-E_0)\backsimeq(2|H|0)/E_{\text{isob}} \tag{110}$$

where $E_{\text{isob}}=3a/2f^2$. We would certainly obtain an upper bound for $(2|H|0)$ if we insert in (108) u_0, v_0 for u_2, v_2 and neglect the other small quantities. This gives for $(2|H|0)$ a value a few times the binding energy of the deuteron, $E_{\text{bind}}=|E_0|$. Hence in this case the approxima-

tion is justified since the upper limit of the ratio (110) is about 0.3, and actually it will be much smaller.

In either case, the validity of the approximation depends on the smallness of the quantity

$$E_{\text{bind}}/E_{\text{isob}}. \tag{111}$$

C. Determination of the Constants

In the present theory the following constants occur: the size of the nucleon a, the strength of the coupling f, and the masses of the pseudoscalar and the vector mesons, κ and μ. Of these, f must be chosen so that the binding energy of the deuteron is equal to the observed value of 2.17 Mev, and κ equal to the observed value of the mass of the meson of ~ 200 electron masses (we take for convenience $\kappa = 177$ m). The tensor force depends on the ratio of the masses μ/κ and vanishes for $\mu = \kappa$. Thus we shall choose μ so that the quadrupole moment of the deuteron comes out equal to the observed value of 2.73×10^{-27} cm^2. However we have the following conditions to satisfy for the validity of our calculation:

(1) small source, i.e., $a\kappa \ll 1$;
(2) strong coupling, i.e., $(f\kappa)^2 \gg (a\kappa)^2$;
(3) small effect of the higher spin states on the ground state, i.e., $E_{\text{bind}}/E_{\text{isob}} \ll 1$.

It is not possible to say *a priori* whether these conditions can be satisfied with the above determination of the constants, but as we shall see below, this is possible.

In order to determine f and μ, we must consider the differential equations (100). f is to be determined so that the lowest eigenvalue E_0 of these equations is equal to $-E_{\text{bind}}$, and μ so that the quadrupole moment[13]

$$Q = \frac{\sqrt{2}}{10} \int_0^\infty r^2 \left(uv - \frac{1}{2\sqrt{2}} v^2 \right) dr \tag{112}$$

agrees with the experimental value. Since the Eqs. (100) cannot be solved in terms of any known function and since the conditions determining f and μ are interdependent, we have to assume some reasonable value for μ, solve (100) approximately, and see whether it gives a good value for Q. Let us first simplify the equations by introducing the dimensionless variable

$$x = 2(M|E_0|)^{\frac{1}{2}} r \tag{113}$$

which transforms (101) to

$$\begin{aligned} &d^2u/dx^2 - \{\tfrac{1}{4} - j(x)\}u = -\sqrt{2}k(x)v, \\ &\frac{d^2v}{dx^2} - \frac{6v}{x^2} - \{\tfrac{1}{4} - j(x) + k(x)\}v = -\sqrt{2}k(x)u, \end{aligned} \tag{114}$$

with

$$\begin{aligned} j(x) &= \frac{\gamma}{x}\{\alpha^2 e^{-\alpha x} + 2\beta^2 e^{-\beta x}\}, \\ k(x) &= \frac{2\gamma}{x^3}\{(\alpha^2x^2 + 3\alpha x + 3)e^{-\alpha x} \\ &\qquad - (\beta^2x^2 + 3\beta x + 3)e^{-\beta x}\}, \end{aligned} \tag{115}$$

where

$$\begin{aligned} &\alpha = \frac{\kappa}{2(M|E_0|)^{\frac{1}{2}}}, \quad \beta = \frac{\mu}{2(M|E_0|)^{\frac{1}{2}}}, \\ &\gamma = \frac{2}{9} f^2 M (M|E_0|)^{\frac{1}{2}}. \end{aligned} \tag{116}$$

The normalization condition (101) becomes

$$\int_0^\infty (u^2 + v^2)\, dx = 1, \tag{117}$$

and the quadrupole moment (112) becomes

$$Q = \frac{\sqrt{2}}{10} \int_0^\infty x^2 \left(uv - \frac{1}{2\sqrt{2}} v^2 \right) dx, \tag{118}$$

and it is now measured in units of $(4M|E_0|)^{-1}$.

We have made an estimate of the constants by carrying out a variational calculation to obtain the minimum value for γ, and approximate expressions for $u(x)$ and $v(x)$ in order to calculate Q. Hulthén[14] has shown that for the simple Schrödinger equation with the potential $e^{-\alpha x}/x$, a good approximate solution is

$$\{a_1(1 - e^{-x}) + a_2(1 - e^{-x})^2\} e^{-x/2}.$$

Hence we have taken this expression for $u(x)$, and an analogous expression for $v(x)$. That is, we take

$$\begin{aligned} u(x) &= \{a_1(1 - e^{-x}) + a_2(1 - e^{-x})^2\} e^{-x/2}, \\ v(x) &= \{b_1(1 - e^{-x})^4 + b_2(1 - e^{-x})^5\} \\ &\qquad \times \left(1 + \frac{6}{x} + \frac{12}{x^2}\right) e^{-x/2}. \end{aligned} \tag{119}$$

[13] Since from now on we consider only the ground state wave function (98), we drop the subscript 0.

[14] L. Hulthén, Arkiv för mat. astr. och fysik **A28**, No. 5 (1942).

They have the required behavior at both small and large values of x. We insert these expressions in the energy which is

$$\frac{1}{4}=\int_0^\infty\Big[u\frac{d^2u}{dx^2}+v\frac{d^2v}{dx^2}-\frac{6v^2}{x^2}+u^2j(x)+2\sqrt{2}uvk(x)+v^2\{j(x)-k(x)\}\Big]dx, \quad (120)$$

and determine the constants a_1, a_2, b_1, and b_2 so that γ is a minimum and the normalization condition (117) is satisfied. The calculation is tedious but straightforward, and we give only the results. Taking $|E_0|=2.17$ Mev, $\kappa=177$ m, and $\mu/\kappa=2$, we obtain

$$\gamma=0.433, \quad (121)$$

$$a_1=3.18, \quad a_2=-2.01, \quad b_1=0.095, \quad b_2=-0.072. \quad (122)$$

(121) gives $(f\kappa)^2=0.375$, and the evaluation of the quadrupole moment with (119) and (122) gives $Q=1.6\times10^{-27}$ cm^2. The latter seems to indicate that the ratio μ/κ should be larger to give the right value for Q. However, it is well known that the variational method may give quite good results for the quantity which is minimized (in this case f), but that the use of the approximate wave functions to calculate other properties may give very bad results. In our case this is quite possible since Q is proportional to $v(x)$ which contributes very little to the energy, and moreover the main contribution to Q comes from the parts of the wave functions at large distances from the origin which do not affect the energy very much. In fact the same calculation made with $\mu/\kappa=3$ actually gives a smaller value for Q. Thus it seems that it is not possible to obtain anything but a rough estimate $\mu/\kappa\sim2$ without going into a much more careful computation.

We can, however, show that the conditions given in the beginning of this part can be satisfied with our estimated values for the constants. Now since $E_{\text{isob}}=3a/2f^2$,

$$\frac{E_{\text{bind}}}{E_{\text{isob}}}=\frac{2(f\kappa)^2}{3(a\kappa)}\left(\frac{E_{\text{bind}}}{\kappa}\right)\leq\frac{0.0056}{(a\kappa)}. \quad (123)$$

Thus there is a region of values for a (and consequently for E_{isob}) for which all the inequalities in the conditions given above hold by a factor of about 10.

D. The Magnetic Moment

The calculation of the magnetic moment of the deuteron is exactly analogous to that given in P-D for a single nucleon. The current vector is[15]

$$\begin{aligned}\mathbf{j}=&\varphi^2\nabla\varphi^1-\varphi^1\nabla\varphi^2\\&+(4\pi)^{\frac{1}{2}}f\textstyle\sum_A\boldsymbol{\sigma}_A(\varphi^1\tau_A{}^2-\varphi^2\tau_A{}^1)U_A\\&+\psi^2\times(\nabla\times\psi^1)-\psi^1\times(\nabla\times\psi^2)\\&+(4\pi)^{\frac{1}{2}}f\textstyle\sum_A\{(\boldsymbol{\sigma}_A\times\psi^1)\tau_A{}^2\\&-(\boldsymbol{\sigma}_A\times\psi^2)\tau_A{}^1\}U_A. \quad (124)\end{aligned}$$

Let us first consider just the part due to the pseudoscalar meson. Inserting in the expansion (46) the value corresponding to the absence of free mesons ($\varphi'^\alpha=0$) and the lowest eigenvalue of the interaction energy (52), we obtain with the aid of (50)

$$\varphi^\alpha=\frac{f}{(4\pi)^{\frac{1}{2}}}\sum_{A,i}e^\alpha_{Ai}\frac{\partial X_A}{\partial x_i}. \quad (125)$$

We have neglected terms in J_{ij}/I in (50) since they only give rise to higher order terms. Putting (125) in the pseudoscalar part of (124), we obtain

$$\begin{aligned}j_k=\frac{f^2}{4\pi}\sum_{A,B,i,j}\Big[&\Big(e^2_{Ai}\frac{\partial X_A}{\partial x_i}\Big)\frac{\partial}{\partial x_k}\Big(e^1_{Bj}\frac{\partial X_B}{\partial x_j}\Big)\\&-\Big(e^1_{Ai}\frac{\partial X_A}{\partial x_i}\Big)\frac{\partial}{\partial x_k}\Big(e^2_{Bj}\frac{\partial X_B}{\partial x_j}\Big)\\&-4\pi\Big\{\Big(e^1_{Ai}\frac{\partial X_A}{\partial x_i}\Big)e^2_{Bk}-\Big(e^2_{Ai}\frac{\partial X_A}{\partial x_i}\Big)e^1_{Bk}\Big\}U_B\Big],\end{aligned}$$

or

$$\begin{aligned}j_k=\frac{f^2}{4\pi}\sum_{A,B,i,j}&\{e^2_{Ai}e^1_{Bj}-e^1_{Ai}e^2_{Bj}\}\\&\times\Big\{\frac{\partial X_A}{\partial x_i}\frac{\partial^2X_B}{\partial x_k\partial x_j}+4\pi\delta_{jk}\frac{\partial X_A}{\partial x_i}U_B\Big\}. \quad (126)\end{aligned}$$

The magnetic moment is given by

$$M_{kl}=\frac{e}{2}\int(x_kj_l-x_lj_k)dV, \quad (127)$$

[15] We have not written down here the terms which would occur if the vector meson had an anomalous magnetic moment, but this will not change our results in any way.

and inserting (126) for j_k, we obtain

$$M_{kl}=\frac{ef^2}{8\pi}\sum_{A,B,i,j}\{e^{2}_{Ai}e^{1}_{Bj}-e^{1}_{Ai}e^{2}_{Bj}\}(A^{ij}_{kl}-A^{ij}_{lk}), \quad (128)$$

where

$$A^{ij}_{kl}=\int\int\left[x_k\left\{\frac{\partial X_A}{\partial x_i}\frac{\partial^2 X_B}{\partial x_l\partial x_j}+4\pi\delta_{jl}\frac{\partial X_A}{\partial x_i}U_B\right\}\right]dV. \quad (129)$$

In the double sum over A, B in (128), the terms with $A=B$ give the moments of the individual particles, and they are just the expressions calculated in P-D. Since it was found there that the moments of the proton and the neutron are equal in magnitude and opposite in sign, these terms will cancel out, and we need only take the terms with $A\neq B$. Since A^{ij}_{kl} is not altered by the interchange of particles I and II, (128) can be written

$$M_{kl}=\frac{ef^2}{8\pi}\sum_{i,j}P_{ij}(A^{ij}_{kl}-A^{ij}_{lk}) \quad (130)$$

with

$$P_{ij}=\{e^{2}_{1i}e^{1}_{11j}-e^{1}_{1i}e^{2}_{11j}+e^{2}_{11i}e^{1}_{1j}-e^{1}_{11i}e^{2}_{1j}\}. \quad (131)$$

We see that P_{ij} is antisymmetric in i, j so that it has only 3 independent components. In order to compute the component of **M** in a given direction, we need the diagonal matrix elements of the P_{ij} in the (S, T, M, N) representation. However the P_{ij} change sign under the operation (85) so that they cannot have any matrix elements between states with the same signature. Thus this theory gives zero magnetic moment for the deuteron.

There is no need to continue the calculation for the vector meson since the reason that the magnetic moment vanishes in the above case is so general that it is clear the same result will be obtained in all cases of the strong coupling theory.

Of course the existence of the tensor force gives a magnetic moment due to the orbital motion of the proton, but this contribution is very small (of the order of a few percent of the observed value).

V. HEAVY NUCLEI

It was shown in S-D that the charged scalar and the neutral pseudoscalar meson theories give rise to nuclear forces which have no saturation property. These results are due to the fact that in these theories, any number of nucleons can be arranged in a symmetrical configuration in such a way that each particle interacts with an attractive potential with all the others: in the charged scalar theory by having the isotopic spin vectors of all the particles in the same direction, and in the neutral pseudoscalar theory by having all the particles lie in a plane with all their spin vectors parallel and perpendicular to this plane. In the neutral mixed theory such configurations do not lead to attractive interaction between the particles.[16] In the symmetrical pseudoscalar and symmetrical mixed theories, we have a system of 3 orthonormal vectors $\mathbf{e}^{\alpha}$ instead of a single spin or isotopic spin vector for each particle. The only symmetrical configuration in these cases is obtained by having all the vectors parallel, and the interaction for this arrangement is repulsive. Thus for these theories the potential energy will be proportional to the number of particles and not to its square as in the cases treated in S-D.

However, for the forces to have the saturation property, it is also necessary that the kinetic energy of the particles increase faster than the attractive potential energy as the radius of the nucleus decreases in order that there exist a minimum for the total energy of the system. This condition is fulfilled in the usual weak coupling theory[17] since, if we denote by r_0 the radius corresponding to the volume occupied by each particle, the kinetic energy increases as r_0^{-2}, and the dependence of the potential energy, of course, is the same as the behavior of the radial potential function, but this cannot increase faster than r^{-1}. In the strong coupling theory however, the existence of isobar states increases the number of allowed states in a given volume of space with the same upper limit for the energy, and this will change the dependence on r_0 of both the kinetic and potential energies.

In order to see how this feature changes our results, we have made a calculation similar to that carried out in Bethe and Bacher. We make

[16] The second configuration gives attraction only when $K(r)>J(r)$. For $\mu/\kappa\sim 2$, this condition holds only when r is greater than about $2/\kappa$ and for such distances, both $J(r)$ and $K(r)$ are very small.

[17] H. A. Bethe and R. F. Bacher, Rev. Mod. Phys. **8**, 82 (1936), in particular §25.

a Hartree approximation for the wave function of the system with free particle solutions for the individual wave functions, both for the spatial and for the spin parts. The latter are hypergeometric functions and have been investigated by Rademacher and Reiche[18] in connection with the quantum theory of a symmetrical top. The integrals which we need are all tabulated there. We shall not give the details of the calculation but just make a few remarks on the points which differ from the calculation given in Bethe and Bacher.

The number of particles N is now the product of N_k and N_s where N_k is the number of states with kinetic energy less than $k_0^2/2M$, and N_s is the number of states with isobar energy less than $(a/4f^2)\{s_0(s_0+1)-\frac{3}{4}\}$. The total energy of the system is

$$E=E_k+E_s+E_p \tag{132}$$

where E_k, E_s, and E_p denote the kinetic, isobar, and the potential energy, respectively. If we consider s_0 to be large compared to 1 and keep only the highest powers of it, then N_k, N_s and E_k, E_s depend on k_0, s_0 in the same way. Thus for (132) to be a minimum,

$$k_0^2/2M=(a/4f^2)s_0^2, \tag{133}$$

and

$$E_k=E_s. \tag{134}$$

Moreover they are proportional to N/r_0. E_p on the other hand turns out to be proportional to $N/(r_0)^4$, and there does exist a value of r_0 at which E is a minimum.

In the above consideration we have neglected the Coulomb energy, and though this may not affect the saturation property, it does bring in a serious difficulty in connection with the stability of heavy nuclei with high charge. As pointed out by Fierz,[19] in a nucleus like that of uranium, the transition of a proton or a neutron to a particle with negative charge is energetically favorable unless the isobar separation is about 50 Mev. However such a value for the isobar separation is inadmissible since we would then have to take the size of the source of the same magnitude as the Compton wave-lengths of the mesons. That is, the size of the source would have to be taken as the same order of magnitude as the range of the nuclear forces, and hence the shape of the source would completely determine the nature of the nuclear forces. Furthermore, such a value also removes the main reason for the introduction of the strong coupling theory; namely, to give a small value for the meson scattering cross section.

VI. CONCLUSIONS

Our results show that the theory considered here suffers from two grave difficulties; it gives a magnetic moment for the deuteron a value only a few percent of the observed value, and it predicts instability of highly charged nuclei. These results seem to be fundamental properties of all strong coupling theories, and there does not seem to be any way of overcoming them.

These difficulties are not present in the weak coupling theory, and it thus seems advisable to go back and reconsider the arguments which led us to take up the strong coupling theory in favor of the weak coupling theory. The main difficulties in the weak coupling theories are the divergences due to the treatment of the heavy particles as a point source, and the large scattering cross section of the meson. As already pointed out by one of us,[20] the first difficulty can be overcome by using the λ-process developed by Wentzel and Dirac, and the second by using the theory of radiation damping developed by Heitler and Wilson. In addition, the weak coupling theory developed in this way has the advantage of relativistic invariance which the strong coupling theory does not have on account of the finite size of the source. Thus there is no reason now to consider the strong coupling theory, and we should go back to the weak coupling theory.

As stated at the end of Part A of Section III, the transition from the strong coupling to the weak coupling theory can be made by a simple replacement of the spin and isotopic spin vectors in place of the vectors $\mathbf{e}^\alpha$. Thus the radial wave functions for the ground state of the deuteron in the weak coupling theory satisfy exactly the

[18] H. Rademacher and F. Reiche, Zeits. f. Physik **39**, 444 (1926), and **41**, 453 (1927).

[19] M. Fierz, Helv. Phys. Acta **14**, 105 (1941).

[20] W. Pauli, Bull. Am. Phys. Soc. New York Meeting, Jan. 22–23, 1943, Abstract No. 25: Phys. Rev. **63**, 221 (1943).

same differential equations (114) except that as shown in the Appendix, γ is redefined as

$$\gamma=2f'^2M(M|E_0|)^{\frac{1}{2}},$$

where f' is the coupling constant in this theory, and there is no longer any approximation due to the higher isobar states since they do not exist. Hence the computation in Part C of Section IV applies just as well for this case, and we obtain $(f'\kappa)^2=\frac{1}{9}(f\kappa)^2\backsimeq 0.042$ for the strength of the coupling. The ratio of the masses is unchanged.

APPENDIX

Calculation of the Matrix Element of e_i^α

The e_i^α satisfy the following commutation relations with s_i and t^α [cf. P-D, Eq. (55)]:

$$\begin{array}{ll}[s_i, e_j^\alpha]=ie_k^\alpha, & i, j, k, \text{ cyclic;}\\ [t^\alpha, e_i^\beta]=ie_i^\gamma, & \alpha, \beta, \gamma, \text{ cyclic.}\end{array} \tag{135}$$

It is more convenient to introduce the imaginary components

$$\begin{array}{llll}s_+=s_1+is_2, & s_-=s_1-is_2, & s_3;\\ t^+=t^1+it^2, & t^-=t^1-it^2, & t^3;\end{array} \tag{136}$$

and

$$\begin{array}{ll}e_+{}^+=e_1{}^1-e_2{}^2+i(e_2{}^1+e_1{}^2), & e_+{}^3=e_1{}^3+ie_2{}^3,\\ e_+{}^-=e_1{}^1+e_2{}^2+i(e_2{}^1-e_1{}^2), & e_-{}^3=e_1{}^3-ie_2{}^3,\\ e_-{}^+=e_1{}^1+e_2{}^2-i(e_2{}^1-e_1{}^2), & e_3{}^+=e_3{}^1+ie_3{}^2,\\ e_-{}^-=e_1{}^1-e_2{}^2-i(e_2{}^1+e_1{}^2), & e_3{}^-=e_3{}^1-ie_3{}^2,\\ e_3{}^3.\end{array} \tag{137}$$

For the matrix elements of the e_i^α between the states (s, m, n) and (s', m', n'), we have the following selection rules:

(1) for any e_i^α, $s'=s-1$, s, or $s+1$;
(2) for e_+^α, $m'=m-1$;
(3) for e_3^α, $m'=m$;
(4) for e_-^α, $m'=m+1$;
(5) for $e_i{}^+$, $n'=n-1$;
(6) for $e_i{}^3$, $n'=n$;
(7) for $e_i{}^-$, $n'=n+1$.

Matrix elements which do not satisfy these conditions all vanish.

The non-vanishing matrix elements of s_i and t^α are:

$$\begin{array}{l}(m|s_+|m-1)=[(s+m)(s-m+1)]^{\frac{1}{2}},\\ (m|s_3|m)=m,\\ (m|s_-|m+1)=[(s+m+1)(s-m)]^{\frac{1}{2}},\end{array} \tag{138}$$

with exactly the same expressions for t^+, t^3, t^- with m replaced by n. Hence in order to satisfy the commutation relations (135), we must have the m dependence of the e_i^α as follows:

$$\begin{array}{l}(s, m, n|e_+^\alpha|s-1, m-1, n')\\ \qquad=-(s, n|c^\alpha|s-1, n')[(s+m)(s+m-1)]^{\frac{1}{2}},\\ (s, m, n|e_+^\alpha|s, m-1, n')\\ \qquad=(s, n|c^\alpha|s, n')[(s+m)(s-m+1)]^{\frac{1}{2}},\\ (s, m, n|e_+^\alpha|s+1, m-1, n')\\ \qquad=(s, n|c^\alpha|s+1, n')[(s-m+1)(s-m+2)]^{\frac{1}{2}},\\ (s, m, n|e_3^\alpha|s-1, m, n')=(s, n|c^\alpha|s-1, n')(s^2-m^2)^{\frac{1}{2}},\\ (s, m, n|e_3^\alpha|s, m, n')=(s, n|c^\alpha|s, n')m,\\ (s, m, n|e_3^\alpha|s+1, m, n')=(s, n|c^\alpha|s+1, n')[(s+1)^2-m^2]^{\frac{1}{2}},\\ (s, m, n|e_-^\alpha|s-1, m+1, n')\\ \qquad=(s, n|c^\alpha|s-1, n')[(s-m)(s-m-1)]^{\frac{1}{2}},\\ (s, m, n|e_-^\alpha|s, m+1, n')\\ \qquad=(s, n|c^\alpha|s, n')[(s-m)(s+m+1)]^{\frac{1}{2}},\\ (s, m, n|e_-^\alpha|s+1, m+1, n')\\ \qquad=-(s, n|c^\alpha|s+1, n')[(s+m+1)(s+m+2)]^{\frac{1}{2}}.\end{array}$$

Similarly to satisfy the commutation relations, the n-dependence must be as follows:

$$\begin{array}{l}(s, n|c^+|s-1, n-1)=-(s|b|s-1)[(s+n)(s+n-1)]^{\frac{1}{2}},\\ (s, n|c^+|s, n-1)=(s|b|s)[(s+n)(s-n+1)]^{\frac{1}{2}},\\ (s, n|c^+|s+1, n-1)=(s|b|s+1)[(s-n+1)(s-n+2)]^{\frac{1}{2}},\\ (s, n|c^3|s-1, n)=(s|b|s-1)[s^2-n^2]^{\frac{1}{2}},\\ (s, n|c^3|s, n)=(s|b|s)n,\\ (s, n|c^3|s+1, n)=(s|b|s+1)[(s+1)^2-n^2]^{\frac{1}{2}},\\ (s, n|c^-|s-1, n+1)=(s|b|s-1)[(s-n)(s-n-1)]^{\frac{1}{2}},\\ (s, n|c^-|s, n+1)=(s|b|s)[(s-n)(s+n+1)]^{\frac{1}{2}},\\ (s, n|c^-|s+1, n+1)=-(s|b|s+1)[(s+n+1)(s+n+2)]^{\frac{1}{2}}.\end{array}$$

To obtain the s-dependence, we use the normalization condition which the e_i^α satisfy [cf. P-D, Eq. (51a)]. Using (137) we find

$$\begin{array}{l}e_+{}^3e_-{}^3+(e_3{}^3)^2=1,\\ e_+{}^+e_-{}^-+e_-{}^+e_+{}^-+2e_3{}^+e_3{}^-=4,\end{array} \tag{139}$$

and from these conditions, we obtain the equations

$$\begin{array}{l}s^2(2s-1)(s|b|s-1)^2+(s+1)^2(2s+3)(s|b|s+1)^2=1,\\ s^2(s-1)(2s-1)(s|b|s-1)^2+s^2(s+1)^2(s|b|s)^2\\ \qquad+(s+1)^2(s+2)(2s+3)(s|b|s+1)^2=2.\end{array} \tag{140}$$

Then from the relation

$$(\mathbf{s}\cdot\mathbf{e}^3)=-t^3 \tag{141}$$

we have

$$(s|b|s)=-1/s(s+1). \tag{142}$$

Thus (140) can now be solved, and we finally obtain

$$\begin{array}{l}(s|b|s-1)=1/s[(2s-1)(2s+1)]^{\frac{1}{2}},\\ (s|b|s+1)=1/(s+1)[(2s+1)(2s+3)]^{\frac{1}{2}}.\end{array} \tag{143}$$

In particular for $s=s'=\frac{1}{2}$, we have the relation

$$(\tfrac{1}{2}, m, n|\mathbf{e}^\alpha|\tfrac{1}{2}, m', n')=\tfrac{1}{2}(m, n|\boldsymbol{\sigma}\tau^\alpha|m', n') \tag{144}$$

which gives the connection between the strong and the weak coupling theories; namely, the only difference for the ground state is the occurrence of a factor $\frac{1}{4}$ in the interaction energy which merely changes the values of the coupling constants.

PHYSICAL REVIEW VOLUME 63, NUMBERS 11 AND 12 JUNE 1 AND 15, 1943

The Antisymmetrical Interaction in Beta-Decay Theory

CHARLES L. CRITCHFIELD*
Research Laboratory of Physics, Harvard University, Cambridge, Massachusetts
(Received March 3, 1943)

Forms of the beta-decay interaction are sought which are totally symmetric and totally antisymmetric to the interchange of any two of the particles involved in the emission. It is found that there is no symmetric interaction and one antisymmetric. The antisymmetric interaction allows transitions without change of parity and with a change of nuclear spin of either 0 or ± 1, including $0 \rightarrow 0$. First forbidden transitions entail a change of parity and $\Delta i = 0, \pm 1$ or ± 2. Second forbidden transitions are characterized by $\Delta i = \pm 2, \pm 3$ and no change in parity. The contributions of electron-neutrino states of definite angular momenta are presented explicitly as an aid in the study of the influence of the nucleus on the light particle waves. The influence of the Coulomb field is discussed.

I. INTRODUCTION

IN the first paper describing a field theory of beta-activity Fermi[1] drew an analogy with electromagnetic theory and assumed the interaction to be the scalar product of a four-vector constructed from the wave functions of neutron and proton with a four-vector constructed from electron and neutrino waves. It is well known that besides the four-vector one can construct from products of two wave functions an axial four-vector, a skew-symmetric tensor, and two scalars, one of which changes sign under reflection and is commonly called a pseudoscalar. Invariant products of any of these five covariant quantities with the corresponding contravariant quantities formed from electron and neutrino wave functions present a fivefold infinite manifold of choices for an interaction between heavy and light particles. The experimental material that may make possible a particular choice of an interaction consists of (1) the selection rules obeyed in beta-emission and (2) the shape of the beta-ray spectrum, particularly the shape of the spectra in forbidden transitions.

An alternative choice of interaction has been proposed by Gamow and Teller[2] who noted that the selection rules imposed by the four-vector interaction were inconsistent with the beta-activity of ThCC′. The same violation of Fermi's selection rules appears to be made in the beta-activity of He^6 and kindred nuclei. The Gamow-Teller selection rules are less stringent than the Fermi rules in that they allow $\Delta i = 0, \pm 1$ (except $0 \rightarrow 0$), whereas the Fermi rules allow only $\Delta i = 0$ (including $0 \rightarrow 0$). Interactions that give G-T rules are the tensor and the axial vector interactions.

Allowed transitions are defined as those transitions that are independent of the small components (i.e., the particle velocity) of the Dirac waves for the nuclear particles and in which the electron and neutrino waves have no node through the nucleus. The shape of the allowed beta-ray spectrum is the same for any one of the five possibilities of interaction listed above. It may be slightly different for linear combinations. Only in forbidden transitions will the spectra of the five possibilities be different.

Uhlenbeck and Konopinski[3] have compared the shapes to be expected from each of the five invariants with the experimental results on Na^{24}, P^{32}, and RaE. Their conclusion is that there is evidence against all these interactions taken singly except the tensor interaction. It is possible that actually none of these interactions is sufficient by itself to explain the experimental results but the tensor interaction cannot be excluded at present because of the great flexibility of this interaction which contains several unknown matrix elements. It is also possible that a linear combination of the five possibilities will account for experiment although no one taken singly is able to do so.

* Now at the Geophysical Laboratory, The Carnegie Institution of Washington, Washington, D. C.

[1] E. Fermi, Zeits. f. Physik **88**, 161 (1934).

[2] G. Gamow and E. Teller, Phys. Rev. **49**, 895 (1936).

[3] E. J. Konopinski and G. E. Uhlenbeck, Phys. Rev. **60**, 308 (1941).

The supposition that a particular one of the five invariants discussed might be a complete description of fact is a kind of extension of Fermi's analogy to electromagnetic theory. It is what we would reasonably expect to obtain if beta-decay occurs in two steps, i.e., the proton emits a meson which then creates a positron and a neutrino. In this description one would naturally form covariant quantities with proton and neutron waves and contract them with the analogous light particle functions. The analogy with electromagnetism then leads to the hope that one of these covariants is enough. If, on the other hand, the beta-process is not analogous to radiation theory in this sense, linear combinations of the five invariants are as acceptable possibilities as the invariants taken singly.

It is the purpose of this paper to present the theoretical predictions of a particular linear combination of the five invariants. The basis on which this combination is chosen is as follows: The beta-process is considered to be an essentially four-particle process, and the requirement on the interaction is that it shall be either totally symmetric or totally antisymmetric to the interchange of role of any two of the participating particles.

II. THE INTERACTION

The symmetry properties of the interaction between fields of the four particles are most easily determined if the beta-process is described as the simultaneous creation of neutron, proton, electron, and neutrino. Since all these particles have spin $\frac{1}{2}h$, this description can be permitted by assuming the Dirac wave equation and the hole theory extension of that equation for all four particles. A hole in the theoretical neutron sea of negative energy is then the experimentally observed neutron. In negative beta-emission such a neutron hole is filled at the same instant that a proton appears to take its place in the nucleus and electron and neutrino are created. Positive beta-emission is then a simultaneous disappearance of four particles: a proton of positive energy and "neutron," electron, and neutrino of negative energy. In this description it is evident that symmetrization of the interaction producing beta-activity is identical with symmetrization of an invariant product wave function of four particles of spin one-half.

Four particles of spin $\frac{1}{2}h$ cannot form a totally symmetrical state that is invariant to Lorentz transformations. This may be seen at once with the aid of the calculation rules of Van der Waerden's spinor calculus.[4] If two of the four-wave functions have dotted indices and two undotted, the invariant forms are not symmetrical because of the skew-symmetry of the ϵ-operator. If all indices are undotted (or all dotted), the symmetric invariant vanishes because of the identity:

$$\epsilon^{\lambda\mu}\epsilon^{\kappa\nu}+\epsilon^{\kappa\lambda}\epsilon^{\mu\nu}+\epsilon^{\mu\kappa}\epsilon^{\lambda\nu}\equiv 0.$$

The symmetrization in this discussion is restricted, of course, to space and spin coordinates. If isotopic spin were introduced, symmetrization would have no significance.

There is one and only one totally antisymmetric invariant wave function constructed of the four Dirac ψ-functions, *viz.*,

$$\chi(\mathbf{x})\equiv\begin{vmatrix}\Psi_1 & \Phi_1 & \psi_1 & \phi_1\\ \Psi_2 & \Phi_2 & \psi_2 & \phi_2\\ \Psi_3 & \Phi_3 & \psi_3 & \phi_3\\ \Psi_4 & \Phi_4 & \psi_4 & \phi_4\end{vmatrix}_{\mathbf{x}}. \qquad (1)$$

Different Greek letters are used to distinguish between particles and, in the following, Ψ shall stand for the neutron wave function, Φ for the proton, ψ, electron, and ϕ, neutrino. All are taken at the same point in space, $\mathbf{x}$. The subscripts in Eq. (1) refer to the four components of a Dirac wave equation, the particular form of which is immaterial as long as it is the same for all particles. That χ is an invariant is readily seen from the fact that the determinants of the matrices that represent Lorentz transformations are unity. Let S be the unitary matrix that represents a certain Lorentz transformation:

$$\psi'=S\psi. \qquad (2)$$

This S applies to all four wave functions in the determinant, Eq. (1), so if we write

$$\chi\equiv|D|,$$

[4] B. Van der Waerden, *Göttingen Nachrichten* (1929), p. 100.

then the new antisymmetric wave function, χ', is

$$\chi' = |S \cdot D| = |S| \times |D| = |D| = \chi, \quad \text{Q.E.D.} \quad (3)$$

For the sake of definiteness the numerical subscripts in Eq. (1) will be assumed to refer to the four rows and columns in their usual order in the α and β matrices in the familiar form of Dirac's equation:

$$\left[i\frac{\hbar}{c}\frac{\partial}{\partial t} - (\boldsymbol{\alpha}, \mathbf{p}) - \beta mc\right]\psi = 0. \quad (4)$$

If we consider the wave functions in Eq. (1) to be quantized, i.e., as operators, the form of the interaction between fields of the elementary particles becomes:

$$H' = g\int [\chi(\mathbf{x}) + \chi(\mathbf{x})^*]d\mathbf{x}, \quad (5)$$

where g is the "Fermi constant" having dimensions of energy times volume, and $\chi(\mathbf{x})$ gives rise to the disappearance of four particles at the point $\mathbf{x}$; $\chi(\mathbf{x})^*$ gives rise to their appearance. The transitions induced by H' are between states of equal energy and therefore the probability of beta-emission is given by the well-known formula

$$P(E)dE = 2\pi\hbar^{-1}|H'|^2\rho_n(w-E)\rho_e(E)dE. \quad (6)$$

In Eq. (6) $\rho_n(w-E)$ is the density of neutrino states of energy $w-E$ and $\rho_e(E)$ the density of electron states of energy E. The energy released by the nucleus is w.

An obvious difference between the form of this theory and that of preceding ones is that H' is an integral over products of Ψ and Φ or over products of Ψ^* and Φ^*. This is only a formal difference from the customary method of calculating matrix elements which contain Ψ^* and Φ together, etc., but it will be convenient all around to introduce Ψ^* in place of Ψ in Eq. (1). Then the physical interpretation of Eq. (5) will be the usual disappearance of a neutron when proton, electron, and neutrino are created or vice versa.

The replacement of Ψ by Ψ^* at the same time that positive and negative energy levels are exchanged has been studied by Furry[5] and Pauli.[6] These authors have shown that there is a unitary operator θ such that

$$\psi^* \rightarrow \psi\theta \quad (7)$$

when positive and negative energy levels are interchanged. In the spin coordinates pertinent to Eq. (4)

$$\theta = -i\beta\alpha_2. \quad (8)$$

Applying θ to the neutron waves in Eq. (1) and substituting in Eq. (5), we get the interaction for positron emission:

$$H_p' = -g\int \begin{vmatrix} \Psi_4(\mathbf{x})^* & \Phi_1(\mathbf{x}) & \psi_1(\mathbf{x}) & \phi_1(\mathbf{x}) \\ -\Psi_3(\mathbf{x})^* & \Phi_2(\mathbf{x}) & \psi_2(\mathbf{x}) & \phi_2(\mathbf{x}) \\ -\Psi_2(\mathbf{x})^* & \Phi_3(\mathbf{x}) & \psi_3(\mathbf{x}) & \phi_3(\mathbf{x}) \\ \Psi_1(\mathbf{x})^* & \Phi_4(\mathbf{x}) & \psi_4(\mathbf{x}) & \phi_4(\mathbf{x}) \end{vmatrix} d\mathbf{x}. \quad (9)$$

Electron emission is given by the complex conjugate of Eq. (9), but since in the expression for the probability of emission only $|H'|^2$ appears, it is sufficient to consider Eq. (9) alone.

It is convenient to expand Eq. (9) for H_p' as a linear combination of the familiar invariants. For this purpose we shall use the Dirac operators, ρ and σ, *acting on the heavy particle waves only*

$$\begin{aligned} &\rho_1 = i\alpha_x\alpha_y\alpha_z, \quad \rho_2 = \beta\alpha_x\alpha_y\alpha_z, \quad \rho_3 = \beta, \\ &\sigma_x = i\alpha_y\alpha_z, \quad \sigma_y = i\alpha_x\alpha_z, \quad \sigma_z = i\alpha_x\alpha_y. \end{aligned} \quad (10)$$

In this formulation Eq. (9) becomes

$$\begin{aligned} H_p' = g\cdot\tfrac{1}{2}\int \Psi^*\Bigg\{ & (\rho_1+i\rho_2)\begin{vmatrix}\psi_1 & \phi_1\\ \psi_2 & \phi_2\end{vmatrix} \\ & -(\rho_1-i\rho_2)\begin{vmatrix}\psi_3 & \phi_3\\ \psi_4 & \phi_4\end{vmatrix} \\ & +\rho_3\left[\begin{vmatrix}\psi_2 & \phi_2\\ \psi_3 & \phi_3\end{vmatrix} - \begin{vmatrix}\psi_1 & \phi_1\\ \psi_4 & \phi_4\end{vmatrix}\right] \\ & -(\sigma_x+i\sigma_y)\begin{vmatrix}\psi_1 & \phi_1\\ \psi_3 & \phi_3\end{vmatrix} \\ & +(\sigma_x-i\sigma_y)\begin{vmatrix}\psi_2 & \phi_2\\ \psi_4 & \phi_4\end{vmatrix} \\ & +\sigma_z\left[\begin{vmatrix}\psi_2 & \phi_2\\ \psi_3 & \phi_3\end{vmatrix} + \begin{vmatrix}\psi_1 & \phi_1\\ \psi_4 & \phi_4\end{vmatrix}\right]\Bigg\}\Phi d\mathbf{x}. \end{aligned} \quad (11)$$

From this expansion selection rules can be

[5] W. H. Furry, Phys. Rev. **51**, 125 (1936); **54**, 56 (1938).
[6] W. Pauli, Inst. H. Poincaré Ann. **6**, 130 (1936).

deduced at once. The terms proportional to the σ's and to ρ_1 constitute an axial vector interaction and give $\Delta i=0, \pm 1$ ($0\rightarrow 0$ excluded) with no change in parity in allowed transitions. The ρ_3 term is the scalar interaction and gives $\Delta i=0$ ($0\rightarrow 0$ included) no change in parity. The ρ_2 term is the pseudoscalar and gives no allowed transitions.

A curious form of the rule for determining the change in parity is evident from Eq. (11). It will be noted that the light particle functions that are associated with ρ_3 and σ (which mix large terms of proton waves with large terms of neutron waves) contain products of one small and one large component of the light particle waves. Thus, if we follow the customary method of giving the electron (and neutrino) the orbital quantum number L that applies to the spin eigenfunction, i.e., the same as the large component, we obtain the rule: There is no change in the parity of the nucleus if the sum of orbital quantum numbers of electron and neutrino is odd; the parity changes if the sum is even. This is just the reverse of the rule that applies to particles of integral spin and also of the rule that applies to the absorption and subsequent emission of a single particle of any spin. The root of the paradox lies in assigning a definite parity to wave functions of spin $\frac{1}{2}\hbar$. The form of the matrix that represents inversion of the coordinate system[5] shows that the phase of these waves is changed by $\frac{1}{2}\pi$ rather than 0 or π, the phase of the large components increasing if that of the small decreases and vice versa. Thus two successive inversions lead to the original wave function but with opposite sign, the same result as that obtained by rotating the coordinates by 360° about some axis. It is well known that there is no paradox in the case of the rotation because the space of all rotations, although continuous, is two-sided.[7]

A short discussion of the above results has been presented in a letter to the editor of *The Physical Review*.[8] It is pointed out in the letter that addition of scalar and axial vector operators increases the lifetimes of the $4n\pm 2$ nuclei relative to the $4n\pm 1$ nuclei in allowed transitions.[9] This improves the agreement of theory with experiment for C^{10} and F^{18} but makes it worse for He^6. Furthermore, the ratio of the transitions to excited and to ground states of the nuclei considered by Grönblom[9] is predicted more closely by the antisymmetric theory than by the axial vector (or tensor) alone. The reason for this is again the relatively stronger transitions without change of spin which the antisymmetric theory predicts.

III. MATRIX ELEMENTS

The shapes of the forbidden spectra under the theory presented in this paper can be derived from the results of reference 3 on the scalar, axial vector, and pseudoscalar interactions. A slight extension is necessary to include some cross product terms in the first forbidden spectra. I have repeated the work of Konopinski and Uhlenbeck insofar as it applies to the antisymmetrical theory of beta-decay by the method which uses the eigenfunctions of both electron and neutrino in polar coordinates. Except for the addition of cross product terms between different kinds of interaction, the results are, of course, the same as in reference 3. Nevertheless an outline of the method is presented, and the results are given in detail for several reasons. The chief reason is to have the contributions of various electron and neutrino angular momenta presented separately because the possible influence of the nucleus on these contributions is very likely different. Beta-spectra may furnish a useful experimental means of determining the influence of nuclei on electron and neutrino waves. It appears certain from the work of Rabi *et al.*[10] that there is no spin dependent force between electron and nucleus except that due to magnetic moments; but it may well be that there are spin-independent forces in addition to the Coulomb field. Another reason for presenting the calculations in polar coordinates is to throw light on the detailed effect of the Coulomb field on the shape of the beta-spectrum and also on the life-

[7] Cf. E. Wigner, *Gruppentheorie und ihre anwendung auf die quantenmechanik der atomspektren* (Braunschweig, F. Vieweg & sohn, 1931), p. 99.

[8] C. Critchfield and E. Wigner, Phys. Rev. **60**, 412 (1941).

[9] E. Wigner, Phys. Rev. **56**, 526 (1939), and in the same issue, B. Grönblom, Phys. Rev. **56**, 508 (1939).

[10] Rabi, Millman, Kusch, and Zacharias, Phys. Rev. **55**, 526 (1939); Kusch, Millman, and Rabi, Phys. Rev. **57**, 765 (1940).

times of the beta-activities. The latter questions are taken up in Section IV.

In this section it will be assumed that there is no interaction between the electron and the electromagnetic field of the nucleus. We have, therefore, to use the eigenfunctions of kinetic energy for both electron and neutrino in Eq. (11) and substitute H_p' in turn in Eq. (6).

The "matrix element" of beta-decay theory, M, is related to our H' by

$$M \equiv -i(2\pi\hbar^2 R/g p_e p_n) H', \tag{12}$$

where R is the radius of the sphere in which quantization is effected, p_e is the momentum of the electron, and p_n is the momentum of the neutrino. Using M in place of H_p' we find the probability of emission of a positron and neutrino (absorption from states ψ and ϕ, respectively) with total angular momentum $j\hbar$ and z-component $m\hbar$ to be

$$P(\psi, \phi)_{j,m} = (g^2/2\pi^3 c^5 \hbar^7) E p_e (w-E)^2 \times |M(\psi, \phi)_{j,m}|^2. \tag{13}$$

An electron and neutrino emitted into a state specified by j and m may cause a maximum change in the nuclear spin of $j\hbar$. The nuclear spin may also change by integral multiples of $\hbar$ less than $j\hbar$ provided that the total angular momentum is conserved. It is necessary to calculate the matrix element only for one particular m, and it is convenient to choose the highest value, $m=j$. The total probability of emission into $(\psi, \phi)_j$ is the sum over all m, and this sum will be considered automatically accomplished in the square of matrix elements.

Consider the particular case in which an electron disappears from an $S_{\frac{1}{2}}$ state of energy $-E$, and the neutrino from a $P_{\frac{1}{2}}$ state of energy $E-w$. If the total angular momentum of these two particles is zero, the state will be denoted by the symbol

$$(S_{\frac{1}{2}} P_{\frac{1}{2}})_0.$$

The electron wave will always be given first. A more expanded form of the wave function is

$$2^{-\frac{1}{2}}[S_{\frac{1}{2}}^{(\frac{1}{2})} P_{\frac{1}{2}}^{(-\frac{1}{2})} - S_{\frac{1}{2}}^{(-\frac{1}{2})} P_{\frac{1}{2}}^{(\frac{1}{2})}],$$

where superscripts denote the values of m for individual waves. Now we may calculate $M(S_{\frac{1}{2}}, P_{\frac{1}{2}})_0$ by substituting this form into Eqs. (11) and (12) and evaluating the expressions at the nuclear radius. Only the leading terms in the series expansions in powers of r/λ_e or r/λ_n will be retained. Under these conditions

$$M(S_{\frac{1}{2}} P_{\frac{1}{2}})_0 = \tfrac{1}{2} a \int \rho_3. \tag{14}$$

Here $\int \rho_3$ stands for $\int \Psi^* \rho_3 \Phi d\mathbf{x}$. In general

$$\int A = \int \Psi^* A \Phi d\mathbf{x}.$$

The factor a and the related factor b which appears later are defined by

$$a \equiv [(E+mc^2)/2E]^{\frac{1}{2}}, \qquad b \equiv [(E-mc^2)/2E]^{\frac{1}{2}}. \tag{15}$$

In some expressions a', a'', b', and b'' will be used for those a's and b's that are changed by the effect of the Coulomb field. Their values in the absence of a field are the same as the unprimed letters.

The calculation for the state $(P_{\frac{1}{2}} S_{\frac{1}{2}})_0$ yields

$$M(P_{\frac{1}{2}} S_{\frac{1}{2}})_0 = -\tfrac{1}{2} b \int \rho_3. \tag{16}$$

In order to simplify the presentation of the formulas, we shall combine related matrix elements into one equation when feasible. Thus Eqs. (14) and (16) may be condensed into

$$M(S_{\frac{1}{2}} P_{\frac{1}{2}})_0 / a = -M(P_{\frac{1}{2}} S_{\frac{1}{2}})_0 / b = \tfrac{1}{2} \int \rho_3. \tag{17}$$

The allowed transitions may also cause emissions into states of unit angular momentum for which:

$$\mathbf{M}(S_{\frac{1}{2}} P_{\frac{1}{2}})_1 / a = -\mathbf{M}(P_{\frac{1}{2}} S_{\frac{1}{2}})_1 / b = \tfrac{1}{2} \int \boldsymbol{\sigma}. \tag{18}$$

Matrix elements (17) and (18) comprise all the allowed transitions, and it is evident from Eq. (15) that the sum of squares of these matrix elements will be independent of light particle wave-lengths. We now present the matrix elements that lead to first forbidden transitions. The latter are of two types: *dipole* matrix ele-

ments which are proportional to ρ_3 and σ but also contain the first power of the momentum of one of the light particles, and *pseudomonopole* matrix elements, proportional to velocity terms of the heavy particle waves, i.e., to ρ_1 and ρ_2. In both cases there is a change in parity, so it is necessary to consider all possible changes in angular momentum:

$$\begin{aligned}
M(S_{\frac{1}{2}}S_{\frac{1}{2}})_0&=\tfrac{1}{2}ia\int(\rho_1-i\rho_2)\\
&\quad+(ap_n+b'p_e)/6\hbar\int(\sigma,\mathbf{r}),\\
M(P_{\frac{1}{2}}P_{\frac{1}{2}})_0&=\tfrac{1}{2}ib\int(\rho_1+i\rho_2)\\
&\quad-(bp_n+a'p_e)/6\hbar\int(\sigma,\mathbf{r}),
\end{aligned}\tag{19}$$

$$\mathbf{M}(S_{\frac{1}{2}}S_{\frac{1}{2}})_1=(ap_n-b'p_e)/6\hbar\int[\rho_3\mathbf{r}-i(\boldsymbol{\sigma}\times\mathbf{r})],$$

$$\mathbf{M}(P_{\frac{1}{2}}P_{\frac{1}{2}})_1=-(bp_n-a'p_e)/6\hbar\int[\rho_3\mathbf{r}+i(\boldsymbol{\sigma}\times\mathbf{r})],$$

$$\begin{aligned}
\mathbf{M}(S_{\frac{1}{2}}D_{1\frac{1}{2}})_1/ap_n&=-\mathbf{M}(D_{1\frac{1}{2}}S_{\frac{1}{2}})_1/bp_e\\
&=\mathbf{M}(P_{\frac{1}{2}}P_{1\frac{1}{2}})_1{}^*/bp_n\\
&=-\mathbf{M}(P_{1\frac{1}{2}}P_{\frac{1}{2}})_1{}^*/ap_e\\
&=(\sqrt{2}/12\hbar)\int[2\rho_3\mathbf{r}+i(\boldsymbol{\sigma}\times\mathbf{r})],
\end{aligned}\tag{20}$$

$$\begin{aligned}
\mathbf{M}(S_{\frac{1}{2}}D_{1\frac{1}{2}})_2/ap_n&=-\mathbf{M}(D_{1\frac{1}{2}}S_{\frac{1}{2}})_2/bp_e\\
&=-\mathbf{M}(P_{\frac{1}{2}}P_{1\frac{1}{2}})_2/bp_n\\
&=\mathbf{M}(P_{1\frac{1}{2}}P_{\frac{1}{2}})_2/ap_e\\
&=(3^{\frac{1}{2}}/6\hbar)\int[\boldsymbol{\sigma}\mathbf{r}],
\end{aligned}\tag{21}$$

where

$$[\boldsymbol{\sigma}\mathbf{r}]_{ik}\equiv\tfrac{1}{2}(\sigma_i r_k+\sigma_k r_i)-\tfrac{1}{3}(\sigma,r)\delta_{ik}.$$

Equations (19), (20), and (21) give all the matrix elements that lead to first forbidden transitions. Following are the results for second forbidden transitions. In these $\rho_3[\mathbf{rr}]$ and $[\mathbf{r}(\boldsymbol{\sigma}\times\mathbf{r})]$ are defined analogously to $[\boldsymbol{\sigma}\mathbf{r}]$ above, and the symbols $[\boldsymbol{\sigma}\mathbf{rr}]$ and $\mathbf{Q}$ will be used:

$$\begin{aligned}
[\boldsymbol{\sigma}\mathbf{rr}]_{ijk}&\equiv\tfrac{1}{3}(\sigma_i r_j r_k+\sigma_j r_i r_k+\sigma_k r_i r_j)\\
&\quad-\frac{1}{15}(\boldsymbol{\sigma}r^2)-\frac{2}{15}\mathbf{r}(\sigma,r),\\
\mathbf{Q}&\equiv\int\{\rho_3[\mathbf{rr}]-i[\mathbf{r}(\boldsymbol{\sigma}\times\mathbf{r})]\}/(12)^{\frac{1}{2}}\hbar^2,
\end{aligned}\tag{22}$$

$$\begin{aligned}
\mathbf{M}(S_{\frac{1}{2}}P_{1\frac{1}{2}})_2&=-(b'p_ep_n/3-ap_n^2/5)\mathbf{Q},\\
\mathbf{M}(P_{1\frac{1}{2}}S_{\frac{1}{2}})_2&=(ap_ep_n/3-b''p_e^2/5)\mathbf{Q},\\
\mathbf{M}(P_{\frac{1}{2}}D_{1\frac{1}{2}})_2&=(a'p_ep_n/3-bp_n^2/5)\mathbf{Q}^*,\\
\mathbf{M}(D_{1\frac{1}{2}}P_{\frac{1}{2}})_2&=-(bp_ep_n/3-a''p_e^2/5)\mathbf{Q}^*,\\
\mathbf{M}(S_{\frac{1}{2}}F_{2\frac{1}{2}})_2/ap_n^2&=-\mathbf{M}(F_{2\frac{1}{2}}S_{\frac{1}{2}})_2/bp_e^2\\
&=-\mathbf{M}(P_{\frac{1}{2}}D_{2\frac{1}{2}})_2{}^*/bp_n^2\\
&=\mathbf{M}(D_{2\frac{1}{2}}P_{\frac{1}{2}})_2{}^*/ap_e^2\\
&=\int\{3\rho_3[\mathbf{rr}]\\
&\quad+2i[\mathbf{r}(\boldsymbol{\sigma}\times\mathbf{r})]\}/30\sqrt{2}\hbar^2,
\end{aligned}\tag{23}$$

$$\begin{aligned}
\mathbf{M}(P_{1\frac{1}{2}}D_{1\frac{1}{2}})_2/a&=-\mathbf{M}(D_{1\frac{1}{2}}P_{1\frac{1}{2}})_2/b\\
&=(p_ep_n/6\cdot3^{\frac{1}{2}}\hbar^2)\int\rho_3[\mathbf{rr}],
\end{aligned}\tag{24}$$

$$\begin{aligned}
\mathbf{M}(S_{\frac{1}{2}}F_{2\frac{1}{2}})_3/ap_n^2&=-\mathbf{M}(F_{2\frac{1}{2}}S_{\frac{1}{2}})_3/bp_e^2\\
&=-\mathbf{M}(P_{\frac{1}{2}}D_{2\frac{1}{2}})_3/bp_n^2\\
&=\mathbf{M}(D_{2\frac{1}{2}}P_{\frac{1}{2}})_3/ap_e^2\\
&=\hbar^{-2}(120)^{-\frac{1}{2}}\int[\boldsymbol{\sigma}\mathbf{rr}],
\end{aligned}\tag{25}$$

$$\begin{aligned}
\mathbf{M}(P_{1\frac{1}{2}}D_{1\frac{1}{2}})_3&=-\mathbf{M}(D_{1\frac{1}{2}}P_{1\frac{1}{2}})_3\\
&=(p_np_e/6\hbar^2)\int[\boldsymbol{\sigma}\mathbf{rr}].
\end{aligned}\tag{26}$$

IV. EFFECT OF THE COULOMB FIELD

The Coulomb field of the final nucleus has an important effect on the beta-spectrum of most forbidden transitions. In fact, it is only for the very light nuclei and (or) rather large electron energies that the effect of the nuclear charge can be neglected. This has already been pointed out by Konopinski and Uhlenbeck.[3] The effect may be described as follows: In the absence of a field, electron waves may be classified as S

waves, P waves, etc., according to the transformation properties of the "large components," the radial dependence of these waves being *one*, r, etc., (r^L in general) near $r=0$. In the presence of the field, the angular dependence remains unchanged, but the radial dependence acquires two new properties. The first is that some of the solutions (total angular momentum $\frac{1}{2}h$) are not bounded at $r=0$. The integral of the square of the wave function is bounded, however, and in calculating transition probabilities for beta-activities the value of the electron wave at the surface of the nucleus is used. This singularity is not important to the shapes of the beta-spectra.

The second, and more important, effect of the electric field is to lower by unity the power of r with which a wave approaches $r=0$. Neglecting the small effect mentioned above, a $P_{\frac{1}{2}}$ wave approaches $r=0$ for the most part as r itself, but there is a small admixture of a wave (with the same angular dependence) which approaches $r=0$ as r^0, i.e., as a finite constant. The coefficient of this S part of the $P_{\frac{1}{2}}$ wave is proportional to $Z/137$ and is usually very small, but the more favorable radial dependence of this part near the origin makes it of importance compared with the P part itself. The physical interpretation of the electron state is that there is a finite probability of finding an electron extremely close to the center of attraction in spite of the fact that the electron has one unit of angular momentum. In the relativistic theory of the electron the increase in kinetic energy that arises upon concentrating the electron within a radius r of the center is proportional to ch/r. On the other hand, the decrease in potential energy in the Coulomb field is also proportional to $1/r$ so that it is possible to have the electron very close to the nucleus although it has angular momentum.

So far as we carry the analysis of forbidden spectra in this paper it is sufficient to consider the amount of S part in the P waves and of the P part in D waves. There are P waves in both $S_{\frac{1}{2}}$ and $P_{\frac{1}{2}}$ eigenfunctions, however, and the coefficient of the S part will be different in the two. In order to determine the coefficients with which these anomalous parts of the wave appear the work of Dirac[11] on the radial functions is used. Neglecting quantities of the order $(Z/137)^2$ compared with unity we find the results are adequately expressed as modifications of the factors a and b in Eqs. (19) and (22) as already indicated by the use of primes. All other matrix elements are unaffected. The values of the primed letters are:

$$\begin{aligned} a'/a &= 1-3Ze^2/2(E+mc^2)\rho, \\ b'/b &= 1-3Ze^2/2(E-mc^2)\rho, \\ a''/a &= 1-5Ze^2/4(E+mc^2)\rho, \\ b''/b &= 1-5Ze^2/4(E-mc^2)\rho, \end{aligned} \tag{27}$$

where ρ is the radius of the nucleus at which the wave functions are evaluated.

V. SHAPES OF SPECTRA

The contributions of the individual matrix elements found above may be changed in different ways by further, non-Coulombic interaction between electron and nucleus. In this section the electric field only will be taken into account. It will be further assumed that the nuclear wave functions are eigenfunctions of the time reversal operator[12] so that the operators in Eq. (11) that change sign under time reversal, σ and ρ_2, lead to different states of the final nucleus than the operators that do not change sign, ρ_1 and ρ_3. This assumption eliminates most of the cross products of different operators in the squares of matrix elements.

The probability of allowed transitions is calculated by adding the absolute squares of all matrix elements leading to such transitions. The positions of the nuclear particles do not matter to those matrix elements, Eqs. (17) and (18), and no change in parity takes place in the transition. Such transitions may thus be called *monopole* radiations. From the values of a and b as given in Eq. (15), the sum of squares of matrix elements, Eq. (17), that apply if initial and final nuclei have spin zero is

$$\sum|M|^2=\tfrac{1}{4}|\int\rho_3|^2 \quad 0\to 0. \tag{28}$$

Similarly, if the nuclear spin changes by one unit the appropriate sum of squares is

$$\sum|\mathbf{M}|^2=\tfrac{1}{4}|\int\boldsymbol{\sigma}|^2 \quad \Delta i=\pm 1. \tag{29}$$

[11] P. A. M. Dirac, *The Principles of Quantum Mechanics* (Oxford, 1935), p. 265.

[12] E. Wigner, *Göttingen Nachrichten* (1932), p. 546.

If the transition involves no change in nuclear spin and the spin is not zero, the sum of (28) and (29) is to be used:

$$\sum|\mathbf{M}|^2=\tfrac{1}{4}|\int\rho_3|^2+\tfrac{1}{4}|\int\boldsymbol{\sigma}|^2\ \Delta i=0\ (i\neq 0). \quad (30)$$

Since Eq. (30) represents a larger factor in the probability of decay than Eq. (29), transitions without change of spin will be more prominent than under the axial vector or tensor theory alone and this is desirable in Grönblom's analysis mentioned above.[7] Equation (13) represents the normal Fermi spectrum of electrons if M^2 is constant so that allowed transitions in the antisymmetric theory give normal spectra.

First forbidden transitions are conveniently divided into three classes: monopole, dipole, and mixed. The monopole radiations differ from the allowed emissions in that a change of parity is entailed, and for this reason the first forbidden monopole transitions are called *pseudomonopole.* The classification of beta-radiations as various multipole radiations is somewhat more convenient than the broader: allowed, first, and second forbidden classification. This is especially true for light nuclei because the matrix elements characteristic of first forbidden transitions, say, may vary in magnitude over a much wider range than the difference between allowed and the strongest first forbidden.[13]

Pseudomonopole matrix elements are proportional to ρ_1 and ρ_2, i.e., to the small components of the nuclear waves. The two operators ρ_1 and ρ_2 appear in Eq. (19) and, according to the assumption stated above, do not mix. The sum of squares of M applicable to pseudomonopole emissions is then

$$\sum|M|^2=\tfrac{1}{4}|\int\rho_1|^2+\tfrac{1}{4}|\int\rho_2|^2 \quad \Delta i=0. \quad (31)$$

The spectrum is normal.

There are four distinct matrix elements that lead to dipole transitions. The sum of squares for each of these will be presented along with the allowed changes in nuclear spin. An indicated change of spin that is primed, as the 0′ in $\Delta i=0'$, 1, means that the sum of spins of initial and final nucleus must be as large as the unprimed number in the same Δi.

$$\sum|M(\sigma,r)|^2=(1/36\hbar^2)\times[(p_n+cp_e^2/E-3Ze^2/2c\rho)^2+m^2c^4p_e^2/E^2]|\int(\sigma,r)|^2, \quad \Delta i=0 \quad (32)$$

$$\sum|\mathbf{M}(\rho_3\mathbf{r})|^2=(1/36\hbar^2)\times[(p_n-cp_e^2/E+3Ze^2/2c\rho)^2+2(p_n^2+p_e^2)+m^2c^4p_e^2/E^2]\times|\int\rho_3\mathbf{r}|^2, \quad \Delta i=0',1 \quad (33)$$

$$\sum|\mathbf{M}(\boldsymbol{\sigma}\times\mathbf{r})|^2=(1/36\hbar^2)\times[(p_n-cp_e^2/E+3Ze^2/2c\rho)^2+\tfrac{1}{2}(p_n^2+p_e^2)+m^2c^4p_e^2/E^2]\times|\int(\sigma\times r)|^2, \quad \Delta i=0',1 \quad (34)$$

$$\sum|\mathbf{M}(\boldsymbol{\sigma}\mathbf{r})|^2=(1/12\hbar^2)(p_n^2+p_e^2)|\int[\boldsymbol{\sigma}\mathbf{r}]|^2 \quad \Delta i=0',1',2. \quad (35)$$

Ordinarily the term containing Z^2 will far outweigh other terms in a given expression and in every one except Eq. (35) the spectrum will be quite the same as the normal one. Deviations from the normal spectrum should be apparent in the high energy transitions in light elements if $\Delta i<2$ or in any case if $\Delta i=2$.

The one mixed transition, between ρ_2 and (σ,r) leads to

$$\sum|M(\rho_2;(\sigma,r))|^2=(1/6\hbar)(p_n+cp_e^2/E-3Ze^2/2c\rho)|\int\rho_2|\times|\int(\sigma,r)| \quad \Delta i=0. \quad (36)$$

Again the Z term should predominate and the spectrum be normal. All first forbidden transitions cause a change in the parity of the nucleus.

So-called second forbidden transitions can be of two types, pseudodipole and quadrupole. There are no pseudodipole transitions in the antisymmetric theory, however, because the only possible matrix elements of this type, $\rho_1\mathbf{r}$ and $\rho_2\mathbf{r}$, do not permit $\Delta i=2$; and $\Delta i<2$, without change of parity, is allowed in monopole transitions. Thus all transitions are quadrupole, $\Delta i=2$ or 3, in the second forbidden category. There are three distinct matrix elements and no cross

[13] Discussions of and formulas for the half-lives of beta-activities have been presented in three independent papers appearing in *The Physical Review* **61** (1942): C. L. Critchfield, p. 249 (light nuclei only); R. E. Marshak, p. 431, and E. Greuling, p. 568.

products under the above assumptions:

$$\sum|\mathbf{M}(\rho_3\tau\tau)|^2=(1/360\hbar^4)[3p_e^4-4cp_np_e^4/E$$
$$+10p_e^2p_n^2-4cp_n^3p_e^2/E+3p_n^4$$
$$+(Ze^2/c\rho)(6p_n^2-10cp_n^2p_e^2/E$$
$$+5p_e^2p_n-3p_e^4/E)+(15/8)(Ze^2/c\rho)^2$$
$$\times(4p_n^2+p_e^2)]|\int\rho_3\tau\tau|^2 \quad \Delta i=2, \quad (37)$$

$$\sum|\mathbf{M}(\sigma\tau\tau)|^2=(1/360\hbar^4)(3p_e^4+10p_e^2p_n^2$$
$$+3p_n^4)|\int\sigma\tau\tau|^2 \quad \Delta i=2',3, \quad (38)$$

$$\sum|\mathbf{M}(\mathbf{r}\sigma\times\mathbf{r})|^2=\{\sum|M(\rho_3\tau\tau)|^2/|\int\rho_3\tau\tau|^2$$
$$-(1/3)\sum|M(\sigma\tau\tau)|^2/|\int\sigma\tau\tau|^2\}$$
$$\times|\int(\mathbf{r}\sigma\times\mathbf{r})|^2 \quad \Delta i=2. \quad (39)$$

If Z is fairly large or the energy particularly small, the normalization factor for waves in a Coulomb field should be included in the electron waves. An approximate form of the squares of the normalization factor is

$$f(\zeta)=\zeta/(e^\zeta-1), \quad \zeta\equiv 2\pi Ze^2E/hcp_e, \quad (40)$$

in which ζ is positive for positron emission and negative for electron emission. The approximation involved in Eq. (40) as well as throughout the calculations on the Coulomb effect is that in which quantities of the order $(Z/137)^2$ are neglected in comparison with unity. Our results thus apply only to light nuclei. The final form of $P(E)$ may be written

$$P(E)=(g^2/2\pi^3c^5\hbar^7)f(\zeta)Ep_e(w-E)^2\sum|\mathbf{M}|^2, \quad (41)$$

in which the sum is taken over all elements that contribute to the transition. The integral of $P(E)dE$ over all electron energies then gives the decay constant. These integrals have been presented in the papers quoted in reference 13.

The foregoing calculations have been carried through for positron emission. In order to apply them to electron emission, it is simply necessary to change the sign of Z throughout.

VI. CONCLUSION

Full application of the results of this paper would require many experimentally determined beta-spectra of forbidden transitions. Furthermore, the spectra must be free of distortion such as introduced by thick sources, etc. The spectra of P^{32} and Na^{24} as determined by Lawson[14] (cf. reference 3) are probably in the desired category. Both transitions are slower than allowed transitions, Na^{24} by a factor 40 and P^{32} by a factor 2×10^4. Assignment of a definite multipole to these transitions is complicated by the fact that we do not know the magnitudes of the matrix elements and also by the intermultiplet character of the transitions (cf. Wigner, reference 9). According to the estimates made of matrix elements in the first reference 13, Na^{24} could be a pseudo-monopole transition that depends upon ρ_2. The Kurie plot predicted for such a transition would be a straight line, and in fact, the high energy end of the experimental curve does appear to be quite straight. The low energy end is probably complicated by another transition.

The high energy end of the Kurie plot for P^{32} is also straight but its lifetime is too long to ascribe the decay to the matrix element $M(\rho_2)$. In addition, the spectrum is probably simple so that the deviation at the low energy end cannot be explained as the influence of a second spectrum. The lifetime of P^{32} suggests the matrix element $M(\rho_1)$ according to the estimates in the first reference 13, but in order to obtain the observed spectrum, it would be necessary for the matrix element to become appreciably dependent upon the energy of the electron when this is low. This or any other elaborate explanation is to be avoided at this stage of the theory of forbidden spectra.

Most of the work presented in this paper was done as a National Research Fellow at Princeton University and The Institute for Advanced Study. I am glad to acknowledge my debt to Professor Eugene Paul Wigner of Princeton University for inspiration and assistance in developing this theory and to Professor Furry of Harvard University for helpful criticism. The whole investigation is the direct result of the Seventh Annual Conference on Theoretical Physics sponsored by The George Washington University and The Carnegie Institution of Washington.

[14] J. L. Lawson, Phys. Rev. **56**, 131 (1939).

On the Silicon Oxide Bands

L. H. Woods
Ryerson Physical Laboratory, University of Chicago, Chicago, Illinois
(Received March 9, 1943)

Pankhurst has described a band spectrum believed by him to belong to an oxide of silicon, possibly SiO_2. A better excitation of the same bands has been obtained from a similar source (a high voltage uncondensed discharge through a constriction in a quartz tube), but in helium gas instead of hydrogen. These bands have been photographed on the 30-foot, 30,000 lines per inch Chicago grating spectrograph. A band near λ3840 has been resolved in the first and second orders and found to be a (0,0) transition, overlapped by a weak (1,1) transition, of the type $^1\Sigma \rightarrow {}^1\Sigma$, having the constants

$$\nu(0,0) = 26{,}015.05 \text{ cm}^{-1}, \quad \nu(1,1) = 25{,}991.44 \text{ cm}^{-1},$$
$$B_0' = 0.7180 \text{ cm}^{-1}, \quad B_1' = 0.704 \text{ cm}^{-1},$$
$$B_0'' = 0.7253 \text{ cm}^{-1}, \quad B_1'' = 0.712 \text{ cm}^{-1}.$$

The coefficients of the spin doubling for the two states are $\gamma_0' = +0.012$ cm^{-1}, $\gamma_0'' = +0.002$ or $\gamma_0'' = +0.022$ cm^{-1}, the value of γ_0'' not certainly fixed as between these two alternatives. The doublet structure and the B values prove that the emitter is SiO^+. Other bands at λ4270 have been resolved with weak intensity and tentatively ascribed to SiO_2.

INTRODUCTION

IN 1940, R. C. Pankhurst[1] described a system of bands lying in the violet region of the spectrum, obtained from a quartz capillary in a hydrogen discharge tube through which passed a heavy current. Part of the system, the region 4400A to 4600A, had been previously described by Cameron[2] and attributed by him to an oxide of silicon. Pankhurst's published photographs show the spectrum to be a series of more or less diffuse regions, the most intense of which had the wave-lengths 4340A, 4270A, and 3840A. He concluded from the general complexity of the spectrum that it was emitted by the triatomic molecule SiO_2.

The general interest in polyatomic molecules stimulated the present investigation of the bands, in particular because until now the spectra of very few polyatomic molecules have been obtained in emission. The large dispersion and high resolving power of the 30-foot Chicago grating have made it possible to resolve the rotational structure of these bands and to find their true emitters. Unfortunately, however, this investigation is incomplete. A band at 3840A was excited with great intensity in helium, and has been analyzed and positively assigned to SiO^+; other bands at 4270A have been resolved with weak intensity and tentatively ascribed to SiO_2; and still others appeared too faintly to allow examination. It was planned to continue these experiments with an atmosphere of hydrogen, in which the 4270A region is excited with greater intensity than is the 3840A region,[1] and to try the effect of other methods of excitation in order to obtain better photographs of the weaker bands, but these plans have necessarily been indefinitely postponed.

EXPERIMENTAL

The general design of the apparatus was like that used by Pankhurst, but with modified electrodes. The bands were obtained by passing an alternating current of 2 amperes at 4000 volts through a discharge tube. Water-cooled steel electrodes were fitted into the glass discharge tube against glass flanges and sealed with Picein. A quartz tube about 1 cm diameter at each end but constricted in the middle of its length to a 2-mm capillary was placed between the electrodes. Concentric with the axis of the quartz capillary, there was a hole through each electrode to permit the light from the capillary to pass to the window of the tube. The quartz tube, itself, was held in position along the axis by two flat doughnut shaped steel disks, on the outer edge of which was a sleeve fitting snugly against the

[1] R. C. Pankhurst, Proc. Phys. Soc. **52**, 707 (1940).
[2] W. H. B. Cameron, Phil. Mag. **3**, 110 (1927).

inside of the glass discharge tube. Likewise the inside circumference of each ring extended in a sleeve slightly smaller in diameter than the quartz tube, which reached into the tube and held it firmly. These snugly fitting steel sleeves, devised to prevent the discharge from leaking around the quartz tube, forced the current to pass through the capillary and heat it. The whole discharge tube was cooled by immersion in a water tank.

Although Pankhurst excited the spectra in an atmosphere of hydrogen, the present experiments were made in helium so that if the same spectrum were found it would be more certain that its carrier was in some way related to quartz. Also helium gives fewer atomic lines than hydrogen in the visible region, and interferes less with the silicon oxide bands. The tube was run for a long time with frequent charges of fresh helium to clean it, for these bands do not appear as long as many impurities are present. Even after many hours of operation, the tube had to be flushed with helium about every twenty minutes during an exposure. Hydrogen and water were the most persistent impurities.

When the tube was clean, the capillary glowed brilliantly yellow in the helium atmosphere and remained red hot for several seconds after the current was shut off. The capillary of a quartz tube which had been used for a long time became coated with sputtered electrode metal, easily removable with acid, and with a glassy brown material which resisted HCL, H_2SO_4, and mechanical scraping. Even aqueous HF did not act on it rapidly. It disappeared, however, if the capillary was heated in an oxygen flame, and the capillary became clear quartz again. This brownish material is thought to be SiO, an hypothesis supported by the disappearance of the brown color inside the capillary when the outside was heated to high temperatures. The identity of the substance was suggested by a review in *Chemical Abstracts* of an article[3] which could not be obtained in this country. The authors, Zintl and others, report that a bright brown powder, whose composition had the formula SiO, was condensed from vapor sublimed from a mechanical mixture of SiO_2 and Si under conditions such that the components themselves were not volatile. Slow condensation of the vapor on a hot surface, conditions which obtained in the discharge tube used here, produced a "brown-black brittle glass or shellac like membrane" also of the composition represented by the formula SiO. The authors further report that both the powder and the glassy material acted like a compound in that each had physical and chemical properties different from those of the parent substances or of the mixture SiO_2+Si.

The same review mentions the reaction of SiO at room temperature with atmospheric oxygen, to form SiO_2, a pyrophoric reaction if the SiO is powdered. This information indicates that the free energy of the reaction $SiO+\frac{1}{2}O_2 \rightarrow SiO_2$ is much greater than that of the reaction $CO+\frac{1}{2}O_2 \rightarrow CO_2$; that is SiO_2 is much more stable against dissociation into SiO than is CO_2 against dissociation into CO. That SiO_2 is more stable than CO_2 against dissociation into the elements is indicated by the heats of formation. Since the spectrum of CO_2 is readily excited in discharges at low currents, it is quite logical that the spectrum of SiO_2 could be excited under the same conditions. The great difficulty in exciting spectra of polyatomic molecules in discharges, namely that the high energy electrons break the molecules less stable than CO_2 into diatomic fragments, might be no difficulty in this case.

After exposures varying from 1 to 30 seconds, on a Hilger E-1 spectrograph, showed the spectrum to be clean and the band at 3840A to be very intense, an exposure of five hours was made on Process plates in the first and second orders of the 30-foot, 30,000 lines per inch, grating spectrograph. The 3840A band was of sufficient intensity to analyze, but the rotational structure of the several bands at 4270A was barely discernible. In hydrogen gas Pankhurst observed the 4270A region to be more intense than the 3840A region by a ratio 5:3. Since the excitation potential of helium is higher than that of hydrogen, electrons in a helium discharge have greater energy than in a hydrogen discharge. That the 4270A bands become less intense in helium than the 3840A band of SiO^+ then indicates that these bands are not emitted by an ionized molecule. The spacing of the rotational structure in these bands is com-

[3] Zintl, Bräuning, Grube, Krings, and Morawietz, Zeits. f. anorg. allgem. Chemie **245**, 1–7 (1940); Chem. Abs. **35**, 1719 (1941).

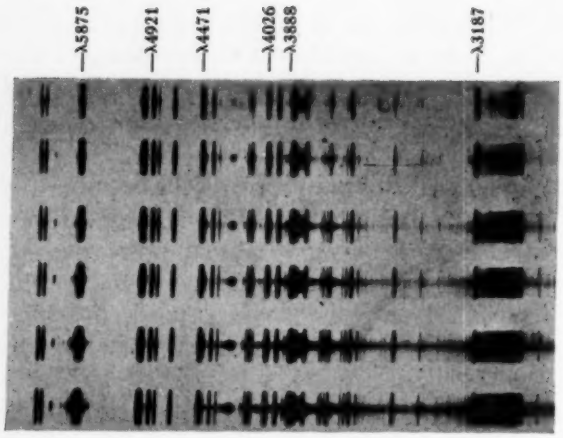

FIG. 1. Photograph from Hilger E-1 spectrograph showing spectrum of helium and some impurities, chiefly water. The small inner spectrum is that of the excited molecules in the quartz capillary. The $^2\Sigma \rightarrow {}^2\Sigma$ band of SiO at λ3840 in helium is much more intense than the group of bands at λ4270.

parable to or less than the spacing of the R branch in the 3840A band of SiO^+ where it is approaching a head. While it is possible that the 4270A bands belong to neutral SiO, it is the belief of the present author, based on the foregoing evidence and supported by the pyrophoric formation of SiO_2 from SiO, that they are emitted by the triatomic molecule SiO_2.

The plates taken on the Hilger E-1 show a possible band at about 6530A of about the same intensity as the 4270A bands, but no attempt has been made yet to photograph it on the big grating. These plates also show, in the region 3650 to 4270A, indications of the several bands reported by Pankhurst, but much less intense than the 4270A bands. It is easy to distinguish between the bands of silicon oxides and the remaining spectrum on the plates from the small spectrograph, because the spectrum from the capillary is distinct from the spectrum of the wider part of the quartz tube. When light from the discharge was focused in a spot on the slit of the Hilger E-1, light from the capillary formed a sharp bright pinpoint of light in the center of the spot. On the photographic plate there were then two spectra: (1) a wide spectrum of helium lines and OH bands through the center of which ran (2) a narrow spectrum of bands of silicon oxides and lines of silicon. See Fig. 1. The group of silicon lines at about 2510A and the many ultraviolet bands of neutral SiO appeared strongly in the spectrum from the capillary.

ANALYSIS

The band at 3840A is a (0,0) vibrational transition of the type $^2\Sigma \rightarrow {}^2\Sigma$, plus a corresponding (1,1) transition. The spin doublet structure is unresolved at low K values, then increasingly widens in the P branch. See Fig. 2. In the R branch, the doublet structure widens but the rotational structure closes up as it approaches the band head, so the spin components for successive values of K approach each other, overlap, and finally form two separate heads. The origin of the $1 \rightarrow 1$ band is displaced toward the red from the $0 \rightarrow 0$ origin. The Condon parabola should be practically a straight line, since as will be seen later the B' and B'' values are nearly equal. No other bands were observed. The wave numbers of lines for the $0 \rightarrow 0$ and $1 \rightarrow 1$ vibrational transitions are given in the Tables I and II.

Because the first P and R lines were diffuse or too faint, the location of ν_0 was uncertain. To find its position, the number of missing lines was determined by linear interpolation, and an arbitrary numbering was made. The actual spin doublet splitting, which in terms of the true K'' values (which are to be determined) must be

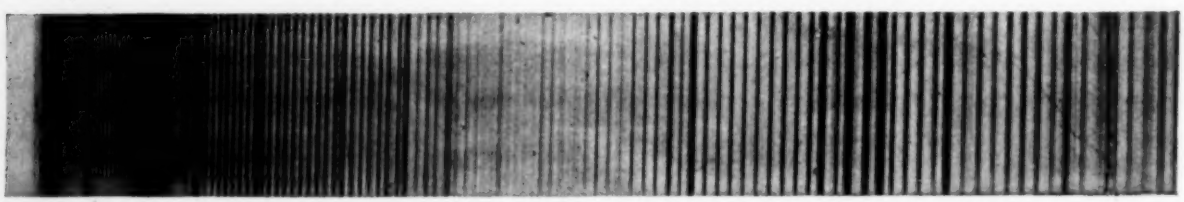

$\leftarrow R \quad P \rightarrow$

FIG. 2. The $^2\Sigma \rightarrow {}^2\Sigma(0 \rightarrow 0)$ 3840A transition of SiO^+. The spin doubling and the doublet heads are clearly visible. At the band origin the spin doublets of the $(1 \rightarrow 1)$ transition can be observed but are of much weaker intensity.

TABLE I. The system $^2\Sigma \rightarrow {}^2\Sigma$ of SiO^+ (cm^{-1}).

	(0→0) vibrational transition				(1→1) vibrational transition				
K''	P_a	P_b	R_a	R_b	K''	P_a	P_b	R_a	R_b
3		26010.75			11		26007.15		
4		26009.20		26022.25	12		26008.32		
5		26007.79		26023.59	13		26009.58		
6		26006.29		26024.98	14		26010.86		
7		26004.77		26026.32	15		26012.00		
8		26003.20		26027.64	16	26012.99	26013.30		
9		26001.68		26028.90	17	26014.14	26014.50		
10		26000.03		26030.19	18	26015.19	26015.63		
					19	26016.34	26016.72		
11		25998.29		26031.43	20	26017.46	26017.90	25960.06	25960.51
12		25996.83		26032.69					
13		25995.12	26031.95	26033.82	21	26018.54	26018.95	—	25958.40
14		25993.51	35.18	35.11	22	26019.52	26019.95	25956.28	25956.72
15		25991.83	36.41	36.28	23	26020.55	—	25954.55	25954.99
16	25990.29	25990.16	—	37.56	24	26021.69	26022.16	25952.80	—
17	88.57	88.40	38.78	38.68	25	26022.73	26023.14	25951.02	—
18	86.90	86.74	39.98	39.88	26			—	—
19	85.22	85.04	41.14	41.00	27			—	—
20	83.51	83.34	42.23	42.13	28			—	25946.09
					29			25943.77	25944.35
21	81.75	81.58	43.39	43.19	30			—	25942.54
22	79.82	79.80	44.50	44.34					
23	78.24	78.05	45.57	45.41	31			25940.06	25940.69
24	76.46	76.24	46.71	46.47					
25	74.59	74.39	47.72	47.49					
26	72.84	72.58	48.70	48.48					
27	71.10	70.75	49.78	49.52					
28	69.27	68.90	50.82	50.47					
29	67.37	67.08	51.85	51.54					
30	65.46	65.15	52.78	52.51					
31	63.60	63.14	53.76	53.45					
32	61.66	61.37	54.71	54.41					
33	59.77	59.43	55.65	55.26					
34	57.88	57.48	56.50	56.21					
35	55.94	55.56	57.49	57.07					
36	53.98	53.53	58.30	57.90					
37	51.96	51.56	59.17	58.79					
38	49.94	49.60	59.98	59.66					
39	48.02	47.58	60.82	60.43					
40	46.02	45.61	61.64	61.25					
41	44.02	43.56	62.45	62.01					
42	41.98	41.52	63.26	62.86					
43	39.90	39.43	64.01	63.59					
44	37.77	36.78	64.78	64.34					
45	35.72	35.25	65.55	65.03					
46	33.66	33.14	66.24	65.80					
47	31.49	31.08	66.96	66.48					
48	29.38	28.83	67.79	67.09					
49	27.12	26.78	68.34	67.78					
50	25.04	24.64	68.99	68.44					
51	22.88	22.44	69.66	69.08					
52			70.26	69.66					
53			70.85	70.26					
54			71.41	70.85					

represented by the equations[4]

$$\Delta\nu_{12}(R) = (\gamma' - \gamma'')K + \tfrac{1}{2}(3\gamma' - \gamma'') \qquad K = 0, 1, 2 \cdots \text{ in } R,$$

$$\Delta\nu_{12}(P) = (\gamma' - \gamma'')K - \tfrac{1}{2}(\gamma' + \gamma'') \qquad K = 1, 2, 3 \cdots \text{ in } P,$$

was then plotted. The two lines obtained by plotting $\Delta\nu_{12}(P)$ against $m = K$ and $-\Delta\nu_{12}(R)$ against $m = -(K+1)$, form a continuous curve whose value at $m = 0$ is $-\frac{1}{2}(\gamma' + \gamma'')$ and whose value at $m = -1$ is $-\frac{1}{2}(3\gamma' - \gamma'')$. The intercept of the curve with the m axis determined the true K numbering of the lines. This gave ν_0 with a small uncertainty. The slope of the curve gave

[4] G. Herzberg, *Molecular Spectra and Molecular Structure* (1939), p. 274.

TABLE II. Constants of the 3840A ($^2\Sigma-{}^2\Sigma$) band of SiO^+ (cm^{-1}).

v'	v''	B'	B''	D'	D''	$\nu(v', v'')$
0	0	0.7180	0.7253	2.25×10^{-6}	2.11×10^{-6}	$26{,}015.05=\nu_{(0,0)}$
1	1	0.704	0.712	"	"	$25{,}991.44=\nu_{(1,1)}$

the value $|\gamma_0'-\gamma_0''|=0.011$ cm^{-1}. From the sum of the intercepts with the two ordinate axes, the value $\gamma_0'=\pm0.012$ cm^{-1} was obtained, and the other possible K numbering gave the value $\gamma_0'=-0.0005$ cm^{-1}. Consideration of the signs of the intercepts and their relation to the signs of the γ's leads to the conclusion that if $\gamma_0'=-0.0005$, then $\gamma_0''=-0.011$, a possibility which was discarded on the grounds that the spin splitting coefficients of the $^2\Sigma$ levels of the analogous molecule CO^+ are positive.[5] If one assumes that SiO^+ and CO^+ are in this respect similar, that is, that $\gamma_0''>0$, then one finds that the conditions $|\gamma_0'-\gamma_0''|=0.010$ and $|\gamma_0'|=0.012$ require $\gamma_0'>0$. It follows that $\gamma_0'=+0.012$ cm^{-1}, and $\gamma_0''=+0.002$ cm^{-1} or $\gamma_0''=+0.022$ cm^{-1}. Further information is needed to fix the value. The determination of γ from combination differences, namely $\gamma=\frac{1}{2}\{\Delta_2T_1(K+\frac{1}{2})-\Delta_2T_2(K-\frac{1}{2})\}$ was found inadequate because of the smallness of the γ's compared with experimental errors.

The quantities

$$[R_1(K+\tfrac{1}{2})-P_1(K+\tfrac{1}{2})]/(4K+2),$$
$$[R_2(K-\tfrac{1}{2})-P_2(K-\tfrac{1}{2})]/(4K+2),$$
$$[R_1(K-1+\tfrac{1}{2})-P_1(K+1+\tfrac{1}{2})]/(4K+2),$$

and

$$[R_2(K-1-\tfrac{1}{2})-P_2(K+1-\tfrac{1}{2})]/(4K+2)$$

were plotted against $K(K+1)$. From the slopes of the lines D' and D'' were determined, and from the intercepts at $K=0$, B' and B'' were determined.[6] The very approximate values $\omega_0'=811$ cm^{-1} and $\omega_0''=851$ cm^{-1} were calculated from the relation $\omega^2=4B^3/D$. Although this relation is an exact one, the values of D are not accurate enough to give good values of ω.

This same procedure was followed to determine the constants of the $1\rightarrow1$ transition (Table II). However, not enough lines could be measured to determine the D values because the transition is severely overlapped by the $0\rightarrow0$ band. The quantity $\nu_{0,0}-\nu_{1,1}=23.61$ cm^{-1} agrees with the calculated difference of the values of ω in order of magnitude.

The B values and the doublet structure of the lines show that the band at 3840A is emitted by the ionized molecule SiO^+.

If the $SiO-SiO^+$ energy level diagrams are roughly analogous to those of $CO-CO^+$ the existence of a $^2\Pi\rightarrow{}^2\Sigma$ band of SiO^+ lying in the infra-red can be expected, probably lying at wave-lengths greater than 8000A.

The writer is very grateful to Dr. S. Mrozowski who suggested this problem, for his kindness, pertinent suggestions, and frequent help, and to Professor R. S. Mulliken for his unfailing interest and valuable advice.

[5] L. H. Woods, Phys. Rev. **63**, 431 (1943).

[6] See reference 4, p. 199.

Note on Spin Doubling in the Doublet Sigma States of CO^+

L. H. Woods
Ryerson Physical Laboratory, University of Chicago, Chicago, Illinois
(Received March 9, 1943)

On the photographic plates of the CO_2 spectrum made by S. Mrozowski from the 30-foot, 30,000 lines per inch, Chicago grating, were found pictures of the first negative bands and the comet tail bands of CO^+ in which the $^2\Sigma$ spin splittings were resolved. From the $^2\Sigma \rightarrow {}^2\Sigma$ transition, the absolute differences of the spin doubling coefficients were measured. The absolute values of γ_0'' and γ_1'' for the lowest $^2\Sigma$ state were measured from the $^2\Pi \rightarrow {}^2\Sigma$ transition, and their algebraic signs determined by consideration of relative intensities of branches. Thus the signs and values of the spin doubling coefficients of $^2\Sigma'$ for $v'=0$ to 4, and of $^2\Sigma''$ for $v''=0$ to 7 have been determined.

INTRODUCTION

THE first negative bands of $CO^+(^2\Sigma \rightarrow {}^2\Sigma)$ are well known from the early days of spectroscopy. Their extensive history, which is well related by Kayser,[1] includes no occasion when the spin doublets of these bands were photographed in such a way that they showed measurable resolution. Recently in his comprehensive study of CO_2 on the 30-foot grating at the Ryerson Laboratory, S. Mrozowski has obtained photographs of the first negative bands in the second and third orders, and of the comet tail bands in the second order, in which the $^2\Sigma$ spin splittings were resolved. These plates provided an opportunity to amplify the known experimental data on spin splitting with which to compare predictions of the theory developed by Van Vleck.[2] Such comparisons have already been made for several molecules by Mulliken and Christy[3] who were able to draw conclusions as to the nature of the electronic states involved.

In the present investigation the absolute value of the difference of the spin splitting coefficients for the upper and lower electronic states $|\gamma'-\gamma''|$ was obtained for the 0→1, 0→2, 0→3, 1→2, 1→3, 1→4, 1→5, 2→4, 2→5, 2→6, 3→5, 3→6, 3→7 vibrational bands of the $^2\Sigma \rightarrow {}^2\Sigma$ transition. From an examination of the 5→0, 6→0, 7→0, and 12→1 vibrational transitions of the $^2\Pi \rightarrow {}^2\Sigma$ bands, the absolute values of γ_0'' and γ_1'' were derived. The R_2 and $^RQ_2$, Q_2 and $^QP_2$ branches of the 5→0 and 6→0 bands were identified by consideration of their relative intensities. The sign of γ_0'' then was determined by the sign of $\Delta\nu = R_2 - {}^RQ_2 = Q_2 - {}^QP_2$. With this knowledge, the signs and values of the spin splitting coefficients were determined for the vibrational levels 0 to 4 of the upper $^2\Sigma$ state and for the levels 0 to 7 of the ground $^2\Sigma$ state. γ' was found to increase very slightly with increase in v' while γ'' showed a rather marked increase with v''. Moreover $\gamma' > \gamma'' > 0$. A similar evaluation of change of spin splitting coefficient with vibrational quantum number was made for the $^2\Sigma \rightarrow {}^2\Sigma$ transition in AlO by M. K. Sen,[4] who found $\gamma' > \gamma'' > 0$, γ' slowly increasing and γ'' slowly decreasing with increase in v. His paper contains a nice discussion of the theory involved in this analysis, but the accuracy of all constants given therein, especially the B values, is overestimated.

ANALYSIS

The spin splitting in the $^2\Sigma \rightarrow {}^2\Sigma$ bands was originally measured on the third-order plates but this set of data was abandoned in favor of that from the second-order plates, which because of greater intensity showed spin splitting to much higher K values, giving more experimental points and therefore more accurate graphs. For each band the separation of the two components of the spin doublets

$$\Delta\nu_P(K) = P_1(K+\tfrac{1}{2}) - P_2(K-\tfrac{1}{2}) = (\gamma'-\gamma'')K - \tfrac{1}{2}(\gamma'+\gamma'')$$

$$\Delta\nu_R(K) = R_1(K+\tfrac{1}{2}) - R_2(K-\tfrac{1}{2}) = (\gamma'-\gamma'')K + \tfrac{1}{2}(3\gamma'-\gamma'')$$

[1] H. Kayser, *Handbuch der Spectroscopie*, Vol. 8.
[2] J. H. Van Vleck, Phys. Rev. **33**, 467 (1929).
[3] R. S. Mulliken and A. Christy, Phys. Rev. **38**, 87 (1931).
[4] M. K. Sen, Ind. J. Phys. **11**, 251 (1937).

TABLE I. Data from graphs of doublet splitting.

$\lvert\gamma'-\gamma''\rvert$	v'	v''	exp. γ values	Theoretical values for pure precession
0.0180	0	1	$\gamma_0''=+0.0102$	−0.026
0.0159	0	2	$\gamma_1''=+0.0110$	−0.025
0.0153	0	3	$\gamma_2''=+0.0122$	−0.025
			$\gamma_3''=+0.0136$	−0.024
0.0172	1	2	$\gamma_4''=+0.0145$	−0.024
0.0158	1	3	$\gamma_5''=+0.0141$	−0.024
0.0150	1	4	$\gamma_6''=+0.0144$	−0.023
0.0159	1	5	$\gamma_7''=+0.0151$	−0.023
0.0149	2	4	$\gamma_0'=+0.0290$	+0.022
0.0153	2	5	$\gamma_1'=+0.0294$	+0.024
0.0150	2	6	$\gamma_2'=+0.0294$	+0.024
0.0153	3	5	$\gamma_3'=+0.0297$	+0.024
0.0153	3	6	$\gamma_4'=+0.0297$	+0.024

$\gamma_0''=+0.0102 : \gamma_1''=+0.0109.$

was plotted against m, where for the P branch $\Delta\nu_P(K)$ was plotted against $m=K$, K having the values 1, 2, 3, $\cdots$ and for the R branch, $-\Delta\nu_R(K)$ was plotted against $m=-(K+1)$, K having the values 0, 1, 2, $\cdots$. The result was a single continuous line from whose slope the absolute value of $(\gamma'-\gamma'')$ was determined.

The differences measured in the $^2\Pi\rightarrow{}^2\Sigma$ bands,

$$\Delta\nu=R_2(K)-{}^RQ_2(K)=Q_2(K)-{}^QP_2(K)$$
$$=Q(K)-{}^QR_1(K)=P_1(K)-{}^PQ_1(K),$$

all of which should be given by the equation $\Delta\nu=T_1''(K+\frac{1}{2})-T_2''(K-\frac{1}{2})=\gamma''(K+\frac{1}{2})$, were plotted against $m=K+\frac{1}{2}$. The slopes of these lines determined the absolute values of γ_0'' and γ_1''. The photographs of these bands were made under conditions more favorable to production of CO_2 spectra than CO^+ spectra, and unfortunately the images of the $^2\Pi\rightarrow{}^2\Sigma$ bands were neither intense nor free of other spectra. Consequently the values of γ'' for higher values of v could not be obtained.

The sign of γ_0'' was found by consideration of the sign of $\Delta\nu$ in the 5→0 and 6→0 transitions of the $^2\Pi\rightarrow{}^2\Sigma$ bands. Since $A/B_0=80$ for CO^+, the $^2\Pi$ state approximates Hund's case a. As the rotational quantum number increases, however, the spin vector uncouples from the internuclear axis, and there is a transition towards case b. The main branches then fulfill the selection rule $\Delta K=\pm1, 0$, because for them $\Delta J=\Delta K$. They remain strong, but the satellite branches suffer decreasing intensity, since for them $\Delta J\neq\Delta K$.[5]

If the lower $^2\Sigma$ level is regular, i.e., $\gamma''>0$, $F(K-\frac{1}{2})$ lies below $F(K+\frac{1}{2})$, Q_2 lies farther to the ultraviolet than does $^QR_2$, and R_2 lies on the ultraviolet side of $^RQ_2$ in the $^2\Pi_{1/2}\rightarrow{}^2\Sigma$ band. In the band $^2\Pi_{3/2}\rightarrow{}^2\Sigma$, $^QR_1$ and $^PQ_1$ must lie on the violet sides of Q_1 and P_1, respectively, if $\gamma''>0$. That is, in the $^2\Pi_{1/2}\rightarrow{}^2\Sigma$ band, the stronger line should lie toward the violet for the Q_2, $^QR_2$ and R_2, $^RQ_2$ branches, and in $^2\Pi_{3/2}\rightarrow{}^2\Sigma$ the stronger line should lie toward the red for the $^QR_1$, Q_1 and $^PQ_1$, P_1 branches. This is true both in the 5→0 and 6→0 transitions of the $^2\Pi\rightarrow{}^2\Sigma$ band; therefore γ_0'' is positive. It is assumed that γ_1'' has the same sign as γ_0''. The 12→1 transition had very low intensity and was so overlapped by other bands that the sign of γ_1'' could not be verified directly from the plates. The data from the graphs of the doublet splitting and the calculated values of the spin splitting coefficients are given in Table I.

The experimental values of the γ's have been obtained by simple algebraic operations with the data. Theoretical values of γ were calculated from Van Vleck's formula

$$\gamma=2AB_vl(l+1)/\nu(\Pi,\Sigma)$$

by assuming a relation of pure precession between the $^2\Sigma$ level considered and the $^2\Pi$ level of the comet tail bands. A is negative for the comet tail $^2\Pi$ level. $\nu(\Pi,\Sigma)$ is obtained by projecting up or down from the $^2\Pi(v')$ level to $^2\Sigma(v'')$ level, and is positive or negative according as the $^2\Pi$ level lies above or below the $^2\Sigma$ level.[3] Hence γ'' is negative and γ' is positive in the theoretical case.

The data indicate a fair degree of likeness to a state of pure precession for the upper $^2\Sigma$ state of CO^+, but very little for the lower $^2\Sigma$ state.

The writer is sincerely thankful to Dr. S. Mrozowski, and to Professor R. S. Mulliken for their guidance and advice.

[5] R. S. Mulliken, Rev. Mod. Phys. **3**, 89 (1931).

The Retardation and Neutralization of Argon Ions in Helium

W. J. HAMM
Department of Physics, Washington University, St. Louis, Missouri

(Received March 21, 1943)

An apparatus is described for making direct measurements of the loss of forward velocity of argon ions in single encounters with helium atoms. Results are given in the form of collision cross sections for given percentage retardations, for ions of energies of 1000, 800, 600, 400, and 200 ev. The cross sections are zero for energy losses greater than 33.1 percent and increase both with decreasing percentage loss and decreasing beam speed. A correction to the readings necessary to obtain the results proves to be of unusual interest because the correction is itself the cross section for charge exchange between the argon ions and the helium atoms. Quantitative values of the cross sections for this unusual charge exchange are thus obtained. The values run roughly from 3.5 to 4.5×10^{-16} cm² per molecule in the energy range studied, compared with 28×10^{-16} cm² for A^+ ions in A and 63×10^{-16} cm² for N_2^+ ions in N_2. All the results are in sufficiently precise form to invite detailed theoretical analysis.

INTRODUCTION

INVESTIGATIONS of the collision of ions and atoms have led to a number of experimental procedures for studying the processes of scattering, neutralization, and retardation, which affect a beam of ions shot through a gas. Various experimenters[1] using the Dempster mass spectrograph technique, and in the majority of cases employing the alkali ions emitted by Kunsman filaments, have published data on the relative importance of these processes for different ion-gas combinations. The experimental procedures were frequently such that quantitative specification of cross sections for the various processes was not possible. This was particularly true when retarding collisions were present, wherein the projectile ions suffered loss of forward speed without undergoing appreciable deviations.

Theoretical considerations by A. V. Hershey[2] indicated that results of the retardation of ions in passing through a gas would involve fewer experimental difficulties and be easier to analyze than angular scattering results. Retardation measurements are most readily made by using ions very much heavier than the gas atoms of the retarding gas as such a combination of masses results in small angular scattering. One of the investigators of the Dempster group, J. S. Thompson,[3] sent Cs^+ ions through helium and hydrogen in apparatus similar to that employed by Mayer[4] in his classic studies of the absorption of electron beams in gases. He developed a method for deriving the cross sections for retardation from the resulting data on multiple collisions. The present paper describes an experiment devised to measure retardation cross sections directly for A^+ ions in helium gas under conditions such that only single collisions occur in the test region to any appreciable extent.

APPARATUS AND EXPERIMENTAL PROCEDURE

The circuit diagram of Fig. 1 illustrates the essential parts of the apparatus. "*S*" represents the ion source, which is a modification of the "High Efficiency Ion Source" described by

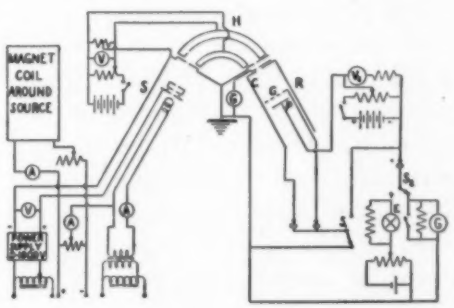

FIG. 1. Schematic diagram of the apparatus.

[1] A. J. Dempster, Phil. Mag. **3**, 115 (1927); R. B. Kennard, Phys. Rev. **31**, 423 (1928); I. W. Cox, Phys. Rev. **34**, 1426 (1929); K. H. Bracewell, Phys. Rev. **54**, 639 (1938).

[2] Private communication. The writer is pleased to acknowledge his indebtedness to Dr. Hershey for furnishing his memoranda on the subject of retardation measurements. Many of his suggestions are incorporated in the experimental procedure.

[3] J. S. Thompson, Phys. Rev. **35**, 1196 (1930).

[4] H. F. Mayer, Ann. d. Physik **64**, 451 (1921).

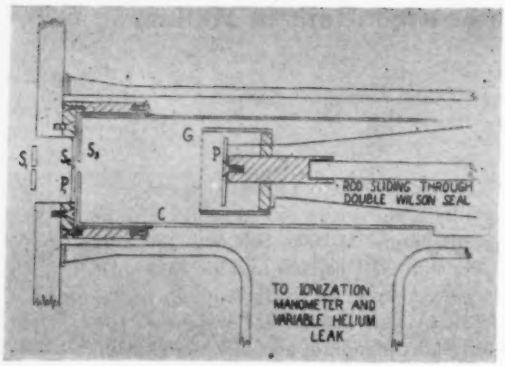

FIG. 2. Details of retardation chamber electrode assembly.

Finkelstein.[5] The source consists essentially of a combined magnetic and electric electron trap which maintains a high electron density in the source and serves the double purpose of using the electrons in a highly efficient way for ionization and of neutralizing the ordinarily inhibitory space charge of the positive ions. The source as used in this experiment is capable of currents of 2 to 10 ma of A^+ ions and has the highly desirable characteristic of operating at extremely low gas pressures. The beam energy used ranged between 200 and 1000 ev. Under these conditions the beam was not too sharply defined but was of such great intensity that it could be collimated with slits and homogenized with an electrostatic velocity selector to give a sharp beam of 10^{-7} amp., highly suitable for the present experiment.

"*H*" represents the velocity selector.[6] "*R*" is the retardation chamber, details of which appear in Fig. 2. The source and retardation electrodes were housed in flanged Pyrex pipe sections (diam. 3 in.) which were attached to a heavy steel box of diamond-shaped cross section containing the 127° selector. This steel box shielded the selector from the axial magnetic field used with the source and served to connect the entire system directly onto the mouth of a three-stage fractionating diffusion pump[7] of 80 liters per sec. speed. Rubber gasket technique was used throughout in making vacuum seals. Argon of 99.6 percent purity was fed into "*S*" through a variable leak,[8] and helium of 98.2 percent purity into "*R*." The gas pressures were measured by a D-79510 ionization manometer connected to a control and measuring unit similar to that described by Bowie.[9]

Power (a.c.) was supplied to the apparatus through a 1 kva Sola constant voltage transformer, and direct current for the source and source magnet coils was supplied by a generator maintained at constant voltage by a General Electric type CD stabilizer. General Radio "Variacs" were used for adjusting accelerating voltages and source-cathode heating current. A shelf of "*B*" batteries suspended by long insulating strips of "Amphenol *A*," a polystyrene derivative, supplied the retardation potentials. These batteries, the switches, and the associated wiring which carried the positive ion currents were well shielded and were supported where necessary with "Amphenol *A*."

The retardation electrode assembly shown in Fig. 2 consisted of a can, a grid, and a plate. The grid and plate were moved as a unit by the sliding motion of the supporting rod through a double Wilson seal.[10] The region between the two seals was kept filled with helium at atmospheric pressure. For most measurements the can and grid were grounded so that the space between S_3 and G was practically field-free. The circuit connections were so arranged that A^+ ions of a chosen energy, V_1, would be shot into He atoms in the field-free space where they would suffer their collisions along a path whose length could be varied at will, after which they would enter the analyzing region between the grid and the plate. The plate was held at a positive potential of V_2 volts with respect to ground so that all ions which had energy less than V_2 electron volts would be unable to reach the plate. Throwing switch S_1 (Fig. 1) upward connected the entire retardation electrode assembly as a Faraday cage by means of which the total ion current I_0 in the beam was measured.

Ideally, if the interaction of an A^+ ions with a helium atom caused the former to be so retarded that its residual energy was less than

[5] A. T. Finkelstein, Rev. Sci. Inst. **11**, 94 (1940).
[6] A. L. Hughes and V. Rojansky, Phys. Rev. **34**, 291 (1929).
[7] L. Malter and N. Marcuvitz, Rev. Sci. Inst. **9**, 92 (1938).
[8] R. D. Fowler, Rev. Sci. Inst. **6**, 26 (1935).
[9] R. M. Bowie, Rev. Sci. Inst. **11**, 265 (1940).
[10] R. R. Wilson, Rev. Sci. Inst. **12**, 91 (1941).

V_2 electron volts, the retarding field would prevent it from reaching the plate. When I_p, the plate current, is plotted as a function of V_2, any ordinate of the curve is proportional to the number of ions retaining energies equal to, or greater than, the corresponding voltage V_2. Energy and momentum considerations show that for the case of an argon ion colliding with a helium atom the minimum velocity retained by the ion is the fraction $(M-m)/(M+m)=0.8179$ of its initial velocity, M and m being the masses of the ion and atom, respectively. Hence the greatest percentage loss of energy that can occur at such an impact is 33.1 percent, this maximum loss corresponding to a perfectly elastic, head-on collision. Any possible inelastic phenomena such as excitation or ionization would have the effect of decreasing this maximum possible percentage loss. The maximum deflection that the ion can experience is given by: $\theta_{max}=\sin^{-1}(m/M)$, or 5° 46′. The geometry of the electrodes was such that for the longest path lengths used (13 cm) all ions so deflected could reach the plate if they were not rejected by the analyzing field.

The graph of I_p against V_2 as it would appear under ideal experimental conditions is shown in Fig. 3 as a dashed curve. A typical actual experimental result is shown as a solid curve. The difference between the two curves may be analyzed as follows: The negative value of I_p at values of $V_2 \geqslant V_1$ could only result from the emission of secondary electrons from the grid by impact of the positive ions and by fast neutral atoms which might be present as the result of the Kallman-Rosen "Umladung" or charge exchange process. A choice of 40×40 mesh grid of 0.007-in. diameter nickel wire was made following preliminary studies on field penetration. At the large values of V_2, all ions of the beam eventually strike the grid because of its relatively negative potential, the ions passing between the meshes on the first passage being deflected back to it. All secondary electrons liberated are collected by the plate. Hence the plate current is solely due to the secondary electrons and is just equal to the correction to be made. At the other extreme of voltage when V_2 approaches zero, the ions which pass through the grid are not deflected back to it, so that only a fraction, 48/73, as many secondary electrons are liberated, the fraction being derived from the effective grid open-area to metal-area ratio. For intermediate V_2 values, the correction was taken as a linear function of V_2, varying between the secondary electron current observed at high V_2 and approximately two-thirds of this value. An assumption made in developing this correction procedure was that neutrals and ions of the same velocity were equally efficient in ejecting secondaries. Other studies[11] support this assumption.

The generous slit dimensions adopted to permit use of a 10^{-7}-ampere ribbon of ions and galvanometer measuring technique allowed some leakage of source gas into the retardation chamber despite the great speed of the pump. The effects of this argon impurity in the target gas (He) were eliminated by taking double sets of readings with and without helium present, which yielded corresponding "helium data" and "foreign gas data." The effect of a slight amount of helium leakage into the source chamber with the consequent generation of a He^+ ion beam

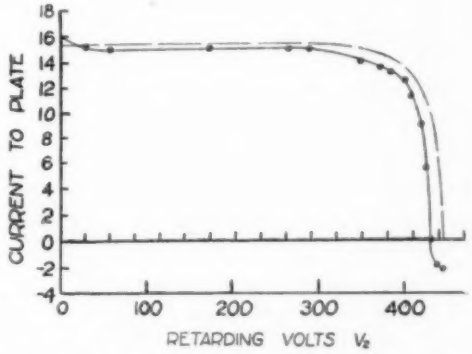

FIG. 3. Graph of the current reaching the plate P, as a function of the retarding voltage V_2. The dashed curve is an ideal one; the solid curve is experimental (helium pressure, 1.07×10^{-3} mm Hg; 430 v A^+ ions; for I_p, one division $=2.4\times10^{-9}$ amp.). The difference is attributed to the emission of secondary electrons from the grid G.

was considered negligible because of the relatively low ionization efficiency of He by electrons of optimum energy for ionizing argon.[12] For a similar reason the ion beam must have contained a negligible percentage of A^{++} ions.[13] No spectrographic investigation of beam quality was attempted.

[11] A. Rostagni, Zeits. f. Physik **88**, 69 (1934).
[12] P. T. Smith, Phys. Rev. **36**, 1293 (1930).
[13] W. Bleakney, Phys. Rev. **36**, 1303 (1930).

The following procedure was used in taking readings: Ions of energy V_1 were shot into the helium-free retardation chamber, and the retarding voltage between grid and plate was made to have values such that energy losses of p percent or greater were studied, where p was successively 0, 5, 10, 15, 20, 33, and also several values between 33 and 100. For each V_2 setting, values of the plate current were recorded as the grid-plate assembly was moved in the retardation tube so as to alter the path length from 4 to 13 cm. The current entering the can was maintained at a constant value for a given ion velocity by frequent measurement of its value as a Faraday cage current and by proper adjustment of the source-magnet current so as to increase or decrease its focusing action on the beam. Similar experiments were next performed with helium in the retardation chamber, the other variables being set at the exact values obtained when no helium was present.

TABLE I. Experimental values of σ, the cross section for specified percentage loss of energy, in units of 10^{-16} cm^2 per molecule.

Energy of ion	1000	800	600	400	200 ev
Energy loss (p% or more)					
33	3.41	3.46	4.02	4.32	4.93
25	3.599	3.747	4.411	4.900	5.635
20	3.996	4.204	4.902	5.770	7.830
15	4.42	4.72	5.49	6.86	—
10	5.08	5.57	6.53	8.67	—
5	—	6.94	—	—	—

The data obtained were analyzed in the following manner: Let I_0' represent the value of the Faraday cage current, the total entering beam strength where path length is zero, and let I_p' represent the plate current in the "foreign gas run" when no helium has been admitted to the retardation chamber. Let I_0 and I_p represent similar quantities in the experiments with helium present. Then, if sufficiently low pressure exists so that the use of single collision equations is justified, the foreign gas effect is given by: $I_p'=I_0' \exp(-\beta x)$, where β is the absorption coefficient representing chiefly the loss of A^+ ions in argon by exchange-neutralization and also by scattering. When helium is admitted to the tube, the law of the beam-intensity decrease becomes: $I_p=I_0 \exp -(\beta+\alpha p)x$, where α is the cross section ($N_1\sigma$) of the atoms in 1 cm^3 of the helium at 1 mm Hg pressure for the ions of velocity determined by V_1, and for a percentage energy loss determined by V_2. Taking the logarithms of these equations and subtracting we find:

$$(\log I_p-\log I_p')+\text{constant}=-\alpha px=-N_1 px\sigma.$$

Hence the curves obtained by plotting ($\log I_p-\log I_p'$) as ordinate against x as abscissa should be straight lines and possess a slope of value $-\alpha p$, or $-N_1 p\sigma$.

RESULTS

Argon ions of energies 1000, 800, 600, 400, and 200 ev were shot through helium gas maintained at a pressure of 1.07×10^{-3} mm Hg. Observed values of I_0 and I_p for different path lengths and different V_2 were tabulated, and the values of I_p corrected for secondary electrons were calculated. A preliminary run was always made to determine the corresponding I_p' values. Curves of ($\log I_p'-\log I_p$) *versus* the path length x were then plotted. From such plots, the slopes which are proportional to the cross sections were derived. Table I gives the total cross section values derived from such graphs for the energy and loss criterion combinations of chief interest in this study. Cross sections remained constant when V_1-V_2 exceeded 33.1 percent.

INTERPRETATION OF DATA

At a single impact, an argon ion colliding with a helium atom cannot lose more than 33.1 percent of its energy. However, in no case did the slope of the ($\log I_p-\log I_p'$) *vs.* x graph, and hence σ, assume a zero value when V_2 was set for energy losses greater than 33.1 percent. The procedure for taking the readings eliminated most of the normal causes for such an apparent discrepancy in the results. Thus a possible divergence of the beam was doubly eliminated, first, because with a divergent beam a graph of

TABLE II. Values of σ_u, the neutralization cross section in units of 10^{-16} cm^2 per molecule, for A^+ ions in He.

Energy of ion	1000	800	600	400	200 ev
σ_u	3.41	3.46	4.02	4.32	4.93

$(\log I_p - \log I_p')$ against x would not have been a straight line, which it was, and second, because the procedure of making the correction for foreign gas also eliminated geometric errors. Multiple collisions were eliminated as a possible cause of the apparent error because the $(\log I_p - \log I_p')$ *versus* x curves would not have been straight lines if multiple collisions had occurred to a measurable extent. Foreign gases were adequately handled by the correction procedure used. Neither foreign gases nor foreign ions would be likely to cause an effect like the one observed, namely, a constant correction independent of the retarding voltage. Finally, it is repeated that no inelastic collisions in the gas can account for the observed effect.

Only one possible explanation for the observed weakening of the beam as a function of path length but not of retarding voltage seems to remain. The effect will appear if A^+ ions are removed from the beam by charge exchange with the helium atoms, the so-called Kallman-Rosen "Umladung" process. Accepting this interpretation, the results of the present experiment provide an excellent quantitative measure of the cross section for such charge exchange. Thus the σ calculated above is composite: It should be written $\sigma = \sigma_u + \sigma_r$, where σ_u, the cross section for exchange neutralization, is the value of σ for the 33.1 percent loss criterion, and σ_r, the retardation cross section, is the difference remaining when σ_u is subtracted from the remaining table entries.

The σ_u values are listed in Table II. These values may be compared with those of 63×10^{-16} cm² for N_2^+ in nitrogen and 28×10^{-16} cm² for A^+ in argon.

The occurrence of charge exchange between an ion of argon and an atom with a very different ionization potential, like helium, has been the subject of some debate. Such measurements as existed indicated that the cross section must certainly be very small. In collisions between ions and atoms of different elements, two possibilities arise: The ionization potential of the projectile may exceed that of the target atom, or vice versa. Quantum mechanical considerations by Morse and Stueckelberg[14] lead to the prediction that there is a certain likelihood of electron transfer in both cases which reaches a maximum when the ionization potentials of the two atoms are the same. Their results also indicate that the probability of transfer of an electron is an even function of the difference of ionization potentials provided the kinetic energy of the ion relative to the atom is large, the same therefore for an A^+ ion meeting a He atom as for a He^+ ion meeting an A atom. The present experiment provides a most promising means for investigating this question further.

TABLE III. Values of σ_r for A^+ ions in He, the cross section for specific percentage loss of energy, in units of 10^{-16} cm² per molecule.

Energy of ion	1000	800	600	400	200 ev
Energy loss in percent					
33	0	0	0	0	0
25	0.189	0.287	0.391	0.580	0.725
20	0.586	0.744	0.900	1.45	—
15	1.01	1.26	1.47	2.54	—
10	1.67	2.11	2.51	4.35	—
5	—	3.58	—	—	—

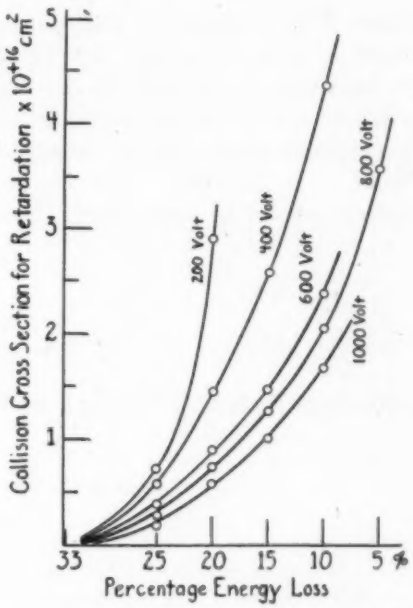

FIG. 4. Collision cross section for energy loss by retardation plotted against percentage energy loss for A^+ ions of various speeds passing through He.

The σ_r values, the cross sections for energy losses at single encounters, are listed in Table III and plotted *versus* percentage energy loss in Fig. 4. The ordinate of any curve gives the

[14] P. Morse and E. Stueckelberg, Ann. d. Physik 9, 589 (1931).

cross section within which the ion must pass if it is to incur at least the percentage energy loss indicated as abscissa. It is believed that the curves will lend themselves in a very satisfactory manner to analysis of the forces existing between the particles.

The author wishes to acknowledge gratefully the guidance and valuable suggestions of Doctor Robert N. Varney who directed this problem by correspondence from the Naval Proving Ground at Dahlgren, Virginia; also the courtesies extended by Professor A. L. Hughes, Professor G. E. M. Jauncey, and Doctor Joseph Keller of this department.

PHYSICAL REVIEW VOLUME 63, NUMBERS 11 AND 12 JUNE 1 AND 15, 1943

Diffusion Rates of Carbon in Iron-Molybdenum and Iron-Tungsten Alloys

R. SMOLUCHOWSKI
Research Laboratory, General Electric Company, Schenectady, New York
(Received March 24, 1943)

Measurements are reported of the influence of tungsten and molybdenum on the diffusion rate of carbon in face-centered iron at 1000°C. Both of these elements slow down the diffusion of carbon, the influence of tungsten being more than twice that of molybdenum. These results are compared with previous measurements on iron-cobalt alloys and other known data. No connection seems to exist between the variation in lattice parameter of face-centered iron and the variation in diffusion rate of carbon.

IN a previous paper[1] a strong accelerating influence of cobalt on the diffusion rate of carbon in face-centered iron was reported.* In continuation of this study, experiments were made with iron-molybdenum and iron-tungsten alloys.

There are relatively few binary systems in which measurements of this type can be made conveniently. The main condition is the existence of a sufficiently wide range of homogeneous face-centered solid solution. It should be possible to vary the concentration of carbon and of the alloying element, within relatively wide limits, to suit the accuracy of the measurements. Both in tungsten-iron and in molybdenum-iron alloys no single phase region with face-centered lattice exists beyond a few percent of the added element. Carbon, however, increases this range somewhat. Accordingly, experiments were made with the following alloys; the tungsten pair: 1.1 atomic percent (about 3.5 wt. percent) tungsten with 2.6 atomic percent (0.58 wt. percent) carbon and with 0.22 atomic percent (0.05 wt. percent) carbon; the molybdenum pair: 1.1 atomic percent (about 1.9 wt. percent) molybdenum with 3.1 atomic percent (0.7 wt. percent) carbon and without carbon, and finally a pair of alloys with the same molybdenum content but with 4.2 atomic percent (about 0.9 wt. percent) carbon, and without carbon. The first two groups of alloys, the tungsten alloys and the molybdenum alloys with lower carbon content, fall within the region of homogeneous face-centered lattice at 1000°C.[2] The third group, the molybdenum alloys with higher carbon, fall into the region where at 1000°C some of the carbides do not dissolve. These alloys were included in the experiments in order to see to what extent the presence of carbides affects the observed diffusion.

The experimental method was essentially the same as that used in the previous investigation. The welded samples were heated for three days at 1000°C and the concentration of carbon in layers parallel to the interface was determined.

[1] R. Smoluchowski, Phys. Rev. **62**, 539 (1942).

* *Note added in proof:* Mr. Malcolm F. Hawkes and Dr. Robert F. Mehl of the Carnegie Institute of Technology kindly informed me that their experiments do not show this strong accelerating influence of cobalt. This point needs thus further experimental clarification in particular in view of reference 6 quoted in reference 1 of this paper.

[2] S. Takeda, Tech. Rep. Sendai **9**, 483 (1930); **9**, 627 (1930); and **10**, 42 (1931). E. C. Bain, *The Alloying Elements in Steel* (Am. Soc. Metals, Cleveland, Ohio, 1939).

An interesting phenomenon was observed in the case of tungsten alloys. In order to prevent decarburization, all samples were enclosed in quartz tubes filled with argon. In each tube were two samples; one with iron containing molybdenum or tungsten and another with pure iron, in order to be able to compare the diffusion rates in iron and in iron alloy under identical conditions. Determination of the carbon concentration in the first heat-treated tungsten-iron samples showed that the carbon-rich side was somewhat decarburized and the carbon-poor side was carburized on the surface. There was a radial gradient of carbon concentration. No such effect was observed on the pure iron sample which was enclosed in the same quartz tube and thus underwent the heat treatment simultaneously with the iron-tungsten sample. An explanation of this effect, on the assumption that the argon used was impure, is difficult to accept because of the absence of this decarburization and carburization in the pure iron sample. Such an effect is, of course, very undesirable because it affects the concentration gradient due to volume diffusion and thus falsifies the results. In order to prevent it, the samples were covered electrolytically with a 0.3-mm thick layer of copper before heat treatment. This protective measure was applied to all samples, and it eliminated the occurrence of these surface phenomena. The computation of the diffusion coefficients was made by the usual Grube method. Because of the presence of the alloying elements on both sides of the interface, the computations were simple, and the use of the corrective formulae derived in the previous paper was not necessary.

The numerical results at various carbon concentrations are given in Table I.

The decelerating influence of both tungsten and molybdenum on the diffusion rate of carbon

TABLE I. Diffusion coefficients of carbon in iron-molybdenum and in iron-tungsten alloys at 1000°C. $D \times 10^7$ cm² sec.$^{-1}$.

Atomic percent carbon	Solvent: Pure Fe	Solvent: 1.1 at. percent Mo	Solvent: 1.1 at. percent W
0.6	2.9	2.5	1.1
1.1	3.2	2.6	1.2
2.2	3.7	2.8	1.25

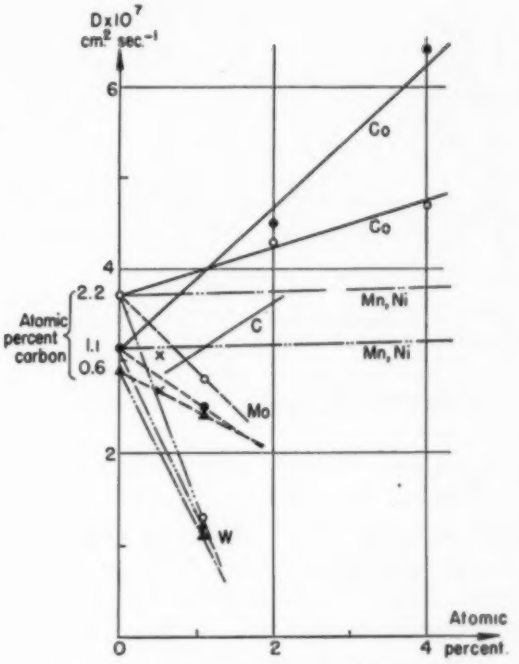

FIG. 1. Diffusion coefficients of carbon in various iron alloys at 1000°C. (Data for Mn and Ni were obtained from reference 3. Crosses indicate values for Mo based on reference 4.)

is clearly seen. For the same atomic percentage of added element, tungsten is much more effective than molybdenum. In Fig. 1 are plotted the diffusion coefficients of carbon in various iron alloys at 1000°C. Former measurements on iron-cobalt alloys[1] are included, also Wells and Mehl's data on iron-nickel alloys and iron-manganese alloys[3] and the recent measurements of Ham, Parke, and Herzig on iron-molybdenum alloys.[4] The latter were made with 0.47 atomic percent (0.80 wt. percent) molybdenum at various temperatures. The corresponding points in Fig. 1 were obtained by interpolation from Table III in Ham, Parke, and Herzig's paper at 1.1 and 2.2 atomic percent carbon. We see that the agreement is satisfactory, the influence of molybdenum being somewhat stronger than that reported here. The difference easily may be due to experimental errors and interpolation inaccuracies.

The diffusion coefficients given in Table I

[3] C. Wells and R. F. Mehl, Trans. A. I. M. E. **140**, 279 (1940).

[4] J. L. Ham, R. M. Parke, and A. J. Herzig, Am. Soc. Metals, Preprint, 1942.

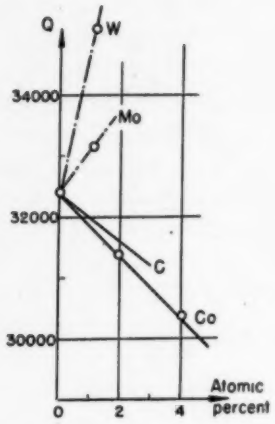

FIG. 2. Activation energies of the diffusion of carbon in various iron alloys.

and Fig. 1 were obtained with alloys which form solid solutions at 1000°C. As mentioned before, experiments were made also with another molybdenum alloy which had a little more carbon than the solubility limit at that temperature. The diffusion coefficients obtained from this alloy were within 15 percent of those given in Table I. This shows only that the few carbides present were quickly dissolved when the concentration of the surrounding solid solution decreased and thus they did not affect appreciably the total diffusion rate. In general, one would expect deviations from the simple concentration distribution law and other complicating effects.

In the previous paper, it was shown that the Dushman-Langmuir equation gives values of the activation energy Q in good agreement with experimental data in the case of iron-cobalt alloys. The same formula was applied here, and we assumed as before that the "free path" δ was 1.8A. We shall not repeat the details and discussion of the limitations of this procedure. The results for 1.1 atomic percent carbon are shown in Fig. 2 where the values for various iron alloys, including those investigated earlier, are plotted against the composition. A strong increase of the activation energy due to the presence of tungsten and molybdenum is apparent. It should be stressed that it is perfectly justifiable not to take into account the variation in δ with composition. A change in the lattice constant of one percent changes the value of Q by about 50 calories, which is, of course, entirely negligible as compared with the effects here observed.

It seemed interesting to see if there is any correlation between the changes in the lattice of iron brought about by the dissolved elements and the change of the rate of diffusion of carbon. Practically no data are available on the lattice constants in the face-centered lattice range of the iron-tungsten and iron-molybdenum alloys. In order to obtain a rough estimate of the influence of these two elements on the lattice of face-centered iron, measurements were made of the density and thermal expansion in the proximity of 1000°C. It turned out that both tungsten and molybdenum expand the iron lattice at a rate which is close to that computed from atomic radii, that is, about 2 percent per 10 percent of added element. Let us compare the change in the diffusion rate of carbon in iron due to the presence of other metallic elements as pictured in Fig. 1 on the one hand, and the change in lattice constants on the other. It turns out that there is no simple relation: cobalt, which leaves the iron lattice constant practically unaltered,[5] accelerates the diffusion markedly. On the other hand, carbon, which accelerates its own diffusion almost as effectively as cobalt, increases the lattice constant of iron rapidly, because of its interstitial location. Molybdenum and tungsten, which both have practically identical atomic radii, decrease this rate to a very different extent. The influence of tungsten is more than twice as strong as that of molybdenum. Nickel has practically no influence on the rate of diffusion, but it decreases the lattice constant of the face-centered iron.[6] Manganese, like nickel, leaves the diffusion rate practically unchanged, but increases the lattice constant of face-centered iron.[7] In the previous paper it was stated that the simple model of carbon atoms diffusing through the crystal lattice of iron, in which only the geometrical factors play a role, is untenable and that only a study of the influence of the alloying elements on the electronic interactions between the iron lattice and the carbon atoms can correlate the observed facts. The results here reported add support to this conclusion.

[5] A. Osawa, Sci. Rep. Tohoku **19**, 109 (1930).
[6] E. A. Owen, E. L. Yates, and A. H. Sully, Proc. Phys. Soc. **49**, 315 (1937): H. Esser and G. Müller, Arch. f. d. Eisenh. **7**, 265 (1933–1934).
[7] E. Öhman, Zeits. f. physik. Chemie **B8**, 81 (1930).

PHYSICAL REVIEW VOLUME 63, NUMBERS 11 AND 12 JUNE 1 AND 15, 1943

Investigations of Ferromagnetic Impurities. II

F. W. CONSTANT, R. E. FAIRES, AND H. E. LENANDER
Duke University, Durham, North Carolina

(Received February 23, 1943)

Continuing previous studies on minute ferromagnetic impurities in ordinary metals, an attempt was made to render such impurities non-magnetic through heat treatment. In the case of copper and brass it was found that heating to 900°C and 750°C, respectively, in hydrogen for two hours or more, followed by quenching, would eliminate the ferromagnetism. This method was not successful with silver. These results are interpreted in terms of the crystal structures of the metals and of iron, which is believed to be the chief magnetic impurity. In the case of copper, reheating to 900°C in an atmosphere containing oxygen caused the ferromagnetism to return strongly. This is explained as due to the diffusion of the oxygen into the copper at high temperatures. The effect of heat treatment at other intermediate temperatures on the magnetic hardness and hysteresis of the impurity was also investigated.

INTRODUCTION

IN an earlier paper[1] (Part I), results are given of measurements on the ferromagnetic impurities found in various commercial materials such as copper, silver, brass, aluminum, etc. The method involved suspending a specimen by a quartz fiber in the magnetic field of a pair of Helmholtz coils. In this way it was possible to measure either the remanent magnetization of the ferromagnetic impurities left after a specimen had previously been exposed to the much stronger field of an electromagnet, or, by means of a second set of magnetizing coils at right angles to the Helmholtz coils, to measure a hysteresis loop for a given specimen. As a result of this work it was found that most commercial metals contained ferromagnetic impurities which could easily be detected magnetically although compared with the remanent magnetization of pure iron, the magnetization of these impurities could represent an amount of impurity far too small to be detected by chemical analysis. The hysteresis measurements showed that the impurities were magnetically "hard."

Since in some cases, such as galvanometer coils, standard inductances, etc., magnetic impurities could be objectionable, it seemed of interest to investigate whether such impurities could be rendered non-magnetic by heat treatment. It was also hoped that in this manner more would be learned about the state of the magnetic impurity in the parent metal. For this purpose three common metals were chosen, namely copper, brass, and silver. The effect of heat treatment in various atmospheres on both the remanent magnetization and hysteresis was investigated.

[1] F. W. Constant and J. M. Formwalt, Phys. Rev. **56**, 373 (1939).

EXPERIMENTAL

A given specimen was surface cleaned, magnetized, and its remanent magnetization measured in the usual way. The coercive force was also found by using increasing negative fields until the remanent magnetization was reduced to zero. The specimen was then placed in a protecting box of molybdenum (which showed no ferromagnetism), and this in turn was introduced into a Leeds and Northrup "Fyrestan" tube situated in a resistance furnace. The tube could be evacuated and various gases run through at one or two atmospheres pressure. The furnace was then heated up to the required temperature and held there for eight hours after which the tube was opened, and the box containing the specimen was removed quickly and quenched in oil. In a few cases the specimen was allowed to cool overnight in the furnace. Although heating to high temperatures would demagnetize a specimen, it did not necessarily follow that the specimen was non-magnetic. Hence after heat treatment each specimen was again placed in a magnetizing field and the remanence, coercive force, or hysteresis measured.

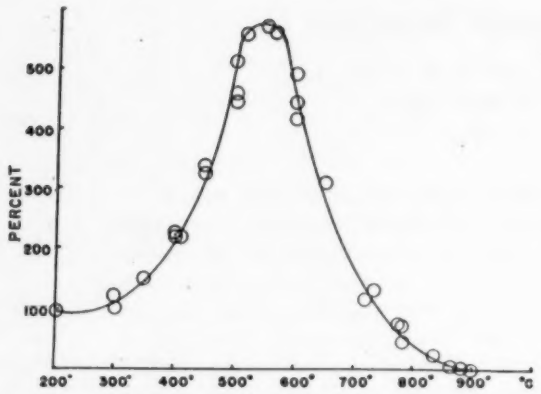

FIG. 1. Ratio of remanence after heat treatment of copper in hydrogen to the original remanence expressed in percent.

RESULTS

1. Copper

Samples were taken from No. 12 D.C.C. magnet wire. As a test for uniformity two or three samples were run through together; the resulting agreement was always good, differences not exceeding a few percent. The remanence was measured both before and after heat treatment, the same magnetizing field being used each time. The new remanence was computed as a percent of the original, and this was plotted against the temperature of the 8-hour run. Figure 1 shows the results for heating in a hydrogen atmosphere, which was naturally tried first in order to keep the specimen "clean." After a slight initial decrease the curve rises to a peak at about 525°C for which the new remanence is some five and a half times as great as the original. Above 525°C the curve falls rapidly to zero at 875°C. Specimens heated to 900°C or higher for two hours or more were completely non-ferromagnetic when cooled. In the case of copper slow cooling gave practically the same results as quenching.

In order to understand better the curve in Fig. 1, hysteresis loops were run on samples before and after heating to 300°, 500°, and 700°C, respectively. These loops were obtained by measuring the period of the specimen when suspended parallel to the magnetizing field. This field exerted a restoring torque proportional to the magnetization which aided the restoring torque of the fiber and hence shortened the period of oscillation. Heating to 300°C produced only a slight change in the hysteresis loop. Figure 2 shows loops before and after heating to 500°C and the heat treatment has evidently made the magnetism "harder," increasing both the remanence and coercive force. This would largely explain the maximum in the curve of Fig. 1 at about 525°C. Heating to 700°C, on the other hand, decreased the remanence somewhat, the coercive force remaining about the same (55 oersteds).

As a further check on the above results a specimen was magnetized in a field of about 4500 oersteds and then placed in a weak field in the opposite direction which could gradually be increased until the remanence disappeared. This gave approximately the coercive force for a larger loop between plus and minus 4500 oersteds. Here again heating to 500°C increased the coercive force from 215 to 320 oersteds whereas heating to 700°C only increased it slightly.

Copper samples were next heat treated in a nitrogen atmosphere. The nitrogen used was ordinary tank nitrogen. The percent of the original remanence after various heatings is shown in Fig. 3. The results differ surprisingly from those shown in Fig. 1 for a hydrogen atmosphere. First, the strong peak at 525°C has disappeared, and secondly, around 900°C an increase in remanence has actually occurred.

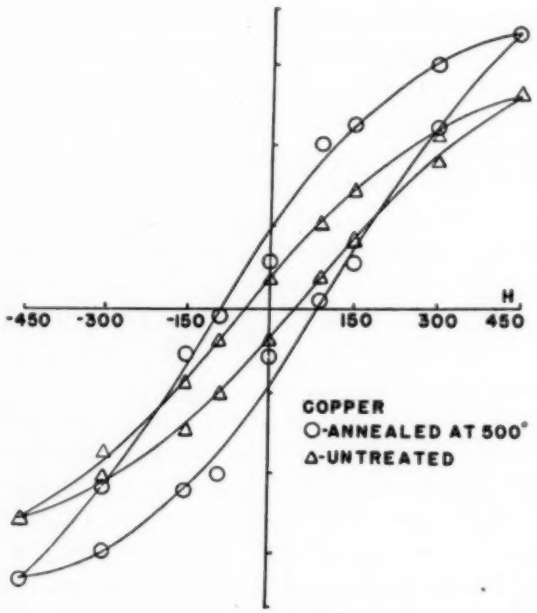

FIG. 2. Hysteresis of copper before and after heating to 500°C.

Finally, temperatures of at least 1000°C were necessary to eliminate the ferromagnetism. Since air gave similar results to nitrogen, it was believed likely that the tank nitrogen contained sufficient oxygen impurity to cause the effect. Attempts were made to purify the nitrogen by passing it over red hot copper and drying it and repeatedly evacuating and refilling the system. As a result the 900°C peak was almost eliminated.

Another interesting point was that a sample which had been rendered non-magnetic in hydrogen at 900°C could be made more magnetic than originally by reheating in air or tank nitrogen at 900°C. This was not a surface effect. This cycle could be repeated indefinitely unless temperatures exceeding 1020°C were used in which case the magnetism returned with more difficulty.

Heating in hydrogen at 900°C or higher always eliminated the ferromagnetism. Although reheating in air at 900°C would cause it to return, heating or annealing at lower temperatures such as 500°C, whether in air or hydrogen, caused no such return. The conclusion was that oxygen diffusing into the copper above about 850°C was responsible for the return of, or increase in, ferromagnetism between 850° and 950°C.

Finally, following the work of Smith[2,3] and Bitter,[4,5] it was found that cold rolling non-magnetic specimens caused a return of the ferromagnetism.

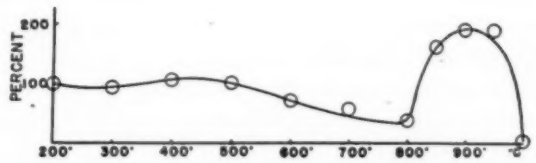

FIG. 3. Ratio of remanence after heat treatment of copper in nitrogen to the original remanence expressed in percent.

2. Brass

The results of heat treating samples of a brass rod in hydrogen at various temperatures are shown in Fig. 4 in which, as in Fig. 1 for copper, the change in remanence is plotted. The brass specimens were about ten times as magnetic as the copper, but the curve is similar except that the peak occurs earlier and magnetism disappears when the heating is carried to about 750°C. Specimens from a different source of brass gave a similar curve except for a much higher peak (650 percent) at 400°C. Above 750°C quenching was necessary if the last 5 percent of remanence were to be removed.

Hysteresis loops were also taken for brass.

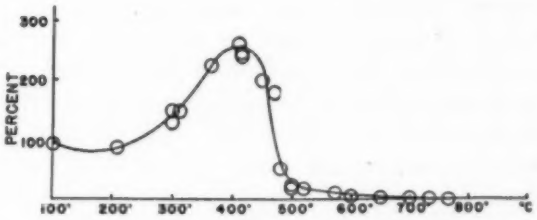

FIG. 4. Ratio of remanence after heat treatment of brass in hydrogen to the original remanence expressed in percent.

However, it was impossible to obtain a loop of any size for untreated specimens because the magnetization was sufficiently "soft" to rotate with the rotation of the specimen or of the resultant field. But after heating to 400°C or 500°C loops could be obtained, indicating, as for copper, an increase in magnetic hardness.

Reheating non-magnetic brass specimens at intermediate temperatures did cause a return of the magnetism. Probably due to the greater amount of impurity in the brass, the solubility limit for the impurity became a factor and the non-magnetic state was then less stable at intermediate or room temperatures.

3. Silver

Similar heat treatments in hydrogen carried out on specimens of silver wire gave much less striking effects, as shown in Fig. 5, where the remanence is again plotted. Heating up to the melting point failed to reduce the ferromagnetic remanence by more than half, and this decrease was probably due to the magnetic impurity becoming magnetically softer.

DISCUSSION

The ferromagnetic impurity was taken to be iron, perhaps picked up by the specimen when

[2] C. S. Smith, Phys. Rev. **57**, 337 (1940).
[3] C. S. Smith, Am. Inst. Min. Metal. Eng., Tech. Pub. No. 1394 (1942).
[4] F. Bitter and A. Kaufmann, Phys. Rev. **56**, 1044 (1939).
[5] F. Bitter, A. Kaufmann, C. Starr, and S. T. Pan, Phys. Rev. **60**, 134 (1941).

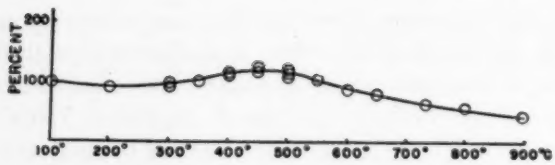

FIG. 5. Ratio of remanence after heat treatment of silver in hydrogen to the original remanence expressed in percent.

drawn through dies, or during cold rolling. The fact that the original remanence was partly retained if copper and brass specimens were heated to temperatures up to 550°C and not remagnetized after cooling indicated that the Curie temperatures for the impurities in these metals did not lie below 550°C. This made it very unlikely that nickel could be the chief ferromagnetic impurity. Further, contamination with cobalt was much less likely than with iron. Finally, brass gave a positive chemical test for iron.

Although the work of Tammann and Oelsen[6] would indicate around one percent impurity when 900°C is required to render a copper-iron alloy non-magnetic, it is very unlikely that in our case as much was present. The 900°C is given as a safe upper limit for rendering copper wire non-magnetic. For one thing, quenching at 900°C exposed the specimen to air (oxygen), which could act on it as mentioned above. Further, longer annealing at 800°C was found equally effective in eliminating the magnetism.

The phase diagram for copper-iron alloys as given by Hansen[7] shows that at 900°C up to two percent of iron will dissolve in copper as a solid solution with the face-centered cubic structure characteristic of copper. This is reasonable since the lattice constant of copper is 3.62A[8] and at high temperatures iron is also face-centered cubic in structure with a lattice constant of 3.60A. At room temperature the solubility of iron in copper is practically nil since iron is then normally body-centered cubic in structure. This latter structure is associated with the ferromagnetic state of iron. However, it now seems evident from the above work and that of Smith[2,3] and Bitter[4,5] that copper containing up to more than one percent iron in solid solution at 900°C may be cooled to room temperature retaining the iron in solution in a metastable, non-magnetic form. Annealing at intermediate temperatures does not restore the magnetism although it may precipitate the iron out in a non-magnetic state. Cold work, however, restores the magnetism, and Smith has shown that there is at the same time a reappearance of a body-centered lattice, presumably through a modification of the iron. Hence the mechanism of rendering a specimen of copper non-magnetic is simply to heat it at a sufficient temperature for a sufficient time to dissolve the iron impurity in the copper lattice. Subsequent cooling or annealing below 850°C will not alone restore the magnetism.

The case of brass would seem similar to that of copper. The lattice constant of brass (face-centered cubic) is almost exactly that of face-centered iron. The solubility of iron in brass takes place even more readily than in copper, a lower temperature for brass than iron being sufficient to dissolve a greater amount of impurity in a given time.

The lack of complete disappearance of the magnetism upon heating silver indicates lack of complete solubility of the impurity in the silver. Although silver is face-centered cubic in structure its lattice constant, 4.60A, differs considerably from that of γ-iron. As even the liquid phases of silver and iron do not mix little solubility can be expected for the solid phases.

Of final interest is the comparison of the effect of an oxygen and a hydrogen atmosphere during heat treatment of copper at 850°C or higher. Both gases have definite effects. However, considerably higher temperatures are required before oxygen can diffuse through copper than in the case of hydrogen, hence the effect of oxygen is noticed only at 850°C or higher. The simplest explanation of the results given above would seem to be that (1) the iron impurity exists partly as an oxide in the copper and this oxide is reduced by hydrogen giving an increase in magnetism at around 550°C, (2) the iron dissolves in the copper lattice at higher temperatures, (3) introduction of oxygen at higher temperatures causes the dissolved iron to be reprecipitated out as an oxide, and (4) reintro-

[6] G. Tammann and W. Oelsen, Zeits. f. anorg. allgem. Chemie **186**, 257 (1930).
[7] M. Hansen, *Der Aufbau der Zweistoffleigierungen* (Julius Springer, 1936).
[8] R. W. G. Wyckoff, *The Structure of Crystals* (Little and Ives, New York, 1924).

duction of hydrogen again reduces the oxide and allows the iron once again to dissolve in the copper.

CONCLUSIONS

Commercial specimens of copper and brass may be rendered completely non-magnetic by heating in hydrogen to a sufficiently high temperature to allow the magnetic impurity to dissolve in the copper lattice. A temperature of 900°C is safe for a two-hour treatment. This method was unsuccessful in the case of silver, but might work for certain other metals with which iron can form solid solutions. The magnetism can be made to return in copper by reheating in air above 850°C, or by annealing plus cold work.

PHYSICAL REVIEW VOLUME 63, NUMBERS 11 AND 12 JUNE 1 AND 15, 1943

Magnetic Properties of Solid Solutions

III. The Paramagnetic Alloys of Copper and Nickel

A. R. KAUFMANN AND C. STARR
Massachusetts Institute of Technology, Cambridge, Massachusetts

(Received December 29, 1942)

The magnetization of the paramagnetic alloys of copper with nickel has been studied as a function of temperature and applied field. It is found that a Curie-Weiss equation cannot represent the results and an equation of the form $\chi = aT + b + (c/T)$ is found to be satisfactory. Alloys in the range from 30 to 38 percent nickel showed a considerable field dependence of the susceptibility at low temperatures.

THE magnetic properties of copper-nickel alloys have been investigated by many people but most of the work has been done at elevated temperatures and on those alloys which are definitely ferromagnetic. The present work was intended primarily to cover the low temperature properties of those alloys which are not ferromagnetic at room temperature, although the investigation was extended to elevated temperatures in order to get a more comprehensive picture of the magnetic behavior. In this alloy series there are compositions which are neither ferromagnetic nor truly paramagnetic even in the Curie-Weiss sense and it is this phenomenon which was looked for in the investigation. It was hoped that such a study would reveal not only the magnetic moment of nickel atoms in dilute solution in copper but also contribute to the knowledge of conditions which lead to ferromagnetism as the concentration of nickel is increased. Copper-nickel alloys are particularly suited for this purpose since they form a complete series of solid solutions in which the added nickel atoms simply replace the copper atoms on the crystal lattice of the latter.

PREPARATION OF ALLOYS

The materials used for the alloys were Mallinkrodt's reagent copper[1] and reagent nickel[2] which were melted together in quantities of about 40 grams. Melting was carried out in an alundum crucible and in a hydrogen atmosphere, the temperature of the furnace being about 1500°C. The alloys were chill cast in a vacuum directly from this melting temperature. These castings were given a homogenizing anneal at 900°C in hydrogen for 36 hours and then were cold swagged with intermediate anneals into the form of $\frac{5}{16}$-inch diameter rods. Short pieces weighing

TABLE I. Composition of alloys, weight percent.

Alloy	Ni	Fe	Alloy	Ni	Fe
J27	—	0.00	J25	20.34	0.016
J7	0.94	0.0023	J24	29.98	0.024
J8	4.99	0.0046	J23	35.59	0.030
J9	10.10	0.0094	J22	38.00	0.029
J26	10.99	0.012	J21	50.16	0.034

[1] Sb −0.01 percent, As −0.001 percent, Fe −0.004 percent, Pb −0.01 percent, Sn −0.01 percent.
[2] Co −0.01 percent, Fe −0.10 percent, Pb −0.01 percent.

TABLE II. Susceptibility per gram of alloy.

	Weight percent nickel									
T −°K	0*	0.94	4.99	10.1	11.0	20.3	30.0	35.6	38.0	50.2
14.0	−0.034	−0.023	0.125		0.581	1.27	4.37†	14.8†	44.7†	
20.4		−0.032	0.104	0.362	0.483	1.10	3.62†	11.0†	31.5†	
77.3	−0.073	−0.052	0.052	0.216	0.274	0.67	1.81	4.01	7.70†	Ferromag.
295	−0.0796	−0.062	0.042	0.185	0.221	0.553	1.277	1.993	2.84	11.8
523	−0.0786	−0.060	0.047		0.232	0.592	1.222	1.675	2.11	
773	−0.0748	−0.055	0.063		0.262	0.635	1.200	1.561	1.85	
1023	−0.0693	−0.045	0.079		0.300	0.687	1.213	1.515	1.74	
1273	−0.0645	−0.043	0.103		0.339	0.735	1.230	1.497	1.69	

* Copper with 0.0025 percent iron described in preceding paper, Phys. Rev. **60**, 134 (1941).
† Measurements showing field dependence. Initial susceptibility given.

about 4 grams were cut from the rods and were used as the specimens for measurement. Immediately adjacent pieces were cut off for chemical analysis for iron and nickel, the results of which are given in Table I. The specimens were given a final anneal in hydrogen and cooled in the furnace in order to remove the effects of cold work.

METHOD OF MEASUREMENT

The same technique and the same magnet were used for these measurements as has been described in the preceding papers[3] of this series. For measurements below room temperature the specimens were suspended from the balance with a silk thread while a sling made of molybdenum foil was used for this purpose at elevated temperatures. No attempt was made to make a correction for the force on the silk thread but a correction was made whenever the molybdenum sling was used.

EXPERIMENTAL RESULTS

The susceptibility of the alloys was determined by plotting the magnetization against the field and taking the slope of the straight line which is found between 10 and 30 kilogauss. This procedure automatically corrects for any traces of ferromagnetic particles since these always are practically saturated in fields of this magnitude. The ferromagnetic inclusions in all cases were almost negligible.

Certain of the alloys, which were normally paramagnetic at room temperature, began to show progressively larger saturation effects in high fields as the temperature was lowered. As with the copper-iron alloys, this effect was considered to be a true property of the alloy and not just simply the result of ferromagnetic inclusions. In such cases the initial slope of the magnetization curves was taken as the initial susceptibility since the room temperature measurements showed an insufficient amount of ferromagnetic particles to affect appreciably this quantity. An example of this type of behavior is shown in Fig. 1 for the case of an alloy with about 40 percent nickel.

The values of mass susceptibility as determined by the above methods are given in Table II. The measurements showing field dependence are indicated and for these the initial susceptibility is given.

It is to be noted, as discussed in an earlier paper,[3] that the relative precision of the values given in Table II for different specimens is not greater than about 1 percent because of the difficulty in locating the specimens at exactly the same point in the magnet. On the other hand, the relative accuracy of the values obtained for any given specimen at different temperatures above room temperature is much greater than this, since the position of the specimen was not altered throughout the run. This position could not change appreciably as a result of thermal expansion since the heated zone in the furnace is only a few inches long. This conclusion is of importance in evaluating the small but consistent changes in susceptibility which are observed above room temperature. Fortunately, this conclusion is substantiated by the measurements themselves since it is found that both dia- and paramagnetic susceptibilities change in the

[3] F. Bitter and A. R. Kaufmann, Phys. Rev. **56**, 1044 (1939); Bitter, Kaufmann, Starr, and Pan, Phys. Rev. **60**, 134 (1941).

proper direction as the temperature is varied; that is, the paramagnetic values become greater when the diamagnetic values decrease. If the observed changes with temperature were due simply to a shift in position of the specimen, then the dia- and paramagnetic susceptibilities would both either increase or decrease depending on the direction of the shift.

DISCUSSION OF RESULTS

The susceptibility at room temperature is plotted as a function of nickel content in Fig. 2, and the results of previous workers are shown for comparison. Our results lie along a smooth curve which is in qualitative agreement with previous measurements[4, 5] except for the work of Williams[6] who found a bulge at about 30 percent nickel. The quantitative agreement of the various workers is not too good. It seems likely that the reason for this is to be found in the purity and treatment of the alloys rather than in the methods of measurement. For example, at room temperature 0.1 percent iron will change the susceptibility of copper to the same extent as 4 percent of nickel and hence the iron impurities of the alloys up to about 20 percent nickel may influence considerably the value obtained for the susceptibility. Above 30 percent nickel the susceptibility increases very rapidly with concentration and, therefore, it becomes increasingly important to be sure that the alloys are well homogenized before measurement. The fluctuation in nickel concentration throughout a specimen as solidified from the liquid state can easily be great enough to give an erroneous value for the susceptibility corresponding to the average composition of the specimen.

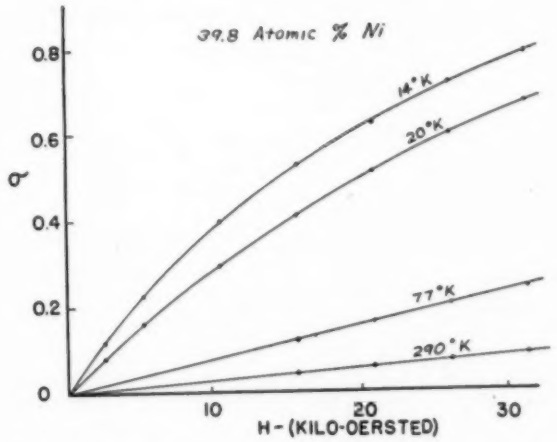

FIG. 1. Magnetization curves [specific intensity of magnetization (σ)] at low temperatures.

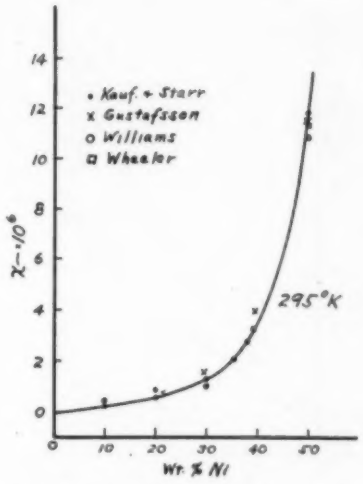

FIG. 2. Mass susceptibility as a function of nickel content at room temperature.

It is not beyond the realm of possibility that at least a partially ordered structure might occur in the composition range of Cu_3Ni and that such an occurrence would affect the susceptibility. This might account for the irregularity in the susceptibility *versus* concentration curve as reported by Williams.[6] In order to check this, the authors slowly cooled the 30 percent nickel alloy from 820°C to 220°C over a period of ten days, since this should allow an ordered structure to form. The susceptibility of this specimen agreed with the value obtained previously to within the experimental error. As a further test the susceptibility of the slowly cooled specimen was measured at 50°C intervals up to 450°C, since the breaking up of an ordered structure should give a discontinuous change in the observed values. No such effect was observed and hence it was concluded that the specimen did not have an ordered structure, or at least that if there were an ordered structure it caused less than a 1 percent change in the susceptibility.

From Fig. 2 it is evident that the susceptibility does not vary linearly with the concentration of nickel and that the deviation from linearity becomes more and more marked as the ferro-

[4] G. Gustafsson, Ann. d. Physik **28**, 121 (1937).
[5] M. Wheeler, Phys. Rev. **56**, 1137 (1939).
[6] E. H. Williams, Phys. Rev. **38**, 828 (1931).

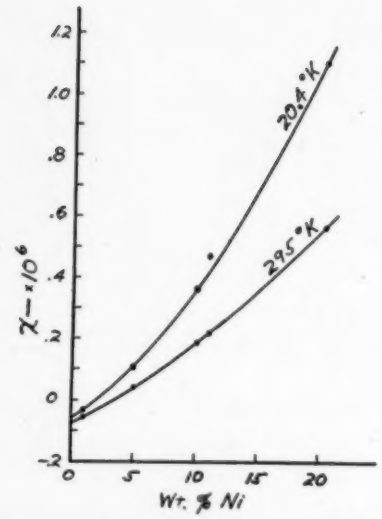

FIG. 3. Non-linear variation of susceptibility with concentration in dilute solutions.

magnetic compositions are approached. This behavior is true at all temperatures down to 14°K and it is true even for small concentrations of nickel as shown in Fig. 3.

The observed low temperature susceptibility values were corrected for the susceptibility of copper and the dissolved iron impurities, and the reciprocals of these quantities were plotted against the absolute temperature as shown in Fig. 4. It is apparent that a Curie-Weiss law does not describe the results for the low nickel alloys and that it tends to become more satisfactory as the nickel content approaches the ferromagnetic compositions. In view of this behavior no attempt was made to calculate Bohr magneton values for the nickel atoms by means of the Curie-Weiss equation although this was done by a different method as will be explained shortly.

Because of the failure of the Curie-Weiss equation to describe the results below room temperature, the measurements were extended to 1300°K. The susceptibility values over the entire range of temperature are plotted in Fig. 5. It is immediately apparent that the susceptibility of all the alloys increases at high temperature, although this effect is concealed by the tendency toward a Curie-Weiss behavior in the higher nickel alloys. This high temperature behavior is undoubtedly the same phenomenon as has already been reported for pure copper[7] although the effect seems to become much greater as nickel is added.

For purposes of comparison the measurements of Gustafsson[4] are also shown in Fig. 5. It is apparent that the temperature range covered by his work did not allow him to observe the phenomenon now reported and that his work is in agreement with ours over the corresponding ranges of temperature.

It is obvious from Fig. 5 that the Curie-Weiss equation cannot represent the results at high temperatures and hence an expression of the form

$$\chi = aT + b + (c/T) \qquad (1)$$

was fitted to the curves by substituting experimental values at three temperatures and solving for the constants. This procedure is quite arbitrary, of course, and can only be justified if the curve calculated from the constants represents the experimental curve accurately. In the present case there was satisfactory agreement between the computed and the experimental curves for all the alloys from 10 to 35 percent nickel. That is, the difference between the two curves was not greater than a few percent except at 14°K. At this temperature and for the other alloys at other temperatures as well, the difference was as large at 10 percent. In spite of this it seems worth while to present briefly the results obtained and accordingly the constants are tabulated in Table III.

The values in Table III were found when the

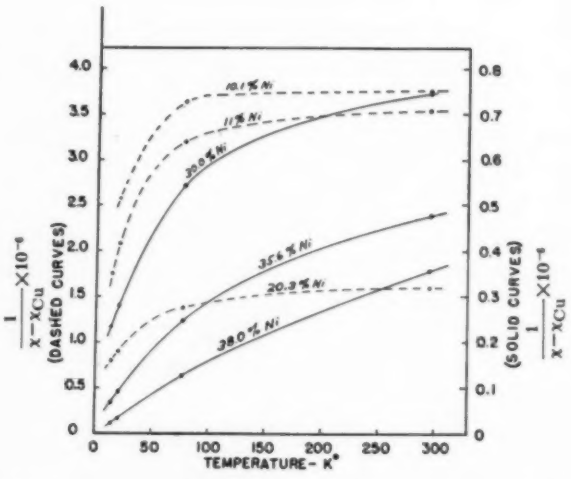

FIG. 4. Reciprocal of mass susceptibility corrected for copper as a function of temperature.

[7] Bitter, Kaufmann, Starr, and Pan, Phys. Rev. **60**, 134 (1941).

susceptibility data obtained at 20.4°K, 290°K, and 1270°K are used for the simultaneous solutions. A choice of different temperatures would lead to somewhat different values for the constants. Also, if one of the terms in Eq. (1) is small compared with the other terms, then that constant is relatively more subject to error because of the limited experimental accuracy. This reason presumably accounts for the erratic variation of the constants a and b when c becomes large.

The first term in Eq. (1), which indicates an increase in susceptibility with increasing temperature, is not accounted for by any of the present theories of magnetism. Such behavior has been reported, however, for the alkali metals[8] and has been attributed by Stoner to a decrease in the number of electrons per unit volume caused by the thermal expansion of the crystal. This explanation is fairly consistent with the present observations on pure copper since it is possible to calculate a temperature coefficient for the mass susceptibility which is only about six times smaller than the value for a which is given in Table III. This calculation was made with the equation for the susceptibility of free electrons and on the assumption that the change in the number of electrons per unit volume is proportional to the temperature coefficient of thermal expansion for copper. Such a calculation is not nearly as satisfactory for the alloys since the coefficient of thermal expansion changes only slightly with addition of nickel to copper, but the constant a changes by at least a factor of 10 when only 20 percent of nickel is added. However, the other factors which may change with alloying such as the number of free electrons per atom and the shape of the energy band could easily mask any effect due to differences in expansion coefficient.

TABLE III. Constants in Eq. (1) and Bohr magneton numbers (p_B).

Alloy	Wt. percent nickel	$a\times10^{10}$	$b\times10^{6}$	$c\times10^{6}$	p_B
J27A	0.00	0.237*	−0.097*		
J7A	0.94	0.217	−0.071	0.787	0.199
J8A	4.99	0.67	0.017	1.756	0.129
J26A	10.99	1.38	0.160	6.34	0.165
J25A	20.3	2.22	0.444	13.29	0.176
J24A	30.0	0.91	1.073	51.95	0.286
J23A	35.6	0.31	1.302	197.7	0.512
J22A	38.0	5.42	0.510	632.0	0.886

* Values at 290°K, 770°K, and 1270°K used in simultaneous solution.

[8] E. C. Stoner, *Magnetism and Matter* (Methuen & Company, London, 1934), p. 509.

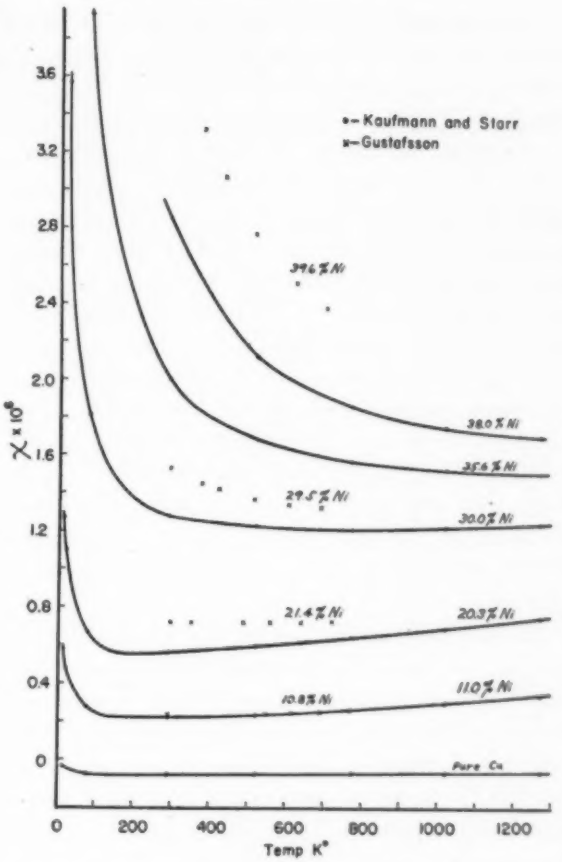

FIG. 5. Mass susceptibility as a function of temperature for different nickel contents.

The constant b of Eq. (1) may be considered as the sum of the diamagnetism and temperature independent electron paramagnetism. It is interesting to note, first of all, that this treatment of the experimental data leads to a value of -0.097×10^{-6} for the temperature independent mass susceptibility of copper instead of the ordinary room temperature value of -0.085×10^{-6} and that this new value is in somewhat better agreement with the calculated value for copper.[9]

The values of b increase continuously with nickel content until c becomes so large that b can no longer be satisfactorily determined. At

[9] E. C. Stoner, *Magnetism and Matter* (Methuen & Company, London, 1934), p. 511.

30 percent nickel b has become about 15 times as large as the theoretical free electron susceptibility of copper. In terms of the band theory of susceptibility this would mean that the number of states at the top of the energy band has increased by this factor since the electronic susceptibility is proportional to the number of states. However, an increase of this magnitude hardly seems compatible with the published energy band shape for copper[10] in spite of the fact that the alloys are approaching an unfilled d band. If the nickel and copper atoms of the alloys form a common set of bands, then the d band should not begin to be unfilled until 40 percent nickel is reached. The present determination of b means either that this perfect sharing of electrons does not occur in the alloy or else one must conclude that b does not have the significance attributed to it here.

The last term in Eq. (1) offers further evidence that a common $3d$ band for the copper and nickel atoms does not describe the results accurately. The reason is simply that this term indicates a normal paramagnetic susceptibility whereas the band picture would alloy only a temperature-independent electronic susceptibility up to 40 percent nickel. There can be no doubt that the low nickel alloys exhibit a large temperature dependence, but whether or not this is correctly represented by a term in $(1/T)$ is open to dispute. At any rate the constant c as here determined shows a continuous variation with nickel content becoming rapidly larger as a concentration of 40 percent is approached. If one regards c as the ordinary Curie constant, the Bohr magneton values per nickel atom may be obtained from the formula $p_B=2.84(cM/K)^{\frac{1}{2}}$, where M is the molecular weight of nickel and K is the fraction of nickel by weight in the alloy. From Table III it can be seen that the Bohr magneton values remain fairly constant up to about 20 percent nickel and then increase rapidly. The significance of this is not clear since the values of p_B are about ten times smaller than that found for pure nickel above its Curie temperature.

Finally, we must discuss the field dependence of the susceptibility which was observed at low temperatures in the alloys with 30 percent and more of nickel. The careful measurements of Weiss and Forrer[11] have shown that the magnetization curve of pure nickel shows no discontinuity at the Curie temperature and that the curve becomes linear within the experimental error only after 40 degrees above the Curie temperature has been reached. It seems reasonable to suppose that this same phenomenon exists also in the ferromagnetic copper-nickel alloys. From this it follows that in varying the composition from ferrromagnetic to paramagnetic alloys at any given temperature the paramagnetic compositions close to the boundary will show field dependence. Our observations must be part of this phenomenon in spite of the fact that the Curie temperature has been supposed to reach absolute zero at 40 percent nickel.

The ordinary Weiss theory will lead to a large field dependence of the susceptibility above the Curie temperature as may readily be verified by numerical substitution in the equation. For nickel this calculated field dependence becomes smaller than 1 percent at 30°C above the Curie temperature and this is in agreement with the measurements. (The calculated magnetization, however, is only about one-half as large as the measured values in fields up to 20,000 oersted.) This result substantiates the idea that the observations on low nickel alloys are to be correlated with the tendency toward ferromagnetism. A more detailed discussion of this problem will be undertaken at a later time after more observations of the same sort have been made on similar alloy systems.

[10] J. C. Slater, Phys. Rev. **49**, 537 (1936).

[11] P. Weiss and R. Forrer, Ann. de physique **5**, 153 (1926).

PHYSICAL REVIEW VOLUME 63, NUMBERS 11 AND 12 JUNE 1 AND 15, 1943

Electrical Conduction and Recrystallization in Thin Pb Films Deposited at Low Temperatures*

EDGAR L. ARMI**
Cryogenic Laboratory, Norman Bridge Laboratory of Physics, California Institute of Technology, Pasadena, California

(Received March 26, 1943)

By evaporation in high vacuum, thin Pb films were deposited on glass plates cooled by liquid hydrogen. Beginning of electrical conduction was observed in films of a nominal thickness of 7A. Aging of these films at various temperatures revealed the existence of two regions of different behavior; decrease of resistance below and increase of resistance above an equilibrium temperature. Possible explanations are offered.

As numerous workers have shown, thin metal films condensed out of their vapor are unstable and undergo structural changes while aging. Various factors have an influence on these changes by affecting the mobility of the metal molecules involved, in particular the nature of the backing, thickness of the film, temperature, presence of gases, etc. Thus either an increase or decrease of the electrical resistance of the film may be observed.

Starting with investigations by Anderson[1] and Foster[2] on the electrical conductivity of thin Ag and Pb films, the range of the present research was extended to temperatures of liquid and solid hydrogen. It was the purpose of this investigation to study the behavior of thin films of heavy metal atoms deposited at temperatures sufficiently low to eliminate disturbing thermal effects. These films were found to possess a "critical" temperature (in the neighborhood of 100°K or higher, depending on the individual data of the film investigated), below which the electrical resistance decreases with time until it reaches a stable value, and above which it increases at a rate rapidly growing with higher temperatures.

APPARATUS AND METHODS

Figure 1 shows a lengthwise cut through the evaporation chamber. Constructed of Pyrex glass, it has wide bore ground joints at both ends. The Pb to be evaporated is held in an iron crucible and placed in an electrical furnace. Stray evaporation is cut only by a cylindrical shield around the axis of the beam. Two shutters are provided and operated by an electromagnet from the outside, the first closing the opening of the cylindrical shield, the second immediately in front of the deposit surface.

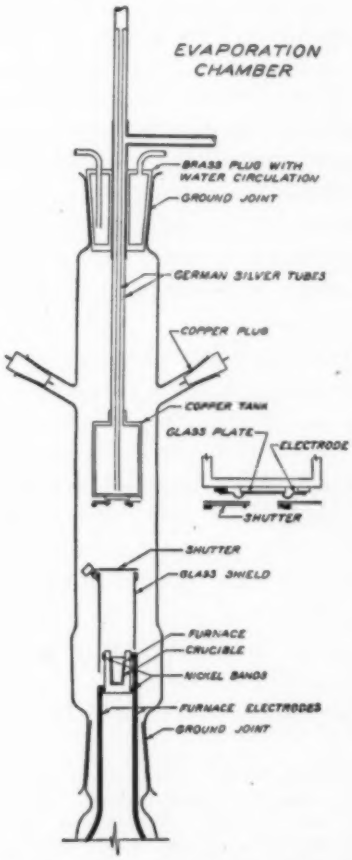

FIG. 1. Evaporation chamber. Lengthwise cut and detail of shutter and electrodes.

* E. L. Armi, Thesis, June 1941, California Institute of Technology.

** Now at the Department of Physics, Alabama Polytechnic Institute, Auburn, Alabama.

[1] A. B. C. Anderson, Thesis C.I.T. (1933); A. B. C. Anderson and A. Goetz, Phys. Rev. **45**, 293 (1934).

[2] M. G. Foster, Phys. Rev. **57**, 42 (1940) and Thesis C.I.T. (1939).

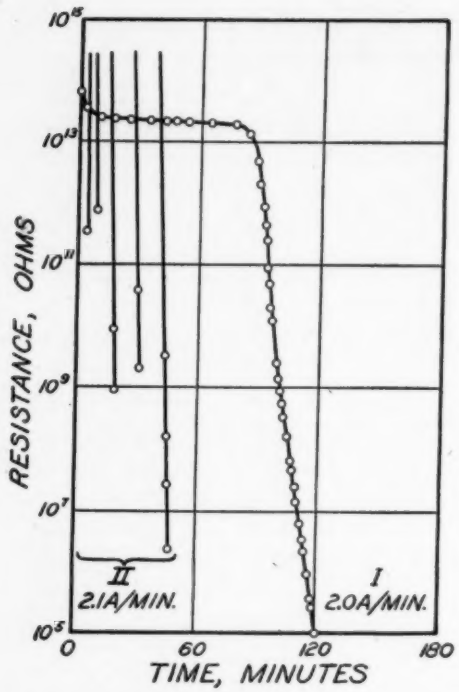

FIG. 2. Continuous deposits. Curve I room temperature deposit. Curve II low temperature deposits.

Deposits were made on 0.2 mm microscope cover glasses provided with platinized contact strips, the film area being 1.3 cm by 1.4 cm. The backs of the cover glasses were platinized and copper plated before being inserted; in order to assure good heat transfer with the copper cooling reservoir, they were soldered to the latter, in vacuum, by induction.

Film thicknesses were calculated from the experimental evaporation data, with the density of Pb taken as that of the metal in bulk (11.3 g/cm³). Evaporation rates were established by running the furnace at fixed temperatures for extended periods of time and weighing on a microbalance the deposits obtained; the values thus found (between 1×10^{-8} and 1×10^{-6} g cm^{-2} min.$^{-1}$ for temperatures in the neighborhood of 500°C) were in good agreement with those calculated from kinetic theory.[3]

Vacua were measured either with an ionization gauge connected directly to the evaporation chamber or with a McLeod manometer. A high frequency induction furnace was used to outgas metal parts before evaporation was started. All glass parts were carefully cleaned and a fresh cover glass inserted for each run. Vacua obtained were of the order of 10^{-6} mm Hg.

The electrical circuit, described previously by Anderson[1] and Foster,[2] permits resistance determinations up to 10^{15} ohms by use of a leakage compensation method. Five condensers of different sizes are provided to cover a wide range of resistance values. A string electrometer serves as null instrument.

The experiments fall into two groups, depending on the temperature of the film. In the first group, deposits were made on a backing at room temperature. In the second group, the tank behind the backing was filled with a cooling agent. Liquid air was siphoned directly into the reservoir and, by reducing the pressure over the liquid air, it was solidified; similarly, after precooling with liquid air, liquid hydrogen was siphoned into the revervoir and solid hydrogen was obtained by reducing the vapor pressure.

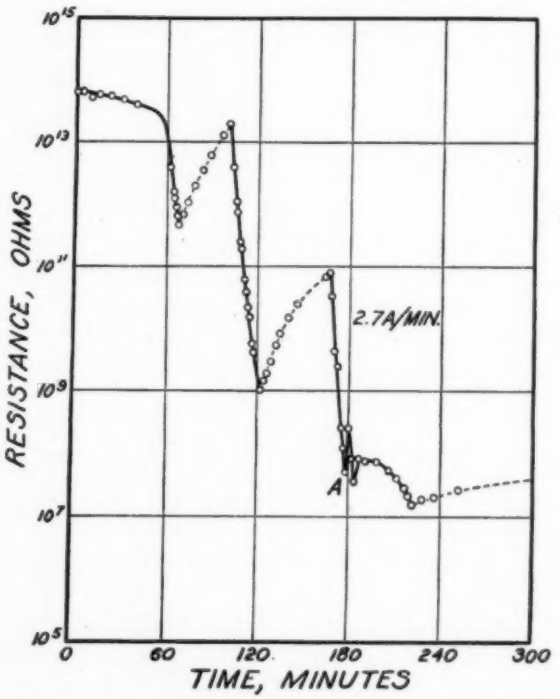

FIG. 3. Interrupted deposit (room temperature). Solid lines show depositing periods, broken lines interruption periods. At A, a small quantity of air was admitted.

[3] The formula for effusion from a small opening was used. $p=(dN/dt)(2MRT)^{\frac{1}{2}}(760)/dS d\omega \cos\theta(1.0132\times10^{6})$. In this p is taken from the vapor pressure formula $\log_{10} p = -52.23A/T+B$. ($A=188.5$, $B=7.82$) (p vapor pressure in mm Hg, M molecular weight, R gas constant per mole, T absolute temperature, dN/dt number of moles per second effusing from an opening of area dS cm² into a solid angle $d\omega$, at an angle θ with the normal to dS.)

RESULTS AND DISCUSSION

(a) Room Temperature Deposits

Curve I on Fig. 2 may be regarded as typical for room temperature deposits. At the beginning of the depositing period, the resistance measured is that of the glass plate at room temperature; after heat influx from the furnace has acted for several minutes, a small drop in the resistance of the glass plate is observed. No effect of the deposited Pb is seen until the film has reached a considerable thickness; in this case only after 80 minutes depositing time (corresponding to a thickness of the film of 160A) a point is reached where the resistance decreases rapidly with each new layer of metal atoms added.

Figure 3 shows how the resistance of a room temperature film increases when the deposit is interrupted (dotted lines); the increase is the more rapid the higher the resistance at the time of interrupting. At *A*, a small amount of air is admitted during the depositing process (to a pressure of 10^{-3} mm Hg), with the immediate effect of stopping the decrease of resistance; only after a considerable length of time does the resistance resume its downward move.

On Fig. 4, the behavior of films under the influence of air is studied in more detail. While

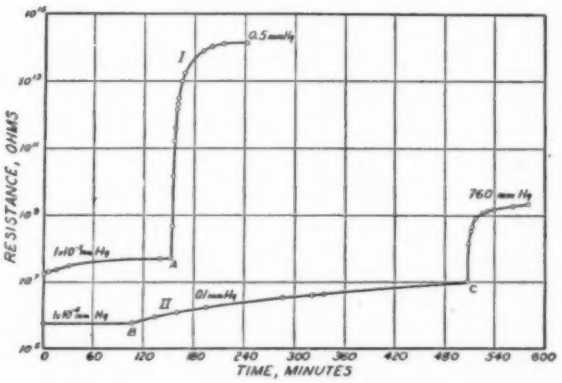

FIG. 4. Air admission to room-temperature films. Film I, initial resistance 2×10^8 ohms; film II, initial resistance 6×10^6 ohms. At *A*, *B*, and *C*, air was admitted to the pressures indicated.

in film I (initial resistance 2×10^7 ohms) the resistance of the background is reached in a few minutes, a considerable conduction is maintained in film II (initial resistance 6×10^5 ohms) after exposure to air even at full atmospheric pressure.

It can be assumed that, apart from the phenomena discussed further below, gas adsorption and oxidation play an important role. Thus, while very thin films are easily attacked by gases even under reduced pressure,[4] heavier films may

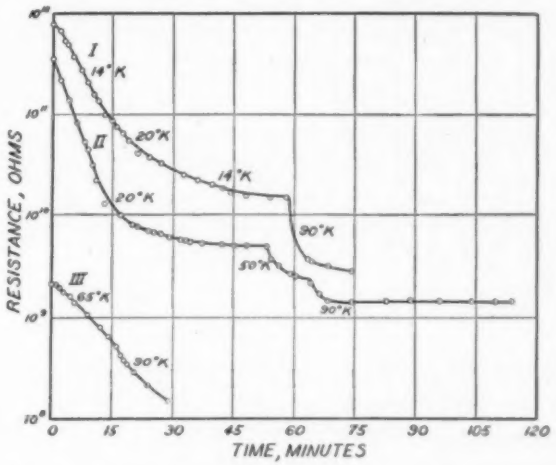

FIG. 5. Aging of several low-temperature films at low temperatures.

conserve their inner layers intact for electrical conduction. Also, while a film is being deposited, bound gas atoms will impede the formation of continuous metallic layers. The maintenance of a high vacuum during the depositing process is therefore imperative, as the thickness at which conduction sets in will depend largely upon the vapor pressure in the evaporation chamber at the time of deposit.

(b) Low Temperature Deposits

Curve II on Fig. 2 represents a group of low temperature deposits, with the backing cooled by liquid hydrogen. Here conduction sets in at thicknesses as small as 7A. Warming up the films to room temperature destroys all traces of conduction; it is thus possible to deposit several films on top of one another, having essentially the same curve of resistance against time, with only a lengthening of the exposure time required to obtain conduction in successive deposits.

Figure 5 displays the behavior of some of these films, after the molecular beam is shut off. In all cases a *decrease of resistance* is found, in contrast

[4] M. C. Johnson and T. V. Starkey, Proc. Roy. Soc. **40**, 126 (1933).

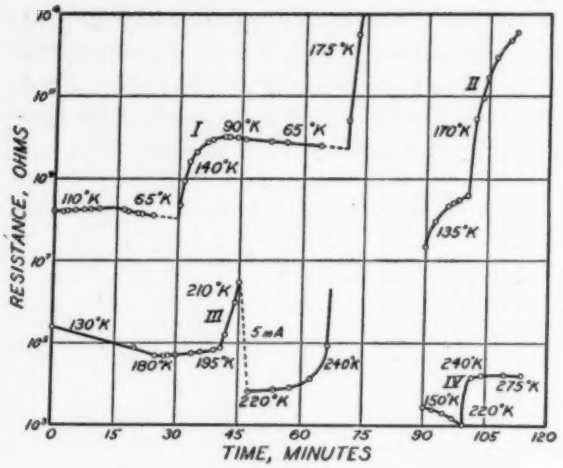

FIG. 6. Aging of several low temperature films at raised temperatures.

to the observations on room-temperature deposits. After about one hour, stable values of resistance are finally reached, at a level which depends upon the initial resistance and the temperature of the film. Raising the temperature will fasten the "reaction" and reduce the value of the final resistance reached.

Plotting the observed decrease of resistance for any given temperature, it is found that a law of the form

$$\log (R-R_T)=\log (R_0-R_T)-K_T t^s$$

is obeyed, in which R_T is the final resistance and K_T the "reaction constant" for a given temperature, and the exponent s has a value of approximately $\frac{3}{2}$.

Turning to Fig. 6, it is seen that by raising the temperature to higher values than in Fig. 5, an *increase* instead of a decrease of the electrical resistance is observed, the rate of this increase going up rapidly with the temperature. A "critical" temperature is found, separating the two regions of opposite behavior; this "critical" temperature depends upon the initial resistance of the film (and hence upon its thickness and structure).

To interpret this behavior, it may be assumed that the reduced mobility of Pb molecules at low temperatures permits only small-scale regrouping from the random positions into which these molecules had been deposited; thus, by a slow formation of crystallites and bridges, a gradual increase of the electrical conduction is achieved. With raised temperature and increased mobility, that process is speeded up, resulting in a maximum conductivity at the "critical" temperature. Above this temperature, the agglomerations, growing larger at the expense of their immediate neighborhood, become surrounded by zones of relative depletion, which in turn diminish the possibilities for electrical conduction. Finally, at high enough temperatures, no current will pass, as the film then is broken up entirely.

Accordingly, in films deposited at higher temperatures, much heavier deposits will be needed before conduction can be established, since the agglomeration and recrystallizing process occurring will inhibit any film formation until enough material is deposited. The thickness at which conduction sets in, in thin films, may thus be linked to the mobility of the constituent molecules. Complicating the phenomenon is the presence of bound gas atoms which act as a hindrance to the formation of a continuous metal film. The results obtained here seem to confirm very satisfactorily the views expressed in recent papers by Suhrmann and Berndt[5] and Weber and O'Brien.[6]

Mention may finally be made of the influence of electric currents upon the conductivity of the films. Curve III in Fig. 6 shows how, by passing a current of 5 mA, the resistance is made to drop by several powers of 10 and the "critical" temperature increased by about 40°, a phenomenon which may be explained by the high local current densities occurring.

The author wishes to express his appreciation to Professor A. Goetz for his stimulating direction of the work, to Dr. A. B. Dember for untiring help and advice and to Drs. A. B. C. Anderson and M. G. Foster, whose apparatus and methods were used as a starting point in this investigation.

[5] R. Suhrmann and W. Berndt, Zeits. f. Physik **115**, 17 (1940).
[6] A. H. Weber and D. F. O'Brien, Phys. Rev. **60**, 574 (1941).

Proceedings of the American Physical Society

Minutes of the Meeting of the New York State Section held at Rochester, New York, April 2–3, 1943

THE Spring Meeting of the New York State Section of the American Physical Society was held at the Strong Memorial Hospital and at the Memorial Art Gallery, Women's Campus, University of Rochester, on Friday evening, April 2, 1943 and Saturday, April 3, 1943. An attendance of over 100 members and visitors was recorded at each of the sessions.

On Friday evening the Section was guest of the University of Rochester School of Medicine and Dentistry. Dr. Stafford L. Warren discussed the work of the Biophysical Laboratories of the School of Medicine, and after the lecture trips were conducted through the various laboratories.

At the Saturday meeting the following program of invited papers was presented:

Address of Welcome. President Alan Valentine, *University of Rochester.*
Microwaves. George K. Town, *Stromberg-Carlson Manufacturing Company.*
Vacuum Pumps in the Development of Industry. K. Hickman, *Distillation Products.*
Resistance of Glass to Thermal and Physical Shock. C. D. Oughton, *Bausch and Lomb Optical Company.*
Animal Electricity. W. O. Fenn, *School of Medicine and Dentistry, University of Rochester.*
Discussion: Education of Physicists for War and Post-War Conditions.
Colleges and Universities. R. C. Gibbs, *Cornell University.*
Secondary Schools. E. L. Manning, *State Education Department.*
Industry. J. T. Littleton, *Corning Glass Works.*

W. R. Fredrickson
Secretary

Proceedings of the American Physical Society

Minutes of the Meeting of the Metropolitan Section held at Columbia University, New York, April 2, 1943

A MEETING of the Metropolitan Section of the American Physical Society, being the only one for the season 1942–1943, was held on Friday, April 2, 1943 at Columbia University. The meeting began with dinner in the Men's Faculty Club. The session for the presentation of papers was held in the Pupin Physics Laboratories beginning at eight o'clock. The following papers were presented:

Contributed Paper: **Formation of Centers of Condensation in Supercooled Phases.** Peter G. Bergmann (Abstract below).
Invited Paper: **The Elasticity of High Polymers as Bearing on the Synthetic Rubber Problem.** Hermann Mark (*Introduced by Karl K. Darrow*).

The following officers were elected for the season 1943–1944: *Chairman:* Helen A. Messinger; *Vice Chairman:* L. H. Germer; *Secretary-Treasurer:* W. S. Gorton; *Elected Members of the Executive Committee:* W. E. Lamb, Jr., C. M. Slack.

W. S. Gorton
Secretary-Treasurer

The Formation of Centers of Condensation in Supercooled Phases. PETER G. BERGMANN, *Lehigh University.*—In the investigation of the spontaneous formation of a more stable phase in the interior of a supersaturated or supercooled phase, it is usually assumed that a count of the centers of condensation which become visible per unit time furnishes us directly with the rate at which new centers are being formed. This assumption is objectionable, because new centers will not necessarily continue to grow, but may redissolve before they become visible. In fact, it is well known that for every degree of supercooling, there exists a "critical" size below which the droplet is more likely to dissolve than to grow. To overcome this difficulty, the author has considered the change to which an arbitrary size distribution of droplets or crystals is subject in the course of time. If the number of droplets containing between μ and $\mu+d\mu$ moles at the time t is $Z(\mu, t)d\mu$, then Z satisfies the equation

$$\frac{\partial Z}{\partial t}=\frac{1}{N^2}\frac{\partial}{\partial \mu}\left[v(\mu)\left(\frac{\partial Z}{\partial \mu}+\frac{Z}{kT}\frac{df(\mu)}{d\mu}\right)\right],$$

where $v(\mu)$ is the rate at which droplets of size μ annex or drop one molecule, and $f(\mu)$ is the free energy per droplet. It is proposed to discuss this equation with the help of Heaviside calculus.

Proceedings of the American Physical Society

MINUTES OF THE MEETING OF THE SOUTHEASTERN SECTION HELD AT AUBURN, ALABAMA, APRIL 2–3, 1943

THE ninth annual meeting of the Southeastern Section of the American Physical Society was held at the Alabama Polytechnic Institute, Auburn, Alabama, on Friday and Saturday, April 2–3, 1943. Approximately sixty-five members and guests attended the meeting. Local arrangements were made by a committee headed by Fred Allison.

The regular program consisted of eight papers, abstracts for five of which are appended hereto. Abstracts of other papers will be found in the June issue of the *American Journal of Physics*. Additional features of the program were a talk by M. H. Trytten on "The Manpower Situation in the Profession of Physics" and a panel discussion on "Physics and the War Emergency," led by A. E. Ruark.

At the business meeting the election of the following officers for the year 1943–44 was announced: *Chairman*, C. W. Edwards; *Vice Chairman*, R. C. L. Mooney; *Secretary*, E. Scott Barr; *Treasurer*, C. B. Crawley; and *Member of the Executive Committee*, K. L. Hertel.

The invitation extended by the University of Tennessee to hold the 1944 meeting of the Section in Knoxville, Tennessee, was accepted.

E. SCOTT BARR, *Secretary*

ABSTRACTS OF CONTRIBUTED PAPERS

1. The Single Scattering of Fast Electrons in Light Gases. T. N. GAUTIER,* *University of North Carolina.*—The single scattering of RaE electrons has been studied in air, hydrogen, and argon. The scattering angles were mainly between 10° and 30° and the primary energies were between 200 kev and the upper limit of the RaE spectrum. Compared to the scattering in argon, the scattering in hydrogen and air was found to agree with the predictions of the Mott formula for nuclear scattering and the Möller formula for electronic scattering, within the limits of instrumental and statistical error. The probable error was about 5 percent for the hydrogen-argon comparison, and about 2 percent for air-argon comparison.

* Now at the National Bureau of Standards.

2. Measurement and Analysis of Noises by an Improved Method. DANIEL S. ELLIOTT AND JOHN L. MCLUCAS, *Tulane University.*—In a previous paper an improved method for studying noises was outlined. This method consists primarily of two parts: (1) a device for tabulating rapidly varying intensities so as to determine the manner in which the intensities are dispersed; and (2) facilities for recording noise samples on a phonograph disk "in the field" and subsequently reproducing them in the laboratory to be analyzed by means of a commercial sound analyzer. In the present study a number of noises of various kinds have been analyzed by this method. Furthermore a modification has been made in the apparatus which now makes possible studies where the ordinary commercial

electric lines are unavailable. Comparisons have been made of the same situations using the energy from the ordinary commercial electric lines and from the new modification which uses a portable energy source.

3. Generalization of Bateman's Differential Equations. ARTHUR E. RUARK, *University of North Carolina.*—Bateman worked out the system of differential equations governing the functions $W_n(t)$, which represent the chance that n events will occur in time t; the chance that an event will occur in time dt is the only datum required to make the solution definite. The generalization of Bateman's ideas to the case where W_n depends on several variables is briefly presented.

4. X-Ray Diffraction Measurements with Geiger-Mueller Tube. R. PEPINSKY, *Alabama Polytechnic Institute,* AND P. WEISZ, *Bartol Research Foundation.*—The time-rate of development of crystalline conditions due to physical or chemical action in materials is often of interest. Examples are the dependence of hysteresis or drift in rubber or other polymers upon the rate of molecular alignment due to stretching, the chronology of polymorphic changes in crystalline forms, or structural changes in alloys with various treatments. Because of exposure times required for photographic recording of x-ray diffraction patterns, reactions occurring in minutes or seconds have in general been unobservable. The possibility of use of Geiger-Mueller tubes as rapid indicators of diffraction maxima and their history during reactions was explored. A preliminary survey was made with a compact GM-tube circuit for audible counting of x-ray quanta, the apparatus being of general interest because of its simplicity and wide applicability. A GM tube with argon-ether filling and 0.0005″ Pyrex window was used, the x-ray beam penetrating the length of the cylinder. The counter supplied positive pulses to the grid of a tube normally biased to cut-off; with practically no current demanded by the circuit, its B voltage could be obtained from the GM-tube high voltage supply. Observations with this apparatus indicated that the GM tube can be successfully utilized for the diffraction studies.

5. The Near Infra-Red Absorption Spectra of Some Vegetable Oils. E. S. BARR AND W. R. HARP, *Tulane University.*—The near infra-red absorption spectra of castor, cottonseed, olive, palm, and peanut oils have been measured in the region between 1μ and 5μ. A pronounced absorption at 3.43μ was observed in each case and attributed to the C-H valency vibration. The other observed absorption positions did not in general appear at the same positions, which permits differentiation among these materials. Since cell thicknesses of 0.06 mm proved best, only small amounts of the oils were needed. The changing composition of such oils with aging seemed likely to produce corresponding changes in spectra. This was investigated, particularly for peanut oil, and marked changes were found in the samples subjected to various amounts of aging. Differences resulting from variations in the preparation of the oils were considered. For example, natural and "tasteless" castor oil spectra differed in the region of 2.5μ. Work on these materials is being continued, and it is planned to include other oils of vegetable origin in the general project.

Proceedings of the American Physical Society

MINUTES OF THE MEETING OF THE NEW ENGLAND SECTION HELD AT WELLESLEY, MASSACHUSETTS, APRIL 3, 1943

THE twenty-first regular meeting of the New England Section of the American Physical Society was held at Wellesley College, Wellesley, Massachusetts, on Saturday, April 3, 1943. Forty-six members were in attendance. The invited papers were as follows:

The M.K.S. System of Units. WENDELL H. FURRY, *Harvard University.*

Physics at Wellesley College. LOUISE S. MCDOWELL, *Wellesley College.*

"Automatic Volume Control" of the Ear. HAROLD P. KNAUSS, *Ohio State University.*

Entropy and Probability. K. K. DARROW, *Bell Telephone Laboratories.*

Four short papers were presented, one of these being by title. Those pertaining to research are as follows:

Radiations from the 100-Day Arsenic Activity. L. G. ELLIOTT AND M. DEUTSCH, *Massachusetts Institute of Technology, Cambridge.*—Sagane *et al.*[1] have isolated an arsenic activity of about 100-day half-life from germanium bombarded with deuterons which they assigned to As^{77} because it was found to emit negative electrons. By studying the radiations in the magnetic lens beta-ray spectrometer we found these electrons to be due to the internal conversion of a 0.052±0.003-Mev gamma-ray. The conversion in the K shell was found to be about 5 times as strong as that in the L shell. K x-rays were also observed.

In order to determine whether the gamma-rays follow orbital electron capture or are due to an isomeric transition, coincidences between conversion electrons and K x-rays were observed. The electrons due to conversion in the L shell were found to be accompanied, on the average by half as many x-rays as those from the K shell. We conclude from this that the 100-day activity decays by orbital electron capture followed, within less than 10^{-6} second, by a highly converted 0.052-Mev gamma-ray. The previous assignment must therefore be in error. Positrons are emitted, if at all, in less than 2 percent of all the disintegrations.

[1] Sagane *et al.* Proc. Phys.-Math. Soc. Japan, 21, 660 (1939).

Absorption Bands in 240–185 mμ Region in Spectra of Aromatic Amino Acids. GLADYS A. ANSLOW AND SALWA C. NASSAR, *Smith College.*—An analysis of the end absorption in the spectra of the aromatic amino acids reveals three independent bands, which in phenylalanine set in near 225, 205, and 198 mμ. In tyrosine, tryptophane, and also in histodine these are shifted to longer wave-lengths, more in tyrosine than in the other two. The latter two bands have intensities and locations similar to the 205 and 185 mμ bands typical of the cyclic hydrocarbons, and may originate from energy absorption in the respective rings. These bands shift more than the weaker 225 mμ band, which tends to merge with the 205 band. A detailed investigation of the longer wave-length band, which occurs in all fatty acids between 225 and 240 mμ, reveals that the tyrosine band is unique in having a long wave-length component. This must result from energy absorption in the ring near the OH substitution, as is also indicated by its existence in the spectrum of hydroquinone. Thus, the seat of the absorption is in the C—C—OH configuration, and is independent of

the nature of X.

Definition and Measurement of Absolute Electrode Potentials. DAVID C. GRAHAME, *Amherst College* (*Read by title*).—The absolute electrostatic potential of a point in space is defined unambiguously in terms of the properties of a unit plus charge. By a slight extension of this definition, the electrostatic potential of a conducting surface can also be defined unambiguously. But the potential of a point within a conductor varies enormously from point to point if one takes into account the discrete structure of matter, as one must in many problems. To avoid this difficulty one may define the potential of an isotropic conductor as the potential of a point in a cavity within the conductor. This definition is in accord with most usage and does not conflict with the basic definition of potential mentioned above. Its particular advantage is that *it makes possible an experimental determination of the electrostatic potential difference between two phases.* By a very slight modification of the original Kelvin method it becomes possible to carry out measurements of liquid junction potentials and of absolute electrode potentials without theoretical difficulties. From such measurements one can calculate individual ionic activities, energies of hydration of gaseous ions, and related quantities.

Another paper, concerned with instruction, has been sent to the *American Journal of Physics.*

MILDRED ALLEN, *Secretary-Treasurer.*

Proceedings of the American Physical Society

And of its Ohio Section

COLUMBUS MEETING, APRIL 30 AND MAY 1, 1943

THE spring meeting of 1943, being the 254th meeting of the American Physical Society, was held in the buildings of the Ohio State University in Columbus on Friday, April thirtieth, and Saturday, May first. As all but our very newest members will recall, the spring meeting was for many years without exception held in Washington, and only in 1942 was it transposed to Baltimore, the latter city becoming itself overcrowded before the advent of 1943. Though not distrustful of the hospitality of the Ohio State University, the officers of the Society were hardly overconfident of the prospects of a meeting held so far from its traditional place, and their fears seemed at first to be justified by the scantiness of contributed papers. The event dispelled their premonitions: The meeting was large by any standards excepting only those of the Washington meetings of the past, with 166 registrants and two hundred in attendance at the dinner. The Local Committee, headed by Dean Alpheus W. Smith, made excellent preparations for the meetings. The Ohio Section of the Society, and Section F of the Ohio Academy of Sciences, merged their meetings with ours.

Part of the success of this meeting was due to the invited papers, the givers of which are to be thanked for their speeches and for the journeying they did. Those of R. B. Barnes, J. R. Downing, H. H. Nielsen, and E. E. Bell formed a symposium on applied infra-red spectroscopy, admirably introduced by the first-names; Norman Wright took the chair. Two—those of Henry Crew and L. T. More—would have been given at the New York meeting of December, 1942 as part of the Galileo-Newton symposium of the A.A.A.S., had that organization not cancelled its meeting. It is a satisfaction to have provided a hearing for these papers; I am informed that they are to appear in the *Scientific Monthly*. The titles of these five, and that of K. Lark-Horovitz which opened the invited programme, are subjoined:

K. LARK-HOROVITZ, *Purdue University:* **Biological Applications of Radioactive Tracers.**

HENRY CREW, *Northwestern University:* **Galileo, the Pioneer Physicist.**

LOUIS T. MORE, *University of Cincinnati:* **Newton's Philosophy of Nature.**

R. BOWLING BARNES, *American Cyanamid Company:* **Applied Infra-Red Spectroscopy.**

J. R. DOWNING, *DuPont Experimental Station:* **Application of Infra-Red Spectroscopy to Chemical Research.**

H. H. NIELSEN AND ELY E. BELL, *Ohio State University:* **Automatic Recording Vacuum Infra-Red Grating Spectrometer.**

Sixteen ten-minute papers were contributed, three of these (2, 10, 11) being read by title: The abstracts are appended at the end of these proceedings.

The dinner of the Society was held on Friday evening in the Deshler-Wallick Hotel, President Hull presiding. The after-dinner programme consisted of talks by Charles F. Kettering of the General Motors Research Corporation and by R. L. Edwards of Miami University.

The Council met at intervals throughout Friday and Saturday. It elected one candidate to Fellowship and seventy-five to Membership. Their names follow. On receipt and after discussion of a petition signed by forty Fellows and Members, the Council voted to establish a Division of Electron and Ion Optics in the American Physical Society under Article IX of the Constitution thereof. This Division is now in process of organization, and members wishing to join it will shortly have an opportunity.

The Society has lost through death one Fellow (A. F. Kimball, General Electric Company) and one Member (H. A. Pidgeon, Bell Telephone Laboratories).

Elected to Fellowship: P. Pringsheim.

Elected to Membership: Kenneth L. Andrews, Ernest Carl Barkofsky, Gordon Edward Becker, Winston H. Bostick, Wayne M. Bowers, Joseph M. Brogan, W. Byron Brown, Royal C. Bryant, Richard C. Burns, Robert Van Duyne Campbell, H. W. Cobb, Frederick Coensgen, Philip Cooperman, Charles D. Coryell, Donald W. Crouch, Elsie

Margaret Dollmann, Richard Ehrlich, Milton Walter Franke, Urie Funaroff, Kenneth William Gardiner, Thomas N. Gautier, Jr., H. E. Greene, Leonard Gross, Dwight T. Hamilton, E. J. Hellund, J. Ross Heverly, David Lawrence Hill, Rosalie C. Hoyt, Albert A. Hudimac, Margaret Catherine Jenkel, W. E. Johnson, Albert E. Keheler, Jr., John M. Kopper, Ralph Werner Krone, Jerome Kurshan, Theodore James La Chapelle, Jr., Leo R. Landrey, Christian LaPointe, Howard Carlton Latham, Lester E. Lighton, Gustave A. Linenberger, Jr., Bernard Lippmann, Luther Leo Lowry, Arthur L. Lutz, Lloyd B. Macurdy, I. Paul Maizlish, N. Marcuvitz, Roland E. Meyerott, Charles Frank Miller, James F. Miller, Jr., Arnold R. Moore, Roger M. Morrow, Vernon W. Myers, I. Opatowski, Doris H. Paul, T. F. Protzman, Robert S. Rasmussen, Charles Ravitsky, W. Joseph Riegger, Emery H. Rogers, Sylvan D. Rolle, Ben Z. Rubin, James J. Shipman, William C. Skinner, O. J. Snow, H. Cecil Spicer, Edwin Garnet Stanford, Lorenzo Sturkey, George Clifford Sziklai, J. A. Van Horn, Frank Verbrugge, C. V. Weaver, Mitchel Weissbluth, E. M. Wise, Adrian Ziolkowski.

KARL K. DARROW, *Secretary*

ABSTRACTS OF CONTRIBUTED PAPERS

1. On the Linear Stress-Strain Curves of the Hexagonal Metals. J. S. KOEHLER, *Carnegie Institute of Technology.*—Taylor[1] supposed that in the work-hardened state a crystal contains many line dislocations, all of which are parallel to one another. He obtained the parabolic stress-strain curve of the face-centered cubic metals by assuming that the dislocations are present in a two-dimensional square lattice. We have been able to obtain linear stress-strain curves by using a rectangular dislocation lattice. The resulting formulas have been used to fit the measured stress-strain curves of single crystals of Mg, Zn, Cd.[2] The dislocation spacing in highly work-hardened hexagonal metals is about 10^{-6} cm in agreement with previous estimates. In the case of Cd at low temperatures the stress-strain curves show a sudden change of slope. Our expressions fit the lower straight-line section only. The change in slope may possibly be due to a change in the mechanism of plastic deformation. It may be that twinning plays a role in the deformation occurring at large stresses.

[1] G. I. Taylor, Proc. Roy. Soc. **145**, 362 (1934).
[2] E. Schmid and W. Boas, *Kristallplastisität* (Springer, 1935), p. 158.

2. Cathode Drop and Current Density in Welding Arcs. G. H. FETT, *Department of Electrical Engineering, University of Illinois.*—Experiments to determine the cathode drop of welding electrodes in air at atmospheric pressure and to compute the electron density in the arc were continued using the method previously described.[1] The cathode drop for certain d.c. welding electrodes used for hard-surfacing was greatly influenced by the coating, the values changing from 9.4 to 14 volts after the coating was removed in the extreme case. Mild steel electrodes showed little or no change with coating removal. The electron density computed values was not proportionately influenced by the coating. Experiments involving currents less than one ampere indicate that with these electrodes the current density increases with a decrease in current. At values of current above 5 amperes the current density is constant for any given electrode, and is influenced by the type of electrode more than the coating. The energy lost by the arc due to convection varies directly with the arc perimeter. Hence the current density must increase as the current decreases in order that the arc temperature within the core be held constant. This proportional increase in loss with reduction in current may account for the fact that arc currents below a certain minimum, usually about 0.3 ampere, cannot be maintained despite the use of fairly high potentials.

[1] G. H. Fett, Welding J. Res. Supp. **21**, 27 (1942).

3. Magnetic Potential Energy. F. W. WARBURTON, *University of Kentucky.*—Treatment of magnetic energy as external (potential) energy in the sense of a modification of electrostatic energy due to electron motion, makes use of the classical Lagrangian function for the energy of the electron in a magnetic field. However, a Hamiltonian function defined in terms of the mechanical momentum rather than the classical canonical momentum differs from the classical Hamiltonian by including explicitly the magnetic potential energy, and equals the total energy. The change in magnetic potential energy upon adding a magnetic field is equal in a first approximation to the Larmor precession increase in rotational kinetic energy. The two give a change in energy proportional to e/mc and provide a simple interpretation of the gyromagnetic experiments and the so-called electron spin. The omission of the canonical momentum and the proof that the Hamiltonian remains constant in time, is not violation of conservation of energy, and it permits an electron-proton pair to release part of their energy in radiation in accord rather than at variance with the added requirements of quantum theory.

4. A Physical Mechanism for the Nebular Red Shift. L. H. THOMAS, *Ohio State University.*—It seems possible to account for the nebular red shift by a second-order effect of ordinary coherent refraction. When a wave train, regarded as plane and infinite in lateral extent, but finite in length, advances through a refracting medium, the parts of which are not elastically anchored in position, the me-

dium receives as the front of the wave train advances over it an average velocity in the direction of propagation of the wave train. This results from the second-order effect of the magnetic field of the wave train on the first-order transverse velocities, lagging in phase, of the material particles. If there is no "frictional" resistance, this velocity is lost as the back of the wave train passes, the medium is left undisturbed, and the wave train is propagated undisturbed. If "frictional" resistance (which may be the statistical effect of waves passing in other directions) damps out the velocity in the direction of propagation, the wave train as a whole is gradually reddened. The whole process is coherent and occurs even in the approximation of geometrical optics. It would not be expected that it should be possible to observe it under laboratory conditions, because a velocity of the medium in the direction of propagation of the wave train is then opposed by elastic restoring forces.

5. A Recording Relay For An Infra-Red Spectrograph. ELY E. BELL, *Ohio State University.*—A recording photoelectric bridge has been constructed for use with an infrared, grating spectrograph which is able to reproduce the 2.7-mu water vapor band with detail equivalent to that previously obtained with point-by-point measurements under similar conditions. A single base, mounting a light source, a Moll bifilar galvanometer, and a pair of photo-tubes is supported inside of a heavy metal tank containing the spectrograph. Here the relay is relatively free from temperature fluctuations and from vibrations. An unbalance of light on the photo-tubes is applied to commercial recording milliammeters through a bridge circuit similar to that of McAlister, Matheson, and Sweeney[1] except that an additional stage of amplification has been added. A provoked potential of 10^{-6} volt in the thermocouple is recorded as readily distinguishable from the background.

[1] E. D. McAlister, G. L. Matheson, and W. J. Sweeney, Rev. Sci. Inst. 12, 314 (1941).

6. The Infra-Red Spectrum of Methyl Fluoride at 9.5μ. K. P. YATES AND V. MILLER, *Ohio State University.*—The infra-red band, ν_5, at 9.5μ in the spectrum of methyl fluoride was first investigated under high dispersion by Bennett and Myer in 1928 who showed it to be of the parallel type. The data seemed to indicate, however, that some of the rotational lines, particularly in the *P* branch, were complex in structure. This has been investigated by the writers under higher dispersion than that available to Bennett and Myer. The curve obtained agrees with that of Bennett and Myer in general details, but most of the rotational lines in both the *P* and *R* branches are split up into component structure. The effect appears to be related to the convergence of the lines in the band and it seems reasonable to ascribe it as due principally to a Coriolis resonance interaction between the parallel type vibration ν_5 at 1048 cm^{-1} and the perpendicular type vibration ν_6 at 1200 cm^{-1}. The contour of the band ν_6 of CH_3F is at present being obtained in order to determine in what manner the resonance interaction affects this vibration.

7. Raman Spectra of Diisobutylene, Cyclohexene, and Dipentene. FORREST F. CLEVELAND, *Illinois Institute of Technology.*—In continuing work on olefinic hydrocarbons, Raman frequencies, relative intensities, and depolarization factors have been obtained for diisobutylene, cyclohexene, and dipentene. The relative intensities and depolarization factors were obtained by use of a Gaertner microdensitometer. Diisobutylene is a mixture of the two isomers 2,4,4-trimethyl-1-pentene and 2,4,4-trimethyl-2-pentene, the present sample containing only about 15 percent of the latter isomer. Raman frequencies and estimated intensities for the two isomers have been obtained previously (Rank and Bordner), but the present investigation provides the first polarization data and more accurate measurements of the intensities. Raman frequencies and estimated intensities have also been reported for cyclohexene and dipentene, but only qualitative polarization data for cyclohexene seems to exist in the literature. Dipentene has a ring structure identical with that of cyclohexene and it is thus of interest to compare the spectra of these two compounds. The olefinic frequencies at 1653(447)0.14, 3022(508)0.19, and 3058(19) in the cyclohexene spectrum appear at 1682(219)0.35, 3012(54)P, and 3050(26)P in the spectrum of dipentene. The olefinic frequencies previously observed at 1303(52)0.64, 1414(108)0.81, 1653(203)0.20, 1674(55)P, 2978(253)P, and 3077(47)0.70 for 2-methyl-1-heptene, which contains the group $XYC=CH_2$, appear at 1236(104)-0.63, 1410(155)0.62, 1644(161)0.33, 1658(51)0.60, 2977-(790)P, and 3072(32)0.71 for diisobutylene and at 1290-(46)0.72, 1376(127)0.70, 1648(213)0.38, 2983(115)P, and 3078(16)D for dipentene.

8. Magnetolysis and the Electric Field Around the Magnetic Current. FELIX EHRENHAFT, *New York City.*—Between the vertical cylindrical poles (magnetodes) of an electromagnet of soft Swedish iron, whose bases form a horizontal gap (pole diam. 8 mm, gap 1–2 mm) acidulated water (one percent H_2SO_4 by volume) is decomposed into oxygen and hydrogen gas. Hereby the old problem of the alchemists about the decomposition of water through the magnet has been solved. As long as the two poles immersed in the solution are not magnetized we get pure hydrogen, but as soon as the two poles are magnetized we get a mixture of hydrogen and oxygen (about 2–12 percent oxygen). The amount of gases evolved magnetically is proportional to the magnetic field (first magnetolytic law). Microscopic observation shows that magnetically evolved gas bubbles carry either a North or South magnetic charge.* Magnetolysis and electrolysis have been superposed. After a swarm of positive electrically charged hydrogen bubbles are produced, the magnetodes were short-circuited electrically. Each of these positive charged gas bubbles moves in a circle around the gap between the magnetodes, through which a constant magnetic current flows, reversing its direction on reversion of the magnetic field, exactly as a single magnetic pole would circulate around the constant electric current, reversing its direction with the reversal of the electric field (Oersted, Faraday). The magnetic current is surrounded by circular electric lines of force (second

method of measuring the magnetic current). Photographs demonstrating these phenomena will be shown. The experiments can be seen at C. Zeiss Inc., New York, whom the author thanks for their hospitality.

* Papers by F. Ehrenhaft: *Science* 1941, 1912; *Phys. Rev.* 1941, 1942, 1943; *J. Frank. Inst.* 1940, 1942; *Phil. Sci.* 1941—some of which with L. Banet.

9. Combined Electron Diffraction and Microscope Apparatus. A. F. PREBUS, *The Ohio State University. (Introduced by Alpheus W. Smith.)*—A modified magnetic electron microscope is described which permits the observation of both highly magnified images and transmission electron diffraction patterns of identical microscopic specimen areas.

10. Investigation of Large Cosmic-Ray Bursts in Iron. R. E. LAPP, *The University of Chicago.*—During the past year experiments have been carried out with a Model C ionization chamber operated specifically to record cosmic-ray bursts. The steel chamber was completely shielded by 35 cm of iron and bursts with 150 to 3000 particles were recorded. Mesotrons producing bursts of such magnitude must have energies up to 6×10^{11} ev. Comparison of the size frequency distribution curve of large bursts in 35 cm of iron was made with the theoretical calculations of Christy and Kusaka.* The observed burst frequency was in agreement with a mesotron having spin 0 or $\frac{1}{2}$, but was in definite disagreement with spin 1. In addition, the recording system of the ionization chamber was coupled so as to record simultaneously coincidences of G-M counter coincidence sets placed above the apparatus. The counters in each 2-fold set were separated by from 2 to 10 meters to detect air showers. Preliminary results indicate that bursts under 35 cm of iron are not coincident with air showers to an accuracy of less than 10 percent. With the chamber completely unshielded and with negligible material in the vicinity, coincidences were observed between bursts and air showers. The experiments are being continued with 2-, 3-, and 4-fold coincidence sets and experiments are also in progress with a 12-cm iron shield around the ionization chamber.

* R. F. Christy and S. Kusaka, Phys. Rev. **59**, 414 (1941).

11. Measurements of Cascade Showers Produced by Ionizing and Non-Ionizing Radiation in the Stratosphere. JULIUS TABIN AND MARCEL SCHEIN, *University of Chicago.*—By using a cosmic-ray balloon apparatus, electron-produced and photon-produced cascade showers were measured below a 2-cm lead plate. The showers were detected by means of four Geiger-Müller counters placed below and an additional anticoincidence counter placed above the lead. The apparatus reached an altitude corresponding to 2.5 cm of Hg pressure. At a pressure of 3 cm Hg (first radiation unit from the top of the atmosphere) it was found that 71 percent of the showers below the lead were produced by non-ionizing and 29 percent were produced by ionizing radiation.

12. Factors Influencing the Plateau Characteristics Of Self-Quenching G-M Counters. W. SPATZ, *New York University.*—Investigations of factors influencing the starting potential and plateau slope of self-quenching G-M counters show: I. Impurities such as air or oxygen increase the plateau slope and starting potential of argon-alcohol counters. II. Operation of the counter causes changes in plateau characteristics as follows: (a) Immediately after use, the plateau slope increases slightly, (b) With continued use the plateau slope becomes steeper. (c) For moderate use the counter recovers when inactive, but never to the original characteristics. (d) With further use, the counter loses its plateau and does not recover. (e) The pressure in an argon-alcohol counter was observed to increase as a function of the total number of counts recorded. III. For argon-alcohol counters the useful life in these experiments was found to be about 10^9–10^{10} counts; for argon-methane, 10^7–10^8 counts. The lifetime may be seriously shortened by operating at high overvoltages, by allowing breakdown to occur, or by using any circuit permitting large currents to flow. The observed changes of characteristics are presumably due to the decomposition of the organic vapor by the discharge.

13. Threshold for the Nuclear Photo-Effect. G. C. BALDWIN AND H. W. KOCH, *University of Illinois.*—With the method previously described[1] for controlling the peak energy of the x-rays from the 20-Mev betatron, (γ, n) reactions have been observed and their thresholds determined in the following elements since the last report: Zn (39 min.) 11.6±0.4 Mev; N (10 min.), 11.1±0.5 Mev; In (1.1 min.), 9.5±0.6 Mev; Ag (2.3 min.), 9.3±0.5 Mev; Se (17 min.), 9.7±0.5 Mev. These values are upper limits for the thresholds. Ag and Se also show strong 25- and 57-minute activities, respectively. Analysis of decay curves taken at varying energies indicates that these activities have higher thresholds than those listed above. An improved determination of the $O^{18}(\gamma, n)O^{15}$ threshold has been made, giving 16.3±0.4 Mev. This and the nitrogen threshold are in fair agreement with values predicted from mass data. Chief sources of error in the method are (1) gradual change in energy calibration with time and (2) low ratio of activity to counter background near threshold, making estimation of a lower limit difficult.

[1] G. C. Baldwin and H. W. Koch, Phys. Rev. **63**, 59 (1943).

14. The Relative Intensities and Characteristic Radiations of Radioactive Scandium. CARL T. HIBDON, M. L. POOL, AND J. D. KURBATOV, *Ohio State University.*—A reinvestigation of the radioactive isotopes of scandium has yielded a new isotope of half-life 3.4 days. This isotope emits electrons of 0.46 Mev but no gamma-rays. Other data obtained by appropriate bombardments of K, Ca, Sc, Ti, and V with alpha-particles, deuterons, protons, slow and fast neutrons include the following:

Isotope	Half-life	Energy of β in Mev	Energy of γ
Sc^{43}	3.92 hr.	1.13 positrons	1.65 Mev
Sc^{44}	3.92 hr.	1.33 positrons	1.33 Mev
Sc^{46}	2.44 day	1.33 positrons	0.28 and 1.33
Sc^{48}	1.83 day	0.57 electron	1.33 Mev

No evidence was found for the existence of the 13.2-day nor the 2.62-day periods previously assigned to Sc^{43} and Sc^{47}, respectively. The Ca(p, n) reaction yielded Sc^{43} and Sc^{48} but not Sc^{44}. With deuteron bombardment of calcium the most abundantly produced isotope is Sc^{46}; the isomers of Sc^{44}, however, are not produced by this reaction in equal proportions as they are by the Sc(n, $2n$) and K(α, n) reactions. The scandium oxide used was of high purity and kindly furnished by Professor Quill of the University of Kentucky.

15. The Artificial Radioactivities of Cerium. M. L. POOL AND J. D. KURBATOV, *Ohio State University.*—Four new radioactive isotopes have been produced and assigned positions in cerium and praseodymium. Ce^{140}, which has a half-life of 140 days, is obtained by the reactions $Ba^{137}(\alpha, n)$ and $La^{139}(d, n)$. The fact that gamma-rays only (of 0.21 Mev) are emitted by this isotope is consistent with the isomeric assignment. A 30-day activity is assigned to Ce^{141} and has been obtained by the reactions $Ba^{138}(\alpha, n)$, $Ce^{140}(d, p)$, $Ce^{140}(n, \gamma)$, $Ce^{142}(n, 2n)$, and $Pr^{141}(n, p)$. The isotope emits beta-particles of 0.65 Mev and gamma-rays of 0.2 Mev. Ce^{141} is of particular interest because of the unusual arrangement of stable isotopes in the cerium region. A 36-hour activity, assigned to Ce^{143}, has been produced by the reactions $Ce^{142}(d, p)$ and $Ce^{142}(n, \gamma)$. This substance forms a chain reaction by disintegrating into Pr^{143}. Pr^{143} in turn disintegrates with a half-life of 13.5 days by the emission of 0.95 Mev beta-particles. No gamma-rays are emitted. The study of the above radioactive isotopes and the clarification of certain meagerly detailed published data on radioactive cerium has been made possible and expedited by improved methods used in the separation of cerium from praseodymium and lanthanum.

16. Progress Report on the Radioactivities in the Illinium Region. J. D. KURBATOV AND M. L. POOL, *Ohio State University.*—A continuation of comparative studies of the radioactivities of Pr, Nd, Il, Sm, and Eu has led to the following results. The nuclear reaction Nd(p, n) produces the periods 2.7 hours and 5.3 days. Both activities disintegrate with the emission of gamma-radiation and 2-Mev electrons; this suggests an isomeric position for the two isotopes in illinium. The nuclear reaction Nd(d, n) produces, in addition to the above, a period of 16 days. The disintegration takes place with the emission of gamma-radiation and 1.7-Mev electrons. The same activation yields a long period of about one year. Gamma-rays of 0.7 Mev constitute the principal radiations emitted. The activation of samarium with deuterons results in several periods. The Sm(d, n) reaction yields a 40-day activity and a one-year activity. Both are associated with europium and disintegrate mainly by the emission of gamma-rays. Absorption measurements of the gamma-rays of this one-year period presents results comparable to those of the one year period obtained by deuteron bombardment of Nd. Thus a chain reaction of four elements is suggested.

AUTHOR INDEX TO ABSTRACTS OF THE COLUMBUS MEETING

Baldwin, G. C. and H. W. Koch—No. 13
Bell, Ely E.—No. 5

Cleveland, Forrest F.—No. 7

Ehrenhaft, Felix—No. 8

Fett, G. H.—No. 2

Hibdon, Carl T., M. L. Pool, and J. D. Kurbatov—No. 14

Koch, H. W.—see Baldwin, G. C.
Koehler, J. S.—No. 1
Kurbatov, J. D.—see Hibdon, Carl T.
—— see Pool, M. L.
—— **and M. L. Pool**—No. 16

Lapp, R. E.—No. 10

Miller, V.—see Yates, K. P.

Pool, M. L.—see Hibdon, Carl T.
—— see Kurbatov, J. D.
—— **and Kurbatov, J. D.**—No. 15
Prebus, A. F.—No. 9

Schein, Marcel—see Tabin, Julius
Spatz, W.—No. 12

Tabin, Julius and Marcel Schein—No. 11
Thomas, L. H.—No. 4

Warburton, F. W.—No. 3

Yates, K. P. and V. Miller—No. 6

Author Index to Volume 63

References with (A) are to abstracts of papers presented at meetings of the American Physical Society. References with (L) are to Letters to the Editor and those with (T) designate title only.

Adams, G. D. and R. K. Clark. Absorption of high energy quanta—60(A)

Adams, R. V., Jr. (see Katz, L.)—140(A)

Almy, G. M. and P. R. Gillette. Quantum yield of diacetyl fluorescence—64(A)

Anslow, Gladys A. and Salwa C. Nassar. Absorption bands in 240–185 mμ region in spectra of aromatic amino acids 458(A)

Anthony, R. L. and S. L. Dart. Temperature rise in rubber on fast stretching—62(A)

Armi, Edgar L. Electrical conduction and recrystallization in thin Pb films deposited at low temperatures—451

Auger, P. Problems in the theory of atmospheric cosmic-ray showers—58(T)

Bachman, C. H. and Simon Ramo. Simplified electron microscope—224(A)

Baldwin, G. C. and H. W. Koch. Thresholds for the nuclear photo-effect—59(A), 462(A)

Banerji, A. C. Cepheid theory of the origin of the solar system—55(L)

Barnes, R. Bowling. Applied infra-red spectroscopy—459(T)

Barr, E. S. and W. R. Harp. Near infra-red absorption spectra of some vegetable oils—457(A)

Barschall, H. H. (see Klema, E. D.)—18

Bateman, H. The influence function for a cubic lattice—141(A)

Beers, Yardley. Direct determination of the charge of the β-particle—77

Bell, Ely E. Recording relay for an infra-red spectrograph—461(A)

—— (see Nielsen, H. H.)—459(T)

Benford, Frank. Probable accuracy of the general physical constants—212(L)

Bergmann, Peter G. Formation of centers of condensation in supercooled phases—456(A), 455(T)

Beringer, Robert. Angular correlation of successive gamma-rays—23

Berlin, Theodore (see Fajans, Kasimir)—309, 399(L)

Birge, Raymond T. Comments on "The probable accuracy of the general physical constants"—213(L)

Brentano, J. C. M. Measurement of photographic densities by the scatter of x-rays—64(A)

—— **and E. R. Schleiger.** Compensation of random fluctuations in a d.c. bridge amplifier—218(A)

de Bretteville, Alexander, Jr., and James W. McBain. X-ray diffraction investigation of sodium stearate from room temperature to the melting point—223(A)

Brillouin, Léon. Theory of the magnetron. III—127

Burbank, Burr G. Direct and fluorescence excitation of the L_{III} level in thick targets of thorium—139(A)

Chamberlain, C. W. Molecular absorption of vibration—219(A)

Chase, C. T. (see Shull, C. G.)—29

Clark, J. R., S. T. Pan, and A. R. Kaufmann. Magnetic properties of iron-cerium alloys—139(A)

Clark, R. K. (see Adams, G. D.)—60(A)

Cleveland, Forrest F. Raman spectra of diisobutylene, cyclohexene, and dipentene—461(A)

—— Raman spectra of methylheptenes—224(A)

—— Raman spectra of some octenes and octynes—64(A)

—— (see Hamilton, Dwight T.)—64(A)

—— (see Meister, Arnold G.)—64(A)

—— **and M. J. Murray.** Raman spectra of symmetrical top acetylenes—220(A)

Cohen, Arnold A. Isotopes of cerium and rhodium—219(A)

Constant, F. W., R. E. Faires, and H. E. Lenander. Investigations of ferromagnetic impurities. II.—441

Coon, Jesse B. $\Delta_1 F$ values from some chlorine dioxide bands—63(A)

Copeland, Paul L. Acceleration of decay in the anode effect by partial excitation—61(A)

—— (see Kennedy, William R.)—61(A)

Courant, E. D. On the excitation functions of proton-induced reactions in lithium—219(A)

Cox, R. T. (see Goertzel, Gerald)—37, 216(A)

Crew, Henry. Galileo, the pioneer physicist—459(T)

Critchfield, Charles L. Antisymmetrical interaction in beta-decay theory—417

Cross, Paul C. and G. W. King. Transition probabilities of the asymmetric rotor—220(A)

Dancoff, S. M. (see Serber, R.)—143

Darrow, K. K. Entropy and probability—457(T)

Dart, S. L. (see Anthony, R. L.)—62(A)

Davey, Wheeler P. (see Townes, Charles H.)—223(A)

—— (see Wehner, R. S.)—61(A)

De Benedetti, S. (see Johnson, T. H.)—222(A)

——, **T. H. Johnson, and R. P. Shutt.** Some results obtained with a new high pressure cloud chamber—222(A)

Deeds, W. E. (see Katz, L.)—140(A)

Dees, Bowen C. and Bernard Hamermesh. Small angle scattering of electrons by aluminum—217(A), 297

Demers, Pierre. "Génies" of Poincaré, and Carnot's principle—221(A)

Deutsch, M. (see Elliott, L. G.)—219(A), 321(L), 386(L), 457(A)

Dicke, Robert H. and John Marshall, Jr. Inelastic scattering of protons—86

Downing, J. R. Application of infra-red spectroscopy to chemical research—459(T)

Dresden, M. and Wilfred Kaplan. Dynamical approach to the condensation problem —221(A)

Ehrenhaft, Felix. Decomposition of matter through the magnet (magnetolysis)—216(A)
—— Magnetolysis and the electric field around the magnetic current—461(A)
Eisenstein, A. Structure of liquid carbon tetrachloride—304
Elliott, Daniel S. and John L. McLucas. Measurement and analysis of noises—456(A)
Elliott, L. G. and M. Deutsch. Disintegration scheme of Co^{58}—219(A)
—— **and M. Deutsch.** Nuclear energy levels in Fe^{56} from the decay of Mn^{56} and Co^{56}—321(L)
—— **and M. Deutsch.** Radiations from the 100-day arsenic activity—457(A)
——, **M. Deutsch, and A. Roberts.** Disintegration scheme of Na^{24}—386(L)
Epstein, Paul S. Theory of elastic oscillations in plates and shells—141(A)
Estabrook, G. B. Effect of high electrostatic fields upon the vaporization of molybdenum—352
Ewell, Arthur W. Production, concentration, and decomposition of ozone by ultraviolet light—65(A)

Faires, R. E. (see Constant, F. W.)—441
Fajans, Kasimir and Theodore Berlin. Quantization of molecules, inter- and intramolecular forces—309; Errata —399
Fano, U. Ionization yield of radiation energy—222(A)
Fenn, W. O. Animal electricity—455(T)
Fett, G. H. Cathode drop and current density in welding arcs—460(A)
Focht, Elizabeth F. (see Quimby, Edith H.)—218(A)
Freed, Simon, A. H. Jaffey, and M. L. Schultz. High centrifugal fields and radioactive decay—12
Friederich, L. M. (see Weber, A. H.)—217(A)
Friedlander, Gerhart and Chien-Shiung Wu. Radioactive isotopes of mercury—227
Furry, Wendell H. M.k.s. system of units—457(T)

Gallagher, Charles J. Adsorption of thorium on tantalum —217(A)
Gamertsfelder, G. R. High energy gamma-ray from radioyttrium (100 days)—60(A)
Gautier, T. N. Single scattering of fast electrons in light gases—456(A)
Geballe, Ronald. Production of photons relative to ionization by collision in a Townsend gap—138(A)
Gibbs, R. C. Discussion: Education of physicists for war and post-war conditions. Colleges and universities—455(T)
Gillette, P. R. (see Almy, G. M.)—64(A)
Ginsburg, V. L. Relativistic theory of excited spin states of the proton and the neutron—1
Goertzel, Gerald and R. T. Cox. Effect of oblique incidence on the conditions for single scattering of electrons by thin foils—37, 216(A)
Grahame, David C. Definition and measurement of absolute electrode potentials—458(A)
Greene, Jack B. and Millard F. Manning. Electronic energy bands in face-centered iron—203
Greisen, Kenneth. Intensity of cosmic rays at low altitude and the origin of the soft component—323
Grünberg, G. Suggestions for a theory of the coastal refraction—185
Guth, Eugene (see Peterson, L. E.)—62(A)

Hamermesh, Bernard (see Dees, Bowen C.)—217(A), 297
Hamilton, Dwight T., Forrest F. Cleveland, and M. J. Murray. Raman spectra of some ethane-like molecules —64(A)
Hamm, W. J. Retardation and neutralization of argon ions in helium—433
Harkins, William D. (see Jura, George)—224(A)
—— **and George Jura.** Distance to which the attractive field of a solid extends into a liquid—224(A)
—— **and George Jura.** Method for the accurate determination of the adsorption of a vapor on the surface of a solid—225(A)
Harp, W. R. (see Barr, E. S.)—457(A)
Hazen, Wayne E. Collision electrons accompanying mesotrons in lead at 10,000 feet—140(A)
—— Specific primary ionization of cosmic rays in helium—107
—— Cosmic-ray stars at 10,000 feet—213(L)
Heller, Wilfried. Morphic double refraction in presence of strong intrinsic anisotropy—62(A)
—— **and Etienne Vassy.** Indirect detection of absorption bands in strongly light scattering dispersed systems—65(A)
Henry, D. C. (see Rentschler, H. C.)—217(A)
Hibdon, Carl T., M. L. Pool, and J. D. Kurbatov. Relative intensities and characteristic radiations of radioactive scandium—462(A)
Hickman, K. Vacuum pumps in the development of industry—455(T)
Hillier, J. (see Zworykin, V. K.)—224(A)
Hipple, John A. and D. P. Stevenson. Ionization and dissociation by electron impact: the methyl and ethyl radicals—121
Hirsh, F. R., Jr. Search for element No. 87—93
Holmes, John R. Isotope shifts in some lines of nitrogen —41
Hudson, G. E. Dispersion of elastic waves in solid circular cylinders—46
Hughes, Donald J. (see Wilson, Volney C.)—161
Hulthén, Lamek. On the scattering of neutrons by protons —383(L)
Huntington, H. B. Energies for self-diffusion in zinc—383(L)
Hutter, R. G. E. (see Marton, L.)—140(A)

Iona, Mario, Jr. (see Schein, Marcel)—60(A)
—— **and Marcel Schein.** Slow mesotrons in the stratosphere—60(A)

Jaffé, George. Statistical theory of liquids. II—313
Jaffey, A. H. (see Freed, Simon)—12
Jánossy, L. (see Rochester, G. D.)—52
Jauch, J. M. Meson theory of the magnetic moment of proton and neutron—222(A), 334

Johnson, T. H. (see De Benedetti, S.)—222(A)
——, **R. P. Shutt, and S. De Benedetti.** High pressure cloud chamber of new design—222(A)
Jura, George (see Harkins, William D.)—224(A), 225(A)
—— **and William D. Harkins.** Method for determining the area of a crystalline powder without the assumption of a molecular area—224(A)

Kanne, W. R. (see Wilkening, M. H.)—63(A)
Kaplan, Wilfred (see Dresden, M.)—221(A)
Katz, L., R. V. Adams, Jr., and W. E. Deeds. Preliminary energy distribution curve of cosmic rays—140(A)
Kaufmann, A. R. (see Clark, J. R.)—139(A)
—— **and C. Starr.** Magnetic properties of solid solutions—445
Kennard, E. H. Cavitation in an elastic liquid—172
Kennedy, William R. and Paul L. Copeland. Temperature coefficient of secondary emission and the work function of molybdenum targets coated with beryllium and treated with HCl—61(A)
King, G. W. (see Cross, Paul C.)—220(A)
Kinsey, E. L. (see Krueger, Robert W.)—138(A)
Kirkpatrick, Paul. Continuous radiation in prismatic x-ray spectra—141(A)
—— Theoretical dependence of continuous x-ray intensity and polarization upon several experimental parameters—139(A)
Klema, E. D. and H. H. Barschall. Saturation characteristics for alpha-particles in purified gases—18
Knauss, Harold P. "Automatic volume control" of the ear—457(T)
Koch, H. W. (see Baldwin, G. C.)—59(A), 462(A)
Koehler, J. W. On the linear stress-strain curves of the hexagonal metals—460(A)
Kolin, Alexander. Electromagnetic method for the determination of velocity distribution in fluid flow—218(A)
Krueger, Robert W. and E. L. Kinsey. Polarization of the absorption spectra of neodymium ions in crystals—138(A)
Kurbatov, J. D. (see Hibdon, Carl T.)—462(A)
—— (see Pool, M. L.)—463(A)
—— (see Weimer, Katherine E.)—59(A), 67
—— (see Zumstein, R. V.)—59(A)
—— **and M. L. Pool.** Progress report on the radioactivities in the illinium region—463(A)
Kusaka, S. (see Pauli, Wolfgang)—400
—— **and W. Pauli.** On the theory of a mixed pseudoscalar and a vector meson field—221(A)

Langer, R. M. and G. Potapenko. On the heat transfer from radiating gases to water tubes of a boiler—138(A)
Laporte, O. and J. E. Mack. Spectrum of neutral tungsten, W I—246
Lapp, R. E. Investigation of large cosmic-ray bursts in iron—462(A)
Lark-Horovitz, K. Biological applications of radioactive tracers—459(T)
Lenander, H. E. (see Constant, F. W.)—441
Liebermann, Leonard N. Vibrational analysis of the near ultraviolet system of CS_2—63(A)
Littleton, J. T. Discussion: Education of physicists for war and post-war conditions. Industry—455(T)

Mack, J. E. (see Laporte, O.)—246
MacKeown, S. S. and Victor Wouk. Static charges produced on moving rubber-tired vehicles—140(A)
Mandeville, C. E. Gamma-rays from As^{76}—91
—— Gamma-rays from Na^{24} and La^{140}—387(L)
Manning, E. L. Discussion: Education of physicists for war and post-war conditions. Secondary schools—455(T)
Manning, Millard F. Electronic energy bands in body-centered iron—190
—— (see Greene, Jack B.)—203
Margenau, Henry. Forces between hydrogen molecules—385(L)
Mark, Hermann. Elasticity of high polymers as bearing on synthetic rubber problem—455(T)
Marshall, John, Jr. (see Dicke, Robert H.)—86
Marton, L. and R. G. E. Hutter. Optical constants of electron microscopes—140(A)
McBain, James W. (see de Bretteville, Alexander, Jr.)—223(A)
McCue, J. J. G. Ionization cross section of the silver L_{III} state—218(A)
McDowell, Louise S. Physics at Wellesley College—457(T)
McLucas, John L. (see Elliott, Daniel S.)—456(A)
Meister, Arnold G., Forrest F. Cleveland, and M. J. Murray. Raman spectra of some diacetylenes—64(A)
Meitner, Lise. Simple method for the investigation of secondary electrons excited by γ-rays and the interference of these electrons with measurements of primary β-ray spectra—73; Erratum—384(L)
Middleton, David. Ultra-high frequency oscillations of cylindrical cavity resonators containing two and three dielectric media—343
Miller, V. (see Yates, K. P.)—461(A)
Millikan, R. A., H. Victor Neher, and William H. Pickering. Further tests of the atom-annihilation hypothesis as to the origin of the cosmic rays—234
——, **H. Victor Neher, and William H. Pickering.** Origin of cosmic rays—140(A)
More, Louis T. Newton's philosophy of nature—459(T)
Mrozowski, S. Hyperfine structure in the band spectrum of HgH—63(A)
Muehlhause, C. O. Method for measuring total cross sections for low energy neutrons—60(A)
Murdock, C. C. Shape of the Debye-Scherrer lines—223(A)
Murray, M. J. (see Cleveland, Forrest F.)—220(A)
—— (see Hamilton, Dwight T.)—64(A)
—— (see Meister, Arnold G.)—64(A)
Myers, F. E. (see Petrauskas, A. A.)—389
—— (see Shull, C. G.)—29

Nassar, Salwa C. (see Anslow, Gladys A.)—458(A)
Neher, H. Victor (see Millikan, Robert A.)—140(A), 234
Nereson, Norris (see Rossi, Bruno)—61(A)
Nielsen, Carl E. and Wilson M. Powell. Mesotron mass and heavy tracks on Mt. Evans—140(A), 384(L)
Nielsen, H. H. and Ely E. Bell. Automatic recording vacuum infra-red grating spectrometer—459(T)

Nordheim, Gertrud and H. Sponer. Determination of chlorine vibrations in dichlorobenzenes from intensities and polarizations of their Raman lines—220(A)

Oughton, C. D. Resistance of glass to thermal and physical shock—455(T)

Pan, S. T. (see Clark, J. R.)—139(A)
Parker, H. M. Construction of surfaces of constant normal separation—63(A)
Pauli, Wolfgang. On strong-coupling and weak-coupling theories of the meson field—221(A)
—— (see Kusaka, S.)—221(A)
—— **and S. Kusaka.** On the theory of a mixed pseudoscalar and a vector meson field—400
Pepinsky, R. and P. Weisz. X-ray diffraction measurements with Geiger-Mueller tube—457(A)
Perlman, I. Applications of nuclear physics to the biological sciences—58(T)
Petersen, Max and C. W. Tucker. X-ray line broadening by cold-working alpha-brass—385(L)
Peterson, L. E. and Eugene Guth. Equation of state of synthetic rubbers—62(A)
Petrauskas, A. A., L. C. Van Atta, and F. E. Myers. Measurements on x-ray production and absorption in the range 0.7 to 2.5 Mv—389
Pickering, William H. Improved cosmic-ray radio sonde—140(A)
—— (see Millikan, Robert A.)—140(A), 234
Pool, M. L. (see Hibdon, Carl T.)—462(A)
—— (see Kurbatov, J. D.)—463(A)
—— (see Weimer, Katherine E.)—59(A), 67
—— (see Zumstein, R. V.)—59(A)
—— **and J. D. Kurbatov.** Artificial radio activities of cerium—463(A)
Potapenko, G. (see Langer, R. M.)—138(A)
Powell, Wilson M. (see Nielsen, Carl E.)—140(A), 384(L)
Prebus, A. F. Combined electron diffraction and microscope apparatus—462(A)

Quimby, Edith H. and Elizabeth F. Focht. Error arising from the use of small carbon-lined ionization chambers in the measurement of low voltage x-rays in Roentgens—218(A)

Racah, Guilio. Theory of complex spectra. III—367
Ramo, Simon (see Bachman, C. H.)—224(A)
Randels, W. C. and S. Silver. Lift function for an oscillating airfoil—225(A)
Reid, Walter P. Effect of high electrostatic fields upon the vaporization and resistance of molybdenum filaments—359
Rentschler, H. C. and D. E. Henry. Action of oxygen, nitrogen, and hydrogen in lowering the photoelectric work function of zirconium, titanium, and thorium—217(A)
Roberts, A. (see Elliott, L. G.)—386(L)
Rochester, G. D. and L. Jánossy. Preparation and efficiency of the fast Geiger-Müller counter—52
Rogers, F. T., Jr. Mg II λ4481 line in the spectrum of algol—219(A)
Rose, M. E. Specular reflection of plane wave pulses in media of continuously variable refractive properties—111
Rossi, Bruno and Norris Nereson. Experimental determination of the disintegration curve of mesotrons—61(A)
Ruark, Arthur E. Generalization of Bateman's differential equations—457(A)

Schein, Marcel (see Iona, Mario, Jr.)—60(A)
—— (see Tabin, Julius)—462(A)
—— **and Mario Iona, Jr.** Nature of the primary cosmic radiation—60(A)
—— **and Julius Tabin.** Production of mesotrons by ionizing and non-ionizing radiation—223(A)
Schleiger, E. R. (see Brentano, J. C. M.)—218(A)
Schultz, M. L. (see Freed, Simon)—12
Serber, R. and S. M. Dancoff. Strong coupling mesotron theory of nuclear forces—143
Shull, C. G., C. T. Chase, and F. E. Myers. Electron polarization—29
Shutt, R. P. (see De Benedetti, S.)—222(A)
—— (see Johnson, T. H.)—222(A)
Silver, S. (see Randels, W. C.)—225(A)
Simpson, John A., Jr. (see Trounson, Edmund)—55(L)
Smith, Charles G. Motion of the copper arc in transverse magnetic field—217(A)
Smoluchowski, R. Diffusion rate of carbon in iron alloys—61(A)
—— Diffusion rates of carbon in iron-molybdenum and iron-tungsten alloys—438
Spatz, W. Factors influencing the plateau characteristics of self-quenching G-M counters—462(A)
Sponer, H. (see Nordheim, Gertrud)—220(A)
Starr, C. (see Kaufmann, A. R.)—445
Steadman, L. T. Carbon arc in oxygen for the spectrochemical determination of potassium—322(L); Erratum—399
Stevenson, D. P. (see Hipple, John A.)—121
Swann, W. F. G. Experiments concerning the origin of the second hump in the Rossi curve—222(A)
—— Nature of the primary particles responsible for cosmic-ray phenomena—210

Tabin, Julius and Marcel Schein. Measurements of cascade showers produced by ionizing and non-ionizing radiation in the stratosphere—462(A)
—— (see Schein, Marcel)—223(A)
Thomas, L. H. Physical mechanism for the nebular red shift—460(A)
Town, George K. Microwaves—455(T)
Townes, Charles H. and Wheeler P. Davey. X-ray diffraction study of the age-hardening of a Cu-Al alloy—223(A)
Trischka, J. W. Fine structure in the x-ray absorption edges of potassium chloride—218(A)
Trounson, Edmund and John A. Simpson, Jr. Polarization of electrons—55(L)
Tucker, C. W. (see Petersen, Max)—385(L)

Uhlenbeck, G. E. Theory of random processes—58(T)

Valentine, Alan. Address of welcome—455(T)
Van Atta, L. C. (see Petrauskas, A. A.)—389
Vassy, Etienne (see Heller, Wilfried)—65(A)

Waldman, Bernard and Marcellus L. Wiedenbeck. Nuclear excitation of indium by x-rays and electrons—60(A)
Warburton, F. W. Magnetic potential energy—460(A)
Wataghin, Gleb. Thermal equilibrium between elementary particles—137(L)
Watson, W. W. and D. Woernley. Thermal diffusion with ammonia—181
—— **and D. Woernley.** Thermal diffusion experiments with ammonia and argon—220(A)
Weber, A. H. and L. M. Friederich. Photoconductance of evaporated bismuth films—217(A)
Wehner, R. S. and Wheeler P. Davey. Equilibrium between the alpha- and gamma-phases of pure iron—61(A)
Weimer, Katherine E., M. L. Pool, and J. D. Kurbatov. Radioactive isotopes of lanthanum—67
——, **M. L. Pool, and J. D. Kurbatov.** Transmutation of barium—59(A)
Weinstock, Robert. Inelastic scattering of slow neutrons—139(A)
Weissler, Gerhard L. Positive and negative point-to-plane corona in pure and impure hydrogen, nitrogen, and argon—96
Weisz, P. (see Pepinsky R.)—457(A)
Wiedenbeck, Marcellus L. (see Waldman, Bernard)—60(A)
Wilchinsky, Z. W. X-ray measurement of short range order and long range order in Cu_3Au—223(A)
Wilkening, M. H. and W. R. Kanne. Localization phenomena in G-M counters—63(A)
Wilson, Volney C. and Donald J. Hughes. Cloud-chamber and counter studies of cosmic rays underground—161
Woernley, D. (see Watson, W. W.)—181, 220(A)
Wold, P. I. Graphical treatment of non-linear circuits—218(A)
Woods, L. H. Note on spin doubling in the doublet sigma states of CO^+—431
—— On the silicon oxide bands—426
Wouk, Victor (see MacKeown, S. S.)—140(A)
Wrenshall, Gerald A. Scattering of protons by magnesium nuclei—56(L)
Wu, Chien-Shiung (see Friedlander, Gerhart)—227

Yates, K. P. and V. Miller. Infra-red spectrum of methyl fluoride at 9.5μ—461(A)

Zachariasen, W. H. Theory of x-ray diffraction in mosaic crystals—62(A)
Zumstein, R. V., J. D. Kurbatov, and M. L. Pool. Disintegration of the long-life radioactive isotope of tantalum—59(A)
Zwicky, F. Dimensional characteristics of the large scale condensations of matter in the universe—139(A)
Zworykin, V. K. and J. Hillier. Compact electron microscope with magnetic lenses—224(A)

Analytic Subject Index to Volume 63

References with (A) are to abstracts of papers presented at meetings of the American Physical Society. References with (L) are to Letters to the Editor.

Absorption
Of high energy quanta, G. D. Adams and R. K. Clark—60(A)

Acoustics
Measurement and analysis of noises, Daniel S. Elliott and John L. McLucas—456(A)

Aerodynamics (see also **Hydrodynamics**)
Lift function for oscillating airfoil, W. C. Randels and S. Silver—225(A)

Arcs (see **Discharge of electricity in gases**)

Astrophysics
Dimensional characteristics of large scale condensations, F. Zwicky—139(A)
Line in spectrum of algol, F. T. Rogers, Jr.—219(A)
Nebular red shift, mechanism for, L. H. Thomas—460(A)
Origin of solar system, cepheid theory, A. C. Banerji—55(L)
Thermal equilibrium between elementary particles, Gleb Wataghin—137(L)

Biophysics
Radium applicators, H. M. Parker—63(A)

Conductivity, electrical (see **Electrical conductivity; Discharge of electricity in gases**)

Constants, physical, standards
Probable accuracy of physical constants, Frank Benford—212(L); Raymond T. Birge—213(L)

Cosmic radiation
Atom-annihilation hypothesis origin of cosmic ray, R. A. Millikan, H. Victor Neher, and William H. Pickering—140(A), 234
Bursts in iron, R. E. Lapp—462(A)
Cloud-chamber and counter studies underground, Volney C. Wilson and Donald J. Hughes—161
Cosmic-ray radio sonde, William H. Pickering—140(A)
Electrons accompanying mesotrons, Wayne E. Hazen—140(A)
Energy distribution curve, L. Katz, R. V. Adams, Jr., and W. E. Deeds—140(A)
High pressure cloud chamber, T. H. Johnson, R. P. Shutt, and S. De Benedetti—222(A)
Intensity at low altitude, origin of soft component, Kenneth Greisen—323
Mesotron mass, tracks on Mt. Evans, Carl E. Nielsen and Wilson M. Powell—140(A), 384(L)
Nature of primary particles, W. F. G. Swann—210
Nature of primary radiation, Marcel Schein and Mario Iona, Jr.—60(A)
Origin of second hump in Rossi curve, W. F. G. Swann—222(A)
Production of mesotrons, Marcel Schein and Julius Tabin—223(A)
Results obtained with high pressure cloud chamber, S. De Benedetti, T. H. Johnson, and R. P. Shutt—222(A)
Showers produced in stratosphere, Julius Tabin and Marcel Schein—462(A)
Slow mesotrons, Mario Iona, Jr., and Marcel Schein—60(A)
Specific ionization of cosmic rays in He, Wayne E. Hazen—107
"Stars" at 10,000 feet, Wayne E. Hazen—213(L)

Crystalline state
Age-hardening of Cu-Al alloy, Charles H. Townes and Wheeler P. Davey—223(A)
Area of crystalline powder, George Jura and William D. Harkins—224(A)
Diffraction investigation of sodium stearate, Alexander de Bretteville, Jr., and James W. McBain—223(A)
Diffusion rate of C in Fe alloys, R. Smoluchowski—61(A), 438
Distance attractive field of solid extends into liquid, William D. Harkins and George Jura—224(A)
Electrical conduction and recrystallization in Pb films, Edgar L. Armi—451
Electronic energy bands in body-centered iron, Millard F. Manning—190
Electronic energy bands in face-centered iron, Jack B. Greene and Millard F. Manning—203
Equilibrium between alpha- and gamma-phases of Fe, R. S. Wehner and Wheeler P. Davey—61(A)
Magnetic properties of solid solutions, Albert R. Kaufmann and C. Starr—445
Self-diffusion in Zn, H. B. Huntington—383(L)
Short range order and long range order in Cu_3Au, Z. W. Wilchinsky—223(A)
Stress-strain curves of hexagonal metals, J. S. Koehler—460(A)
X-ray of line broadening, cold-working, Max Petersen and C. W. Tucker—385(L)

Diffusion (see also **Thermal diffusion**)
Diffusion rate of C in Fe alloys, R. Smoluchowski—61(A), 438
Self-diffusion in Zn, H. B. Huntington—383(L)

Discharge of electricity in gases
Cathode drop, current density in arcs, G. H. Fett—460(A)
Decay in anode effect, Paul L. Copeland—61(A)
Motion of Cu arc in transverse magnetic field, Charles G. Smith—217(A)
Photon production relative to ionization by collision, Ronald Geballe—138(A)
Point-to-plane corona, Gerhard L. Weissler—96

Disintegration and excitation of nucleus (see also **Radioactivity**)
Threshold for nuclear photo-effect, G. C. Baldwin and H. W. Koch—462(A)

Dissociation
By electron impact of lead tetra-alkyls, John A. Hipple and D. P. Stevenson—121

Elasticity
Disturbance in elastic lattice system, H. Bateman—141(A)
Elastic waves in solid cylinders, dispersion of, G. E. Hudson—46
Oscillations in plates and shells, Paul S. Epstein—141(A)
Temperature rise in rubber on stretching, R. L. Anthony and S. L. Dart—62(A)
Electrical conductivity and resistance
Charges produced on rubber-tired vehicles, S. S. MacKeown and V. Wouk—140(A)
Of Pb films, Edgar L. Armi—451
Resistance of molybdenum, effect of electrostatic fields, Walter P. Reid—359
Electrolysis
And magnetolysis, Felix Ehrenhaft—216(A); 461(A)
Electromagnetic theory
Magnetic potential energy, F. W. Warburton—460(A)
Oscillations of cylindrical cavity resonators, David Middleton—343
Plane wave pulses in media of continuously variable properties, M. E. Rose—111
Theory of "coastal" refraction, G. Grünberg—185
Theory of the magnetron, Léon Brillouin—127
Electron optics
Combined electron diffraction and microscope apparatus, A. F. Prebus—462(A)
Constants of electron microscopes, L. Marton and R. G. E. Hutter—140(A)
Electron microscope with magnetic lenses, V. K. Zworykin and J. Hillier—224(A)
Simplified electron microscope, C. H. Bachman and Simon Ramo—224(A)
Electrons
Direct determination of β-particle charge, Yardley Beers—77
Electrons, scattering of
Effect of oblique incidence, polarization, Gerald Goertzel and R. T. Cox—37
Electron polarization on scattering, C. G. Shull, C. T. Chase, and F. E. Myers—29; Edmund Trounson and John A. Simpson, Jr.—55(L)
Electrons, secondary
Excited by γ-rays, Lise Meitner—73, 384(L)
Temperature coefficient, work function of molybdenum, William R. Kennedy and Paul L. Copeland—61(A)
Electron tubes (see **Vacuum tubes**)
Electrostatics
Definition of absolute electrode potentials, David C. Grahame—458(A)
Elements
Search for element 87, F. R. Hirsh, Jr.—93
Equations of state
Condensation in super-cooled phases, Peter G. Bergmann—456(A)
Dynamical approach to condensation problem, M. Dresden and Wilfred Kaplan—221(A)
Of synthetic rubbers, L. E. Peterson and Eugene Guth—62(A)
Errata
Carbon arc in oxygen for the spectrochemical determination of potassium, L. T. Steadman—399
Quantization of molecules inter- and intramolecular forces, Kasimir Fajans and Theodore Berlin—399
Simple method for the investigation of secondary electrons excited by γ-rays and the interference of these electrons with measurements of primary beta-ray spectra, Lise Meitner—384(L)
Evaporation
Effect of high electrostatic fields, G. B. Estabrook—352; W. P. Reid—359
Excitation of nuclei (see also **Disintegration and excitation of nucleus, Nuclear structure**)
Excitation functions of proton-induced reactions in Li, E. D. Courant—219(A)
Of indium by x-rays and electrons, Bernard Waldman and Marcellus L. Wiedenbeck—60(A)
Thresholds for nuclear photo-effect, G. C. Baldwin and H. W. Koch—59(A)
Fluorescence
Quantum yield of diacetyl fluorescence, G. M. Almy and P. R. Gillette—64(A)
Heat conduction (see **Thermal conductivity**)
Hydrodynamics
Cavitation in an elastic liquid, E. H. Kennard—172
Hyperfine structure
In band spectrum of HgH, S. Mrozowski—63(A)
Instruments (see **Methods and instruments**)
Ionization by collision
Of methyl and ethyl radicals, John A. Hipple and D. P. Stevenson—121
Saturation characteristics for α-particles in gases, E. D. Klema and H. H. Barschall—18
Ionization by radiation
Ionization yield of radiation energy, U. Fano—222(A)
Isotopes
Of Ce and Rh, Arnold A. Cohen—219(A)
Isotope shifts in N lines, John R. Holmes—41
Liquids (see also **Hydrodynamics**)
Condensation in super-cooled phases, Peter G. Bergmann—456(A)
Statistical theory of, George Jaffé—313
Structure of liquid CCl_4, A. Eisenstein—304
Magnetic Properties
Ferromagnetic impurities, heat treatment, F. W. Constant, R. E. Faires, and H. E. Lenander—441
Of Fe-Ce alloys, J. R. Clark, S. T. Pan, and A. R. Kaufmann—139(A)
Magnetolysis and magnetic current, Felix Ehrenhaft—461(A)
Of solid solutions, Albert R. Kaufmann and C. Starr—445
Mechanics, quantum-molecular structure and spectra
Molecular structure, Henry Margenau—385(L)
Mechanics, statistical
Theory of liquids, George Jaffé—313

Mesotrons
Disintegration curve of mesotrons, Bruno Rossi and Norris Nereson—61(A)
Electrons accompanying mesotrons, Wayne E. Hazen—140(A)
Mesotron mass, Carl E. Nielsen and Wilson M. Powell—140(A), 384(L)
Production by ionizing and non-ionizing radiation, Marcel Schein and Julius Tabin—223(A)
In stratosphere, Mario Iona, Jr., and Marcel Schein—60(A)
Metals (see **Crystalline state**)
Methods and instruments
Absorption of vibration, C. W. Chamberlain—219(A)
Adsorption of vapor on surface of solid, William D. Harkins and George Jura—225(A)
Area of crystalline powder, George Jura and William D. Harkins—224(A)
Bateman's differential equations of probability, Arthur E. Ruark—457(A)
Combined electron diffraction and microscope apparatus, A. F. Prebus—462(A)
Constants of electron microscopes, L. Marton and R. G. E. Hutter—140(A)
Cosmic-ray radio sonde, William H. Pickering—140(A)
Definition of absolute electrode potentials, David C. Grahame—458(A)
Detection of absorption bands, Wilfried Heller and Etienne Vassy—65(A)
Determination of velocity distribution in fluid flow, Alexander Kolin—218(A)
Electron microscope with magnetic lenses, V. K. Zworykin and J. Hillier—224(A)
Error arising in ionization chambers, Edith H. Quimby and Elizabeth F. Focht—218(A)
Fast G-M counters, preparation and efficiency, G. D. Rochester and L. Jánossy—52
Graphical treatment of non-linear circuits, P. I. Wold—218(A)
High pressure cloud chamber, T. H. Johnson, R. P. Shutt, and S. De Benedetti—222(A)
Localization phenomenon in G-M counters, M. H. Wilkening and W. R. Kanne—63(A)
Measurement and analysis of noises, Daniel S. Elliott and John L. McLucas—456(A)
Measurement of photographic densities by x-rays, J. C. M. Brentano—64(A)
Oscillations of cylindrical cavity resonators, David Middleton—343
Production of ozone by ultraviolet light, Arthur W. Ewell—65(A)
Random fluctuations in d.c. bridge amplifier, J. C. M. Brentano and E. R. Schleiger—218(A)
Recording relay for infra-red spectrograph, Ely E. Bell—461(A)
Self-quenching G-M counters, W. Spatz—462(A)
Simplified electron microscope, C. H. Bachman and Simon Ramo—224(A)
Spectrochemical determination of K, L. T. Steadman—322(L)
Surfaces of constant normal separation, H. M. Parker—63(A)
Theory of the magnetron, Léon Brillouin—127
X-Ray diffraction with G-M tube, R. Pepinsky and P. Weisz—457(A)
Molecular structure and constants (see also **Spectra, molecular,** etc., and **Raman spectra**)
Inter- and intramolecular forces; quantization, Kasimir Fajans and Theodore Berlin—309, 399

Nuclear moments and spin
Magnetic moment of proton and neutron, meson theory, J. M. Jauch—222(A); 334
Nuclear structure (see also **Disintegration of nucleus**)
Antisymmetrical interaction in beta-decay theory, Charles L. Critchfield—417
Energy levels in Fe^{56}, L. G. Elliott and M. Deutsch—321(L)
Excited spin states of proton and neutron, V. L. Ginsburg—1
Strong coupling mesotron theory, R. Serber and S. M. Dancoff—143
Theories of meson field, W. Pauli—221(A)
Theory of mixed pseudoscalar and vector meson field, S. Kusaka and W. Pauli—221(A), 400

Optical constants and properties
Double refraction, intrinsic anisotropy, Wilfried Heller—62(A)

Photo-conductance
Of evaporated Bi films, A. H. Weber and L. M. Friederich—217(A)
Photoelectric effect and properties; cells
Photoelectric work function action of O_2, N_2, and H_2, H. C. Rentschler and D. E. Henry—217(A)

Radioactivity (see also **Disintegration of nucleus**)
Angular correlation of gamma-rays, Robert Beringer—23
Of Ba isotope, Katherine E. Weimer, M. L. Pool, and J. D. Kurbatov—59(A)
Of Ce, M. L. Pool and J. D. Kurbatov—463(A)
Disintegration scheme of Co^{58}, L. G. Elliott and M. Deutsch—219(A)
Disintegration scheme of Na^{24}, L. G. Elliott, M. Deutsch, and A. Roberts—386(L)
Of elements in illinium region, J. D. Kurbatov and M. L. Pool—463(A)
Gamma-ray from radio-yttrium, G. R. Gamertsfelder—60(A)
Gamma-rays from As^{76}, C. E. Mandeville—91
Gamma-rays from Na^{24} and La^{140}, C. E. Mandeville—387(L)
Half-life of RaE, charge of β-particles, Yardley Beers—77
High centrifugal fields, radioactive decay, Simon Freed, A. H. Jaffey, and M. L. Schultz—12
Interaction in beta-decay theory, Charles L. Critchfield—417
Isotopes of La, Katherine E. Weimer, M. L. Pool, and J. D. Kurbatov—67

Measurements of primary β-ray spectra, Lise Meitner—73, 384(L)
Of Hg isotopes, Gerhart Friedlander and Chien-Shiung Wu—227
Of 100-day As, L. G. Elliott and M. Deutsch—457(A)
Of Sc; intensities and characteristic of radiations, Carl T. Hibdon, M. L. Pool, and J. D. Kurbatov—462(A)
Of Ta isotope, R. V. Zumstein, J. D. Kurbatov, and M. L. Pool—59(A)

Raman spectra
Chlorine vibrations in dichlorobenzenes, Gertrud Nordheim and H. Sponer—220(A)
Of diacetylenes, Arnold G. Meister, Forrest F. Cleveland, and M. J. Murray—64(A)
Of diisobutylene, cyclohexene, and dipentene, Forrest F. Cleveland—461(A)
Of ethane-like molecules, Dwight T. Hamilton, Forrest F. Cleveland, and M. J. Murray—64(A)
Of methylheptenes, Forrest F. Cleveland—224(A)
Of octenes and octynes, Forrest F. Cleveland—64(A)
Of symmetrical top acetylenes, Forrest F. Cleveland and M. J. Murray—220(A)

Relativity
Relativistic theory of excited spin states of proton and neutron, V. L. Ginsburg—1

Scattering of electrons, neutrons, and ions (see also **Electrons, scattering of; Electron optics**)
Effect of oblique incidence on single scattering of electrons, Gerald Goertzel and R. T. Cox—216(A)
Of electrons in light gases, T. N. Gautier—456(A)
Inelastic scattering of neutrons, Robert Weinstock—139(A)
Inelastic scattering of protons in various metals, Robert H. Dicke and John Marshall, Jr.—86
Neutralization of ions in He, W. J. Hamm—433
Of neutrons by protons, Lamek Hulthén—383(L)
Plural scattering of electrons, Bowen C. Dees and Bernard Hamermesh—217(A), 297
Of protons by Mg, Gerald A. Wrenshall—56(L)
Total cross sections for low energy neutrons, C. O. Muehlhause—60(A)

Secondary electrons (see **Electrons, secondary**)

Spectra, absorption
Of aromatic amino acids, Gladys A. Anslow and Salwa C. Nassar—458(A)
Detection of absorption bands, Wilfried Heller and Etienne Vassy—65(A)
Polarization of spectra of Nd ions, Robert W. Krueger and E. L. Kinsey—138(A)
Of vegetable oils, infra-red, E. S. Barr and W. R. Harp—457(A)

Spectra, atomic
Isotope shifts in N, John R. Holmes—41
Mg II line in spectrum of algol, F. T. Rogers, Jr.—219(A)
Theory of complex spectra, Giulio Racah—367
Of W I, O. Laporte and J. E. Mack—246

Spectra, general
Nebular red shift, mechanism for, L. H. Thomas—460(A)
Spectrochemical determination of K, L. T. Steadman—322(L), 399(L)

Spectra molecular (see also **Molecular structure and constants**)
ClO_2 bands, $\Delta_1 F$ values, Jesse B. Coon—63(A)
Chlorine vibrations in dichlorobenzenes, Gertrud Nordheim and H. Sponer—220(A)
Of CH_3F at 9.5μ, K. P. Yates and V. Miller—461(A)
Of SiO_2 bands, L. H. Woods—426
Spin doubling doublet $^2\Sigma$ states of CO^+, L. H. Woods, —431
Transition probabilities of asymmetric rotor, Paul C. Cross and G. W. King—220(A)
Vibrational analysis of system of CS_2, Leonard N. Liebermann—63(A)

Thermal conductivity
Heat transfer from gases to water tubes, R. M. Langer and G. Potapenko—138(A)

Thermal diffusion
Of NH_3 and A, influence of temperature, W. W. Watson and D. Woernley—181, 220(A)

Thermionic emission; Emitting surfaces
Adsorption of Th on Ta, Charles J. Gallagher—217(A)

Thermodynamics
"Génies" of Poincaré, and Carnot's principle, Pierre Demers—221(A)
Thermal equilibrium between elementary particles, Gleb Wataghin—137(L)

Vacuum tubes
Theory of the magnetron, Léon Brillouin—127

Vaporization (see **Evaporation**)

Wave motion
Media of continuously variable properties, M. E. Rose —111

X-rays, absorption
Error arising in ionization chambers, Edith H. Quimby and Elizabeth F. Focht—218(A)
Fine structure in absorption edges of KCl, J. W. Trischka —218(A)

X-rays, diffraction, scattering, reflection, refraction, and polarization
Continuous radiation in prismatic spectra, Paul Kirkpatrick—141(A)
Diffraction in mosaic crystals, W. H. Zachariasen—62(A)
Diffraction with G-M tube, R. Pepinsky and P. Weisz —457(A)
Shape of Debye-Scherrer lines, C. C. Murdock—223(A)
Structure of liquid CCl_4, A. Eisenstein—304

X-rays, emission (see also **X-rays, spectra and spectroscopy**, etc.)
Cross section of **Ag** L_{III} state, J. J. G. McCue—218(A)
Fluorescence excitation of L_{III} level in Th, Burr G. Burbank—139(A)
Intensity and polarization, dependence on experimental parameters, Paul Kirkpatrick—139(A)
Production and absorption 0.7 to 2.5 Mv range, A. A. Petrauskas, L. C. Van Atta, and F. E. Myers—389

JUL 6 1943

THE PHYSICAL REVIEW

VOLUME 63 *Second Series* NUMBERS 11 AND 12

JUNE 1 AND 15, 1943

Published for the

AMERICAN PHYSICAL SOCIETY

by the

AMERICAN INSTITUTE OF PHYSICS
Incorporated

LANCASTER, PA., AND NEW YORK, N. Y.

THE PHYSICAL REVIEW

A journal of experimental and theoretical physics established by E. L. Nichols in 1893

Published by the American Institute of Physics for the

AMERICAN PHYSICAL SOCIETY

Officers

President

A. W. HULL
General Electric Company
Schenectady, New York

Vice President

A. J. DEMPSTER
University of Chicago
Chicago, Illinois

Secretary

K. K. DARROW
Bell Telephone Laboratories
Office:
Columbia University
New York, New York

Treasurer

G. B. PEGRAM
Columbia University
New York, New York

Local Secretary for the Pacific Coast

R. T. BIRGE
University of California
Berkeley, California

Editor

JOHN T. TATE*
University of Minnesota
Minneapolis, Minnesota

*On leave for 1943.

BOARD OF EDITORS

JOHN T. TATE, *Editor (on leave)* J. W. BUCHTA, *Acting Editor*

Associate Editors

A. C. G. MITCHELL	W. H. FURRY	BRUNO ROSSI
I. I. RABI	LUIS ALVAREZ	MELBA PHILLIPS
G. E. UHLENBECK	E. M. MCMILLAN	W. H. ZACHARIASEN

Manuscripts for publication should be submitted to J. W. Buchta, University of Minnesota, Minneapolis, Minnesota.

Proof and all correspondence concerning papers in the process of publication should be addressed to the Publications Manager, American Institute of Physics, 175 Fifth Avenue, New York, New York.

Subscription Price

United States and Canada $15.00
Elsewhere $16.50

Back Numbers

Complete set: Series 2,[1] Vol. 1, 1913–Vol. 62, 1942—$450.00
Yearly rate: $16.50
Single copies: $1.50 each prior to July, 1929;
$0.75 each July, 1929–December, 1941.
Current issues: $1.50 each.

Subscriptions and orders for back numbers should be addressed to Prince and Lemon Streets, Lancaster, Pennsylvania, or to the American Institute of Physics, 175 Fifth Avenue, New York, New York.

Changes of address in the case of members of the American Physical Society should be addressed to the Treasurer; in the case of other subscribers to the Publications Manager.

[1] For Series 1 inquire of Physics Department, Cornell University, Ithaca, New York.

The Physical Review is published monthly at Prince and Lemon Streets, Lancaster, Pennsylvania.

Entered as second-class matter January 27, 1933, at the Post Office at Lancaster, Pennsylvania, under the Act of March 3, 1879.

Acceptance for mailing at special rate of postage provided for in paragraph 4, section 538, P. L. & R., authorized January 27, 1933.

THE AMERICAN INSTITUTE OF PHYSICS

INCORPORATED

ADMINISTRATIVE STAFF

HENRY A. BARTON, *Director*

MADELINE M. MITCHELL, *Publications Manager*

JOHN T. TATE, *Adviser on Publications*

Office: 175 Fifth Avenue, New York, New York

JOURNALS

THE PHYSICAL REVIEW

REVIEWS OF MODERN PHYSICS

JOHN T. TATE, *Editor (on leave)*

J. W. BUCHTA, *Acting Editor*

JOURNAL OF THE OPTICAL SOCIETY OF AMERICA

GEORGE R. HARRISON, *Editor*

THE JOURNAL OF THE ACOUSTICAL SOCIETY OF AMERICA

FLOYD A. FIRESTONE, *Editor*

AMERICAN JOURNAL OF PHYSICS

DUANE ROLLER, *Editor*

THE REVIEW OF SCIENTIFIC INSTRUMENTS

GAYLORD P. HARNWELL, *Editor*

THE JOURNAL OF CHEMICAL PHYSICS

JOSEPH E. MAYER, *Editor*

JOURNAL OF APPLIED PHYSICS

ELMER HUTCHISSON, *Editor*

GOVERNING BOARD

PAUL E. KLOPSTEG, *Chairman*
Central Scientific Company

GEORGE B. PEGRAM, *Secretary*
Columbia University

For the American Physical Society:

JOHN T. TATE
University of Minnesota

L. A. DUBRIDGE
University of Rochester

GEORGE B. PEGRAM
Columbia University

For the Optical Society:

A. C. HARDY
Massachusetts Institute of Technology

K. S. GIBSON
National Bureau of Standards

R. C. GIBBS
Cornell University

For the Acoustical Society of America:

HARVEY FLETCHER
Bell Telephone Laboratories

FLOYD A. FIRESTONE
University of Michigan

WALLACE WATERFALL
The Celotex Corporation

For the Society of Rheology:

R. B. DOW
Aberdeen Proving Ground

HERMANN MARK
Brooklyn Polytechnic Institute

N. W. TAYLOR
The Pennsylvania State College

For the American Association of Physics Teachers:

A. G. WORTHING
University of Pittsburgh

PAUL E. KLOPSTEG
Central Scientific Company

T. D. COPE
University of Pennsylvania

The American Institute of Physics is a membership corporation of which five societies are the founding members. These five societies are the principal national societies devoted to pure and applied physics in America. Their names, and those of their representatives who form the Governing Board of the Institute, are given above. The principal work of the Institute is the publication of journals sponsored by the societies or by itself. The names and the editors of the journals are also listed above.

The broad purpose of the Institute is to represent, in all matters of wide or common interest, the five thousand or more members and subscribers associated with the Founder Societies and the journals. It aims to advance the science and profession of physics, and to promote cooperation between pure research, the applied sciences and the industries. To achieve these aims, it is greatly in need of an endowment and is empowered by law to administer grants and funds of any kind.

CONTENTS

THE PHYSICAL REVIEW SECOND SERIES, VOL. 63, NOS. 11 AND 12 JUNE 1 AND 15, 1943

Measurements on X-Ray Production and Absorption in the Range 0.7 to 2.5 Mv . . . . . A. A. PETRAUSKAS, L. C. VAN ATTA, AND F. E. MYERS 389

Errata: Quantization of Molecules, Inter- and Intramolecular Forces . . . . . KASIMIR FAJANS AND THEODORE BERLIN 399

Erratum: The Carbon Arc in Oxygen for the Spectrochemical Determination of Potassium . . . . . L. T. STRADMAN 399

On the Theory of a Mixed Pseudoscalar and a Vector Meson Field . . . . . W. PAULI AND S. KUSAKA 400

Antisymmetrical Interaction in Beta-Decay Theory . . . . . CHARLES L. CRITCHFIELD 417

On the Silicon Oxide Bands . . . . . L. H. WOODS 426

Note on Spin Doubling in the Doublet Sigma States of CO^+ . . . . . L. H. WOODS 431

Recombination and Neutralization of Argon Ions in Helium . . . . . W. J. HAMER 433

Diffusion Rates of Carbon in Iron-Molybdenum and Iron-Tungsten Alloys R. SMOLUCHOWSKI 438

Investigations of Ferromagnetic Impurities. II . . . . . F. W. CONSTANT, R. E. FAIRES, AND H. E. LENANDER 441

Magnetic Properties of Solid Solutions. III. The Paramagnetic Alloys of Copper and Nickel . . . . . A. R. KAUFMANN AND C. STARR 445

Electrical Conduction and Recrystallization in Thin Pb Films Deposited at Low Temperatures . . . . . EDGAR L. ARMI 451

Proceedings of the American Physical Society:

Metropolitan Section Meeting, April 2, 1943: Minutes and Abstract 455
New York State Section Meeting, April 2–3, 1943 455
Southeastern Section Meeting, April 2–3, 1943: Minutes and Abstracts 1–5 456
New England Section Meeting, April 3, 1943: Minutes and Abstracts 1–3 457
Columbus Meeting, April 30 and May 1, 1943: Minutes and Abstracts 1–16, Author Index 459

Author Index to Volume 63 464

Analytic Subject Index to Volume 63 469

Volume Table of Contents iii

LANCASTER PRESS, INC., LANCASTER, PA.